

**Development of selective real-time PCR (SPCR)
assays for the detection of K103N resistance mutation
in minor HIV-1 populations.**

by

Mpho Maria Seleka

Submitted in partial fulfilment for the degree

Masters in Medical Science (Virology)



at

Stellenbosch University

Department of Pathology

Faculty of Health Sciences

Supervisor: Prof Susan Engelbrecht

Co-Supervisor: Dr Gert Van Zyl

Date: 1 December 2011

Declaration

I, the undersigned, hereby declare that the work contained in this thesis is my own original work and that I have not previously in its entirety or in part, submitted it at any university for a degree.

Signature

Mpho Maria Seleka

Name in full

Date

Acknowledgements

I extend my sincere thanks to the following people:

Prof. Susan Engelbrecht, my promoter, and Dr. Gert Van Zyl, my co-supervisor, for guiding and encouraging me throughout the course of this research project and compiling the thesis.

Bizhan Romani and Eloise Braaf for support and technical assistance.

Dalene de Swardt and Eduan Wilkinson for the Afrikaans translation of the Abstract.

Poliomyelitis Research Foundation (PRF), National Research Fund (NRF) and National Health Laboratory Service Research Trust (NHLS RT) for funding the study.

My family and friends for their support and encouragement throughout the study period.

Abstract

Background: The conventional sequence analysis is the most common method used for the detection of drug-resistant mutants. Due to its sensitivity limitations, it is unable to detect these mutants when comprising less than 20% (minor populations) of the total virus population in a sample. However, real-time PCR-based assays offer a rapid, sensitive, specific and easy detection and quantification of such mutants. The HIV-1 variants harbouring the K103N mutation are associated with resistance to nevirapine (NVP) and efavirenz (EFV). The persisting drug-resistant mutants decay slowly to low levels, and therefore they are called minor drug-resistant mutants. Consequently, they affect subsequent treatment with the drugs of the relevant class.

Objectives: The objective of this study was to design two TaqMan real-time PCR-based assays called selective-polymerase chain reaction (SPCR), namely the total viral copy SPCR assay and the K103N-SPCR assay. The former detects HIV-1 of subtype C reverse transcriptase sequences, whereas the latter detects K103N drug-resistant variants in these sequences.

Design and Methods: In developing the SPCR assays, sets of appropriate primers and probes for the HIV-1 subtype C reverse transcriptase (*RT*) were developed to use in the K103N-specific reaction and the total copy reaction. Twelve DNA plasmid standards with sequence diversity were constructed for the assay from two HIV-1 subtype C samples known to harbour the K103N mutation (AAC or AAT) in our Department's Resistance Databank. Their *RT* regions were amplified, cloned and verified with sequencing. Site-directed mutagenesis was used to induce mutations at 103 amino acid position in some of these clones to generate more standards with either one of the three codons (AAA, AAC and AAT). The two assays were optimized and validated, and a standard curve was generated for each assay using 10-fold serial dilution (5×10^7 - 5×10^0 DNA copy/ μ L) of a K103N-mutant plasmid standard. The optimized and validated SPCR assays were used to screen 40 nested PCR products of previously genotyped patient samples for minor K103N variants.

Results: Two sensitive and reproducible selective real-time PCR (SPCR) assays, with cut-offs of 8.23 and 10.33 and a detection limit of 0.01% for the K103N resistance

variants, were successfully developed. The assays detected a prevalence of 25.64-46.15% for the K103N resistance mutation in 39 patient samples. The genotyping (population sequencing) missed 40-53.85% of these variants.

Conclusion: In conclusion, sensitive and reliable selective real-time PCR assays to detect and quantify minor K103N variants of HIV-1 in nested PCR products were successfully developed. The assay had a lower detection limit of 0.01%.

Opsomming

Agtergrond: Konvensionele volgorde bepaling analise is die mees algemeenste metode wat gebruik word vir die opsporing van middel-weerstandige mutasies, maar weens beperkte sensitiviteit is dit nie moontlik om hierdie mutante op te spoor wanneer dit minder as 20% (minderheids populasie) van die totale viruspopulasie in 'n monster uitmaak nie. Nietemin, kwalitatiewe PCR-gebaseerd toetse bied vinnige, sensitiewe, spesifieke en makliker opsporings en kwantifisering van sulke mutante aan. MIV-1 variante wat die K103N mutasie bevat word geassosieer met weerstand teen nevirapine (NVP) and efavirenz (EFV). Volhoudende middel-weerstandige mutasies vergaan stadig na laer vlakke en word daarom na minderheids middel weerstandige mutasies verwys. Gevolglik affekteer dit opvolgende behandeling met die middel van die relevante klas.

Doelwitte: Die doel van die studie was om twee TaqMan kwantifiserende PCR gebaseerde selektiewe polymerase ketting reaksies (SPKR), naamlik totale virale kopie SPKR en K103N-SPKR te ontwikkel. Die voormalige toets het die MIV-1 sub tipe C omgekeerde transkriptase volgorde bepaal, waar K103N die middel-weerstand variante in hierdie volgorde opspoor.

Ontwerp en Metodes: 'n Geskikte stel inleiers en peiler was ontwikkel vir die MIV-1 sub tipe C omgekeerde transkriptase (OT) vir gebruik in die K103N-spesifieke en die totaal kopie reaksie. Twaalf DNS plasmied standarde met volgorde diversiteit was saamgestel vir die toets vanaf twee MIV-1 sub tipe C monsters wat volgens ons Departement se weerstand databasis geklassifiseer is vir die besit van die K103N mutasie (AAC of AAT). Die OT streke was geamplifiseer, gekloneer en geverifieer deur volgorde bepaling. Punt-gerigte mutagenese is gebruik om 'n mutasie by die amino suur posisie 103 van sekere klone te induseer om meer standarde te genereer wat een van die drie kodons (AAA, AAC en AAT) bevat. Die twee toetse is geoptimeer en gevalideer en 'n standard kurwe is genereer vir elk van die toetse deur die gebruik van tienvoud serie verdunnings (10^7 -1 DNS kopie/ μ L) van 'n algemene K103N-mutante plasmied standard. Die geoptimeerde en gevalideerde

SPKR toets was gebruik om vir die minderheids K103N variante in 40 “nested” PKR produkte van voorheen gegenotipeerde pasiënt te soek.

Resultate: Twee sensitiewe en herproduseerbare selektiewe kwantitiewe PKR toetse met 'n ΔC_t afsnypunt van 8.23 en 'n deteksie limiet van 0.006% was ontwikkel vir die K103N weerstand variant. Die toets het 'n voorkomsyfer van 25.6 % vir die K103N weerstand mutasie in 40 pasiënt monsters bepaal, waar genotipering (populasie volgorde) 40% van hierdie variante nie opgespoor het nie.

Gevolgtrekking: 'n Sensitiewe en betroubare selektiewe kwantitatiewe PKR toets vir die opspoor en kwantifisering van die minderheids K103N variante van MIV-1 in PKR produkte was ontwikkel. Hierdie toets het 'n laer opsporings limiet van 0.01%.

Table of Contents

Declaration	2
Acknowledgements	3
Abstract	4
Opsomming	6
List of Abbreviations	12
List of Figures	16
List of Tables	18
List of Addendums	20
Chapter 1	21
1.1 Introduction	21
1.2 Literature Review	23
1.2.1 Human immunodeficiency virus type-1 (HIV-1)	23
1.2.1.1 Classification	23
1.2.1.2 Structure and Genome	23
1.2.1.3 HIV-1 life cycle	24
1.2.1.4 Genetic variability	26
1.2.2 The HIV-1 <i>pol</i>	26
1.2.2.1 Reverse transcriptase (RT)	27
1.2.2.2 Reverse transcription	30
1.2.3 Treatment of HIV-1	31
1.2.3.1 Mechanisms of inhibition of HIV-1 replication by NNRTIs	34
1.2.4 Development of HIV-1 drug resistance mutations	36
1.2.4.1 K103N and minor drug-resistant variants	38

1.2.5	Detection methods for drug-resistant mutants of HIV-1	40
1.2.5.1	Genotyping methods	40
1.2.5.2	Phenotyping methods	41
1.2.5.3	Sensitive detection methods	42
1.2.6	Real-time polymerase chain reaction (real-time PCR)	42
1.2.6.1	TaqMan® probes	43
1.2.6.2	Absolute quantification	44
1.2.6.3	Data analysis	45
1.2.6.4	Applications of real-time PCR	47
1.3	Motivation for study	48
 Chapter 2		49
2.1	Materials and Methods	49
2.1.1	Patient samples	50
2.1.2	Analysis of RT gene sequences in Los Alamos HIV database	51
2.1.2.1	Multiple alignments of the RT gene sequences from Los Alamos HIV database	51
2.1.3	Construction of plasmid-derived DNA standards to use in the SPCR assays	51
2.1.3.1	RNA Isolation from Patient samples	51
2.1.3.2	RT-PCR and PCR of the HIV-1 RT gene	51
2.1.3.3	Agarose gel electrophoresis of PCR products	54
2.1.3.4	Cloning	54
2.1.3.5	DNA sequencing	56
2.1.4	Site-directed mutagenesis	57
2.1.4.1	Mutagenic primer design	57
2.1.4.2	Mutant strand synthesis and <i>Dpn</i> I Digestion of the amplification products	58
2.1.4.3	Transformation of XL10-Gold® ultracompetent cells	59
2.1.4.4	Confirmation of the presence of the desired mutations by sequencing	60
2.1.5	Development of primers and probes for the real-time selective-polymerase chain reaction (SPCR) assay	61
2.1.6	Preparation of plasmid DNA standards/controls	63
2.1.7	General conditions and execution of real-time SPCR assay	63

2.1.8	Testing the reactivity of primers and probes for total viral copy SPCR assay	64
2.1.9	Optimization of primers for total viral copy SPCR assay	65
2.1.10	Optimization of probes for total viral copy SPCR assay	66
2.1.11	Construction of standard curve for total viral copy SPCR assay	66
2.1.12	Testing the reactivity of primers and probes for K103N-SPCR assay	66
2.1.12.1	Design of additional K103N-specific primer and its reactivity testing	67
2.1.13	Optimization of primers for K103N-SPCR assay	67
2.1.14	Optimization of probes for K103N-SPCR assay	68
2.1.15	Construction of standard curve for the K103N-SPCR assay	68
2.1.16	Evaluation of the discriminatory ability of K103N-SPCR assay	69
2.1.17	Evaluation of the accuracy of both SPCR assays	69
2.1.18	Detection of K103N minor variants in patient samples	70
2.1.18.1	Total viral copy SPCR assay on patient samples	70
2.1.18.2	K103N-SPCR assay on patient samples	70
Chapter 3		71
3.1	Results	71
3.1.1	Patient samples	71
3.1.2	Analysis of RT gene sequences in the Los Alamos HIV database	71
3.1.2.1	Multiple alignments of the RT gene sequences from Los Alamos HIV database	71
3.1.3	Construction of plasmid-derived standards for the SPCR assays	71
3.1.3.1	RT-PCR and PCR amplification of HIV-1 <i>RT</i> gene	71
3.1.3.2	Transformation using JM109 High efficiency competent cells	73
3.1.3.3	Screening for recombinant clones	73
3.1.3.4	Sequence analysis of pGEM®-T Easy plasmid clones	75
3.1.4	Site-directed mutagenesis	75
3.1.4.1	Mutagenesis of selected recombinant plasmids	75
3.1.4.2	Sequence analysis of site-directed mutagenesis-generated plasmid clones	77
3.1.5	Primers and probes used for two real-time SPCR assays	77
3.1.6	Total viral copy SPCR assay	79

3.1.6.1	The reactivity of total viral copy primers and probes	79
3.1.6.2	Total viral copy primer optimization	81
3.1.6.3	Total viral copy probe optimization	82
3.1.6.4	Standard curve for the total viral copy SPCR assay	83
3.1.7	K103N-SPCR assay	86
3.1.7.1	The reactivity of the K103N-specific primers and probes	86
3.1.7.2	New additional specific primer and its reactivity	87
3.1.7.3	K103N-specific primer optimization	90
3.1.7.4	K103N-specific probe optimization	91
3.1.7.5	Evaluation of the discriminatory ability of K103N-SPCR assay	92
3.1.7.6	Standard curve for the K103N-SPCR assay	94
3.1.8	Accuracy of both SPCR assays	97
3.1.8.1	Accuracy of the total viral copy assay	97
3.1.8.2	Accuracy of K103N-SPCR assay	99
3.1.8.3	The assay cut-off and mutation detection limit	102
3.1.9	Detection of K103N minor variants in patient samples	103
Chapter 4		109
4.1	Discussion	109
4.1.1	The study findings	106
4.1.2	Detection of HIV-1 K103N minor variants in South Africa	107
4.1.3	Detection of HIV-1 K103N minor variants globally	109
4.1.4	Quality control issues	110
4.2	Conclusion	112
References		113

List of Abbreviations

3TC	Lamivudine
°C	Degree Celsius
©	Copyright
®	Registered
α	Alpha
β	Beta
Δ	Delta
μg	Microgram
μL	Microlitre
μM	Micromolar
A	Adenine
ABC	Abacavir
AIDS	Acquired immunodeficiency syndrome
ART	Antiretroviral therapy
ARV	Antiretroviral
Asn	Asparagine
AZT	Zidovudine
BLAST	Basic Local Alignment Search Tool
bp(s)	base pair(s)
C	Cytosine
CA	Capsid
cDNA	Complementary DNA
cfu	Colony forming units
CRF(s)	Circulating recombinant form(s)
Ct	Threshold cycle
d4T	Stavudine
DDDP	DNA-dependent DNA polymerase activity
DDI	Didanosine
DLV	Delavirdine
DNA	Deoxyribonucleic acid
dNTPs	Deoxyribonucleoside triphosphates
dsDNA	Double-stranded DNA

EDTA	Ethylene diamine tetra-acetic acid
EFV	Efavirenz
ENV	Envelope protein
<i>env</i>	Envelope gene
<i>Exo 1</i>	Exonuclease 1
FDA	Food and Drug Administration
FTC	Emtricitabine
G	Guaninine
<i>gag</i>	Group antigen gene
gp	glycoprotein
HAART	Highly active antiretroviral therapy
HIV-1	Human immunodeficiency virus type 1
IAS	International AIDS Society
IN	Integrase
INV	Indinavir
IPTG	Isopropyl-beta-D-thiogalactopyranoside
kb	Kilo-base pairs
KLT	Kaletra (Liponavir/roitonavir)
L	Litre
LANL	Los Alamos National Laboratory
LB	Luria-Bertani
LTR	Long terminal repeat
Lys	Lysine
M	Molar
MA	Matrix
Met	Methionine
mg	Milligram
mL	Millilitre
mM	Millimolar
NASBA	Nucleic acid sequence-based amplification
NC	Nucleocapsid
<i>nef</i>	Negative factor gene
ng	Nanogram
nm	Nanometer

nM	Nanomolar
nt	nucleotide
NNIBP	Non-nucleoside inhibitor binding pocket
NNRTI	Non-nucleoside reverse transcriptase inhibitor
NRTI	Nucleoside reverse transcriptase inhibitor
NtRTI	Nucleotide reverse transcriptase inhibitor
NVP	Nevirapine
PBS	Primer binding site
PCR	Polymerase chain reaction
PI	Protease inhibitor
PIC	Pre-integration complex
pmol	Picomole
pMTCT	Prevention of mother-to-child transmission
<i>pol</i>	Polymerase gene
PPT	Polypurine tract
<i>pr</i>	Protease gene
RDDP	RNA-dependent DNA polymerase activity
<i>rev</i>	Regulator of viral expression gene
Rn	Normalized reporter
RNA	Ribonucleic acid
RNase H	Ribonuclease H
rpm	Revolution(s) per minute
<i>RT</i>	Reverse transcriptase gene
RTC	Reverse transcription complex
RTV	Ritonavir
sdNVP	Single-dose nevirapine
SIVgor	Gorilla simian immunodeficiency virus
SP	Signal peptide
SPCR	Selective polymerase chain reaction
SQV	Saquinavir
ssRNA	Single-stranded RNA
SU	Surface envelope protein
T	Thymine
<i>Taq</i>	<i>Thermus aquaticus</i>

TAR	Trans-activation response element
Tat	Transcriptional transactivator protein
TDF	Tenofovir
T _m	Melting temperature
™	Trade Mark
TM	Transmembrane envelope protein
TMC125	Etravirine
tRNA	transcriptional ribonucleic acid
v	Version
Val	Valine
<i>vif</i>	Viral infectivity factor gene
<i>vpr</i>	Viral protein R gene
<i>vpu</i>	Viral protein U gene
U3	Unique, 3'end
U5	Unique, 5'end
UK	United Kingdom
USA	United States of America
UV	Ultra violet
WHO	World Health Organisation
ZVD	Zidovudine
X-Gal	X-Galactosidase

List of Figures

Figure 1.1: A Schematic representation of a mature HIV-1 particle showing the major viral proteins, lipid bilayer and the RNA genome.	23
Figure 1.2: HIV-1 genome organization.	24
Figure 1.3: HIV-1 life cycle.	25
Figure 1.4: A structure of the HIV-1 RT heterodimer (p66/p51).	29
Figure 1.5: A schematic representation of reverse transcription after entry of HIV-1 RNA genome into a host cell cytoplasm.	30
Figure 1.6: A structure of HIV-1 reverse transcriptase (RT) enzyme showing the binding sites for NRTIs, NtRTIs, and NNRTIs.	35
Figure 1.7: Structure of the p66/p51 heterodimer showing the closed and opened conformation of the hydrophobic binding pocket.	35
Figure 1.8: The structure of polymerase active site of HIV-1 RT showing sites for the NNRTI-associated resistance mutations in the non-nucleoside inhibitor binding pocket (NNIBP).	38
Figure 1.9: The principle of TaqMan sequence-specific detection chemistry.	44
Figure 1.10: An amplification plot/curve showing the kinetic analysis of fluorescent changes during a real-time PCR run.	46
Figure 2.1: The schematic diagram showing the reverse transcription-polymerase chain reaction (RT-PCR) and the polymerase chain reaction (PCR) of the selected HIV-1 <i>RT</i> region which encompasses the amino acid position 103 associated with K103N resistance mutation.	52
Figure 2.2: A structure of pGEM®-T Easy vector showing its multiple restriction sites within the multiple cloning sites.	55
Figure 2.3: A schematic representation showing the positioning of primers and probe for the total copy and the K103N-specific SPCR assays on the HIV-1 HXB2.	56
Figure 3.1: A 0.8% agarose gel image of 804-bp amplicons for samples STV139166 and STV128864 after RT-PCR and nested PCR amplification.	73

- Figure 3.2:** A 0.8% agarose gel image of some of the purified pGEM®-T Easy plasmid clones. 74
- Figure 3.3:** A 0.8% agarose gel photo of the pGEM®-T Easy recombinant plasmid clones after a restriction digestion with *EcoRI*. 75
- Figure 3.4:** A multiple sequence alignment of *RT* Consensus C, consensus *RT* sequences of the four parental plasmids (pGEM® T-Easy) and all 12 mutated plasmid clones generated using Geneious version 4.5.5. 78
- Figure 3.5:** Representative amplification plots showing the amplification curves of all 12 plasmid standards for testing the reactivity of total copy primers and probes. 80
- Figure 3.6:** The average standard (std) curve for the total viral copy SPCR assay. 86
- Figure 3.7:** Representative amplification plots showing the reactivity of K103N specific primers and probes on three (3) plasmid standards. 88
- Figure 3.8:** A representative amplification plot displaying amplification curves generated with the specific forward primer C-103N.3FC for all four AAC-K103N mutant standards. 89
- Figure 3.9:** Amplification plots showing the discriminatory ability of five K103N specific primers on all 12 genetically varying standards. 93
- Figure 3.10:** A plot of standard (std) curve for the K103N-SPCR assay using average Ct values of eight runs. 97
- Figure 3.11:** A representative amplification plot for Run 2 with Ct values of the wild-type/mutant plasmid mixture experiment in the total viral copy SPCR reaction. 98
- Figure 3.12:** A representative of the accuracy of K103N-SPCR assay by comparing the three regression lines (Run 1-3) from three plasmid mixture runs with the K103N-SPCR assay standard curve using pure K103N-mutant standard. 100

List of Tables

Table 1.1: The previous and new HIV-1 treatment guidelines of HAART used in South Africa.	34
Table 2.1: Primers used in RT-PCR and Nested PCR.	53
Table 2.2: Sequencing primers used for plasmid clones.	57
Table 2.3: Site-directed mutagenesis primers used on four of the generated plasmid. clones.	58
Table 2.4: Primers and probes used for total copy and K103N-specific SPCR assays.	61
Table 2.5: Thermal cycling conditions for the real-time SPCR assays.	64
Table 2.6: Total copy reaction setup for testing the reactivity of total copy primers and probes.	65
Table 2.7: PCR master mix setup for five experiments using all three K103N specific forward primers.	67
Table 3.1: Clinical information and demographics of patient samples.	72
Table 3.2: pGEM®-T Easy plasmid clones and their codon at amino acid position 103 of HIV-1 <i>RT</i> .	76
Table 3.3: A summary of site-directed mutagenesis and the mutated plasmids generated.	77
Table 3.4: Mean threshold cycle (Ct) values after three runs of the total copy experiment for testing the reactivity of total copy primers and probes on all 12 standards at low and high DNA copy numbers.	81
Table 3.5: Mean Ct values after three runs for the titration experiment using the total copy primers on the AAC-mutant standard MS15-3 at 5×10^3 DNA copies/ μ l	82.
Table 3.6: Mean Ct values after three runs of the probe titration experiment with total copy primers (900:900 nM; forward: reverse) on the AAC-mutant standard MS15-3 at 5×10^3 000 DNA copies/ μ l.	83

Table 3.7: Threshold cycle (Ct) data for the construction of a standard curve with K103N-mutant standard MS15-3 (AAC) from eight (8) runs using total viral copy SPCR assay.	84
Table 3.8: Assay efficiency and reproducibility results for the total copy SPCR standard curve experiment after 8 runs.	85
Table 3.9: Threshold cycle (Ct) values from Experiments (Exp) 3, 4 and 5 for testing the reactivity of K103N-specific forward primers C-103NT.3F, C-103N.1F and C-103N.2F on four AAT-K103N plasmid standards at 5×10^4 DNA copy/ μ L.	89
Table 3.10: Threshold cycle (Ct) values for all K103N-mutant standards encoding AAC in the reactivity experiment using new specific forward primer C-103N.3FC.	90
Table 3.11: Mean threshold cycle (Ct) values from two primer titration experiments using two K103N specific primers individually.	91
Table 3.12: Mean threshold cycle (Ct) values from the probe titration experiments after using two K103N specific primers individually.	92
Table 3.13: Mean threshold cycle (Ct) values after assessing the discriminatory ability of a mixture of C-103N.3F and C-103NT.3FC on all 12 plasmid standards at low (5×10^3) and high (5×10^6) DNA copy numbers.	94
Table 3.14: Threshold cycle (Ct) values after eight runs for constructing K103N-SPCR standard curve using mutant standard MS15-3 (AAC).	95
Table 3.15: Efficiency and reproducibility data from standard curve experiment using K103N-SPCR assay.	96
Table 3.16: Data of the results from the wild-type/mutant plasmid mixture experiment in the total copy SPCR reaction and the K103N-SPCR reaction.	99
Table 3.17: Data of results for the wild-type/mutant plasmid mixture experiment with 10^6 -0.5 copy/ μ l of MS15-3 K103N-Mut plasmid DNA added to a background of 10^7 copy/ μ l MS10-2 K103-Wt plasmid DNA in the K103N-SPCR reaction.	101

Table 3.18: Data of results for the total copy SPCR and the K103N-SPCR assay standard curves using a common K103N-mutant MS15-3 standard to determine the ΔC_t assay cut-off.	103
Table 3.19: Data from three runs after detecting minor resistance variants of K103N in 40 patient samples using SPCR assay cut-offs of 8.23 and 10.33.	105

List of Addendums

Appendix A: Equipment, reagents and software packages used in this study are listed in Table 1-3.

Appendix B: Multiple alignments of all 2008 HIV-1 RT sequences and consensus C.

Appendix C: Multiple alignments of plasmid standards, SPCR primers and probes

Chapter 1

1.1 Introduction

South Africa has been devastated by the HIV/AIDS epidemic more than any other country with an estimate of 5.7 million people living with the human immunodeficiency virus type 1 (HIV-1) infection. At the end of 2009, the national HIV prevalence was estimated to be 17.8% among the 15-49 year olds (UNAIDS, 2010). There are 2 800 000 to 3 700 000 women and 230 000 to 320 000 children under 15 years living with the infection in South Africa (UNAIDS, 2010). The impact of the epidemic is reflected in the gradual increase of the country's morbidity and mortality rate, with 316, 559 deaths in 1997 to 607,184 deaths in 2007 (<http://www.statssa.gov.za>). A majority of the young women or antenatal clinic attendees in the 25-39 age groups is particularly dying. This group has the highest HIV prevalence 35-42%, whereas in the males the highest HIV prevalence is seen in the 30-34 age groups (South African Department of Health Study, 2009). Half of the country's orphans is attributed to HIV/AIDS related deaths, with 70% children without maternal parents. Since 2006, the premature deaths have significantly increased from 39% to 70% in 2010 (<http://www.statssa.gov.za>).

The most common antiretroviral treatment (ARV) of HIV/AIDS in the developing countries including South Africa, as recommended by World Health Organization (WHO), consists of two drugs from the NRTI class (nucleoside reverse transcriptase inhibitor) combined with one drug from the NNRTI class (non-nucleoside reverse transcriptase inhibitor) or one drug from the PI class (protease inhibitor) boosted with a small dose of ritonavir. Nevirapine (NVP) and efavirenz (EFV) are the widely prescribed NNRTIs in developing countries including South Africa. Selective pressure from these drugs causes high levels of resistance-associated mutations in the reverse transcriptase gene (*RT*) that can be transmitted and account for the majority of treatment failures (Feinberg 1997; Grant, Hecht et al. 2002; Little, Holte et al. 2002; Violin, Cozzi-Lepri et al. 2004).

Several studies using standard genotyping have revealed that NVP selects for resistant HIV-1 variants, commonly the K103N, in 15-50% of mothers who administered intrapartum single-dose nevirapine (sdNVP) (Eshleman, Mracna et al. 2001; Eshleman and Jackson 2002; Martinson, Morris et al. 2009). Genotyping is the most common method used in the developed countries to detect K103N mutations in patient samples. However, it is unable to reliably detect resistance variants comprising less than 20% of the total virus population in a sample (Grant, Kuritzkes et al. 2003; Halvas, Aldrovandi et al. 2006; Hirsch, Gunthard et al. 2008). Typically, the NVP-resistant population harbouring K103N in the plasma decreases to below the limit of detection (50 copies of HIV-1 RNA/mL) by standard genotyping after six months of stopping the treatment (Johnson, Li et al. 2005; Loubser, Balfe et al. 2006; Palmer, Boltz et al. 2006; Palmer, Boltz et al. 2006; Metzner, Giulieri et al. 2009; Saladini, Vicenti et al. 2009; Toni, Asahchop et al. 2009; Wind-Rotolo, Durand et al. 2009). These minor variants persist for a maximum period of five years in the plasma after withdrawal of the relevant drug pressure (Flys, Donnell et al. 2007). They are also found in the latent reservoirs of resting CD4 T cells (Siliciano, Kajdas et al. 2003; Bailey, Sedaghat et al. 2006; Briones, de Vicente et al. 2006; Wind-Rotolo, Durand et al. 2009). Unlike genotyping, real-time PCR-based mutation-specific assays have been shown to detect and quantify minor drug-resistant variants harbouring K103N and other resistance-associated mutations when present in a patient sample at frequencies of 20% or less than 0.1% (Metzner, Bonhoeffer et al. 2003; Halvas, Aldrovandi et al. 2006; Palmer, Boltz et al. 2006; Palmer, Boltz et al. 2006; Johnson, Li et al. 2007; Paredes, Marconi et al. 2007; Balduin, Oette et al. 2009).

This study will investigate a selective real-time PCR assay to detect minor HIV-1 resistant variants harbouring K103N that are not detected with more expensive and laborious genotyping methods.

The literature review section will focus on the classification, characteristics and life cycle of the HIV-1 with more emphasis on the RT. The section will also cover the HIV-1 treatment, mechanisms of treatment by NNRTIs and drug resistance development, the detection methods for the K103N minor/drug-resistant variants and fully describe the sensitive real-time PCR-based assays which include the selective real-time polymerase chain reaction (SPCR) assay which is developed in this study.

1.2 Literature review

1.2.1 Human Immunodeficiency Virus Type 1 (HIV-1)

1.2.1.1 Classification

HIV-1 belongs to the genus *Lentivirus*, a family of *Retroviridae*. Lentiviruses are slow viruses (*lenti-*, Latin for “slow”) which infect many species and are characterized by long-term illnesses and long incubation periods (Levy 1993). They are transmitted as a single-stranded, positive-sense, enveloped RNA virus.

1.2.1.2 Structure and Genome

HIV-1 is approximately 120 nm in diameter and roughly spherical (McGovern, Caselli et al. 2002). A diagram of the HIV-1 structure is illustrated in **Figure 1.1** and the genome organization is illustrated in **Figure 1.2**.

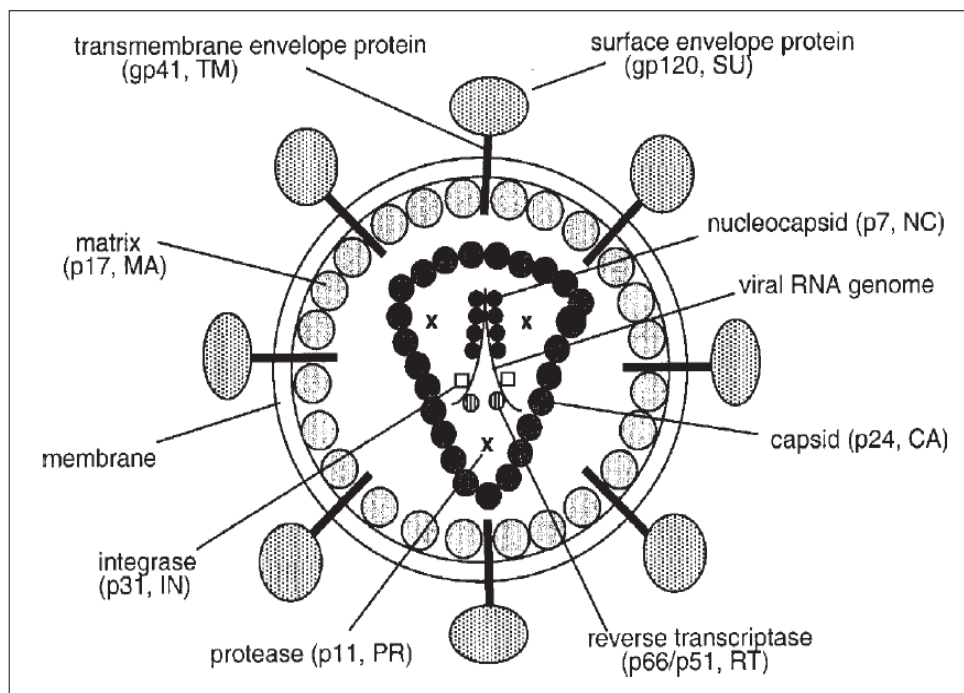


Figure 1.1: A Schematic representation of a mature HIV-1 particle showing the major viral proteins, lipid bilayer and the RNA genome (Freed, 1998).

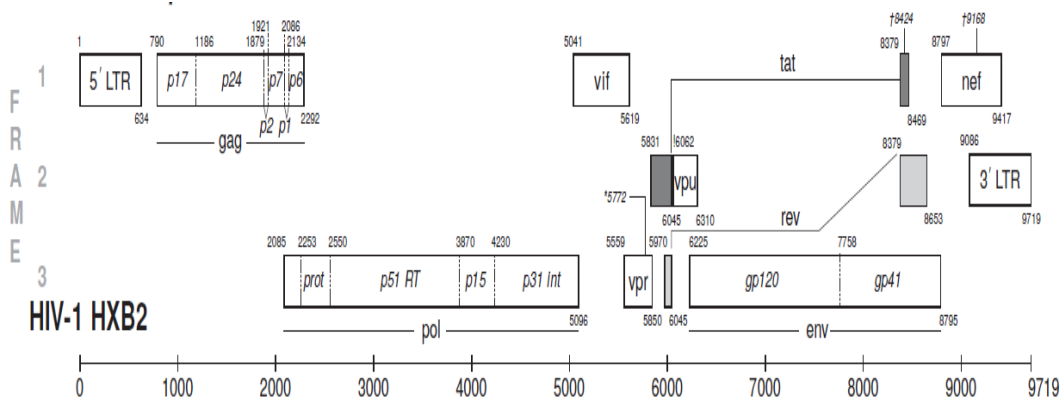


Figure 1.2: HIV-1 genome organization. Gene start and end sites are numbered according to the HXB2 (<http://www.hiv.lanl.gov/>).

All single-stranded RNA viruses contain genes that are required for viral replication and host defence evasion (Watts et al., 2009). HIV-1 RNA genome is composed of nine genes namely, *gag*, *pol*, *env*, *tat*, *rev*, *nef*, *vif*, *vpr*, and *vpu* which encode viral proteins (**Figure 1.2**) (<http://www.hiv.lanl.gov/>). The three structural genes include the *gag* (group-specific antigen) which codes for internal structural proteins, such as the matrix (MA, p17), capsid (CA, p24), nucleocapsid (NC, p7) and p6 proteins; *pol* (polymerase) for encoding protease, reverse transcriptase, ribonuclease H (RNase H) and integrase enzymes necessary for viral replication, and the *env* (envelope glycoprotein) gene which encodes a 30-amino-acid signal peptide (SP) and gp160, the precursor to gp120, an extracellular protein, and gp41, a transmembrane protein (**Figure 1.1**) (Freed 1998; Watts, Dang et al. 2009) (<http://www.hiv.lanl.gov/>). The *tat* and *rev* genes encode regulatory proteins involved in viral propagation, and transcriptional and posttranscriptional steps of virus gene expression. The *vpr*, *nef*, *vif*, and *vpu* are accessory or auxiliary genes encoding proteins that regulate the HIV-1's ability to infect cells, replication or pathogenicity (<http://www.hiv.lanl.gov/>).

1.2.1.3 The HIV-1 life cycle

HIV-1 life cycle includes a series of events which are divided into two phases, early and late, as shown in **Figure 1.3** (Freed 2001).

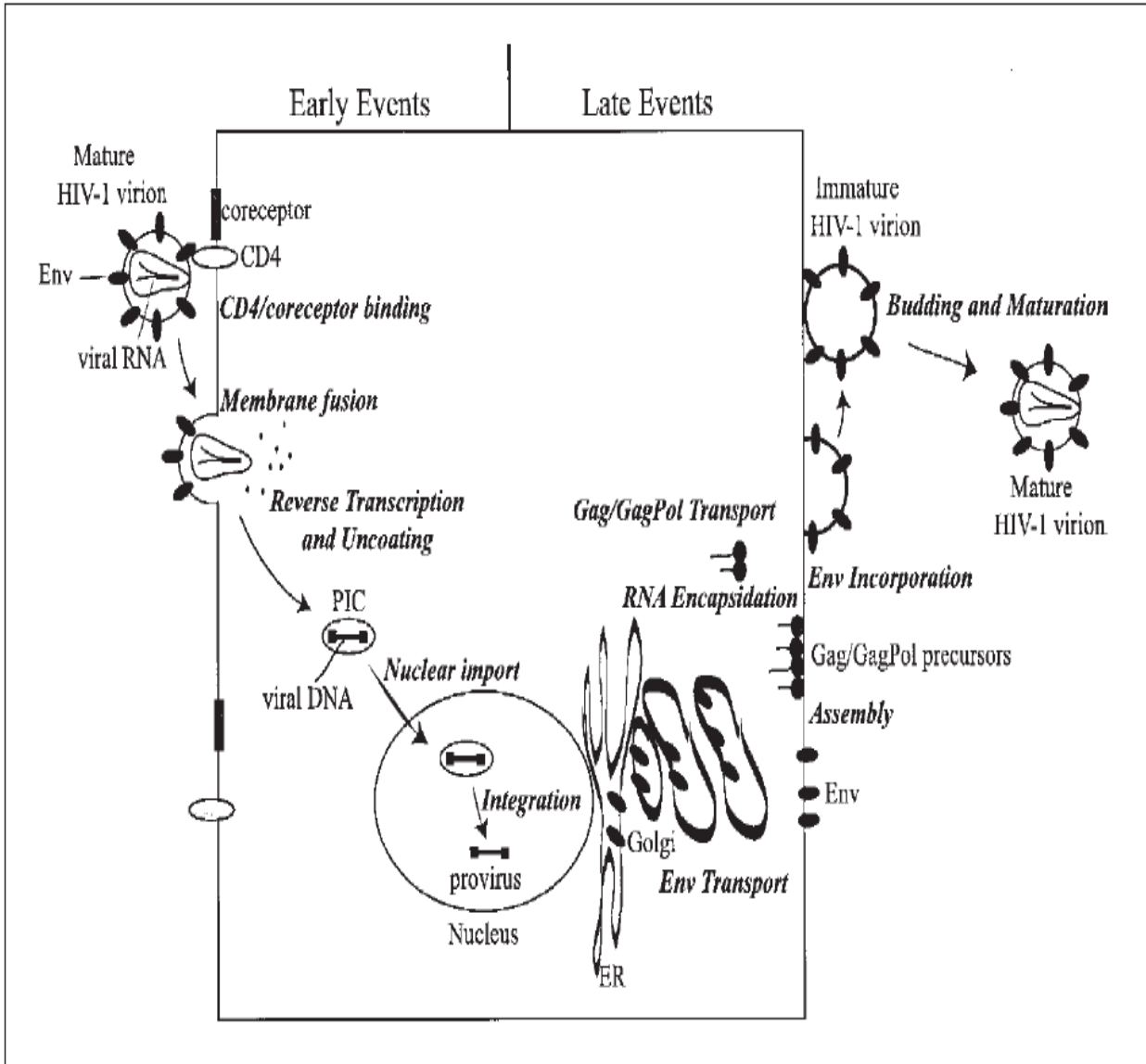


Figure 1.3: HIV-1 life cycle (Freed, 2001).

The early events includes: (1) membrane fusion a process in which the gp120 binds to target cell by interacting with CD4 receptors and co-receptors. Thereby, it causes conformational changes in the gp41 which enables it to facilitate membrane fusion between lipid bilayers of the viral envelope and host cell plasma membrane. The viral core enters the cytoplasm of the host cell through this fusion. (2) “uncoating” - is when the lipid bilayer is removed from the HIV-1 virion leaving a structure called the viral core. RT occurs and then you get assembly of the PIC (pre-integration complex). During “uncoating” event the capsid (CA) is lost whereas the viral RNA, accessory protein Vpr, MA, NC, *pol*-encoded enzyme RT and IN remain associated with the PIC. (3) Reverse transcription – whereby the viral RNA genome is converted to a

double-stranded DNA by the reverse transcriptase (RT) enzyme of the virus particle. (4) Nuclear import of the PIC associated with the viral DNA is translocated to the nucleus of the host cell (Freed 2001). Whilst inside the cell, the HIV-1 virion can either enter a latent state and the infected cell continues to function normally or actively replicate to form a large number of virus particles that are subsequently released to infect neighbouring cells (Freed 2001).

In the late stage the viral RNA is transcribed from the integrated viral genome. Furthermore it is processed to form viral messenger RNA (mRNA) and full-length viral genomic RNA. They are then transported through the nuclear pore into the cytosol and the mRNA is translated to generate viral proteins which are processed. Core particles encompassing the viral genomic RNA and proteins assemble at the host cell membrane. The immature HIV-1 virion is released by budding. Following that, it matures into an infectious virion (Frankel and Young, 1998; Freed, 2001; Miller and Bushman, 1997).

1.2.1.4 Genetic Variability

HIV-1 is divided into four groups, namely the „major’ group M, the „outlier’ group O and two new groups, N (<http://www.hiv.lanl.gov/>) and P (Plantier, Leoz et al. 2009). In general, the M group accounts for a majority of infections by HIV-1. It is divided into nine different subtypes, namely A, B, C, D, F, G, H, J and K. In addition to this, there are also circulating recombinant forms, CRF, as a result of recombination between these subtypes. Group O is found only in west-central Africa. Group N was discovered in Cameroon in 1998 (<http://www.hiv.lanl.gov/>). In 2009 group P was identified in a Cameroonian woman, and it was found to be closely related to gorilla simian immunodeficiency virus (SIVgor) (Plantier, Leoz et al. 2009). The enormous diversity of HIV-1 poses a major challenge in the development of effective drugs and vaccines (<http://www.avert.org/hiv-types.htm>).

1.2.2 The HIV-1 polymerase (*pol*) gene

The viral enzymes encoded by the *pol* gene are initially produced as a Gag-Pol polyprotein precursor, Pr160_{GagPol}, which is later cleaved by the viral PR into a Gag and a Pol polypeptide. The Gag-Pol precursor is produced by ribosomal frame-shifting during translation, which is activated by specific cis-acting RNA elements

located in the 3' end region of the Gag RNA. This event occurs in order to maintain a certain production ratio of Gag and Gag-Pol precursor (Peng, Chang et al. 1991; Parkin, Chamorro et al. 1992; Various 2008). Furthermore, the Pol is processed by viral PR to produce individual enzymes PR, RT (p51), Rnase (p15) and integrase (IN, p31) in the viral maturation step (Parkin, Chamorro et al. 1992). All of the *pol* gene products are located in the capsid of free HIV-1 virions. The PR, as mentioned above, is involved in the cleavage of Gag and Pol polypeptides into major structural proteins and enzymes required for the formation of viral particles (Birk and Sonnerborg 1998). The RT and together with RNase H, which is linked to the carboxyl-terminus of RT, are involved in viral replication, whereas the IN facilitates the incorporation of the HIV proviral DNA into the genomic DNA of an infected cell (Birk and Sonnerborg 1998).

1.2.2.1 Reverse transcriptase (RT)

Reverse transcriptase is used by retroviruses in the reverse transcription step during replication process. It is known as RNA-dependent DNA polymerase that reverse transcribes the two RNA copies of an HIV-1 virion into a single-stranded DNA (cDNA), followed by formation of a double-stranded DNA. The reverse transcriptase enzyme has no error-correction or proofreading mechanism. Therefore, it introduces mutations in every replication cycle. It has been an ideal target for antiretroviral therapy, since the early era of HIV-1 treatment strategies (Larder, Purifoy et al. 1987). HIV-1 reverse transcriptase has five enzyme activities, namely; the RNA-dependent DNA polymerase activity which copies the viral positive(+) RNA strand into a minus(-) viral complementary DNA (cDNA); the ribonuclease activity carried out by RNase H, located in the C-terminal region, which degrades the viral RNA during the synthesis of cDNA; a DNA-dependent DNA polymerase activity that copies the minus (-) cDNA strand into a (+) DNA to form a double-stranded DNA intermediate; strand transfer; and strand displacement (Menendez-Arias 2009).

A mature RT is composed of two polypeptides, p66 and p51. However, a functional RT consists of p66 only, a homodimer, or both p66 and p51 subunits called a heterodimer. The heterodimer is the predominant functional RT. The two subunits are linked by a common amino (N) terminus, with p66 consisting of 560 amino acid residues and p51 with only 440 residues (Sarafianos, Das et al. 2004). A few years

after the discovery of HIV-1, studies showed that the p66 subunit is actually exhibiting the majority of the RT activity, whereas p51 has minute or no activity (Hansen, Schulze et al. 1988; Lori, Scovassi et al. 1988; Lowe, Aitken et al. 1988; Starnes, Gao et al. 1988; Tanese, Prasad et al. 1988). According to crystallographic structures of the HIV-1 RT, p66 contains the two domains, polymerase and RNase H, whereas p51 has only the former. The active sites for both domains are found only on p66, and as for p51, it acts as a structural subunit (Huang, Zhang et al. 1998; Sarafianos, Das et al. 1999; Sarafianos, Das et al. 2004).

The polymerase domain of both subunits is further compartmentalized into four common subdomains, called, the „fingers’ (residues 1-85 and 118-155), ‘thumb’ (residues 237-318), „palm’ (residues 86-117 and 156-236), and „connection’ (residues 319-426) (Huang, Zhang et al. 1998). A structure of the HIV-1 RT heterodimer showing the polymerase subunits (p66 and p51) with its domains and subdomains is shown in **Figure 1.4**.

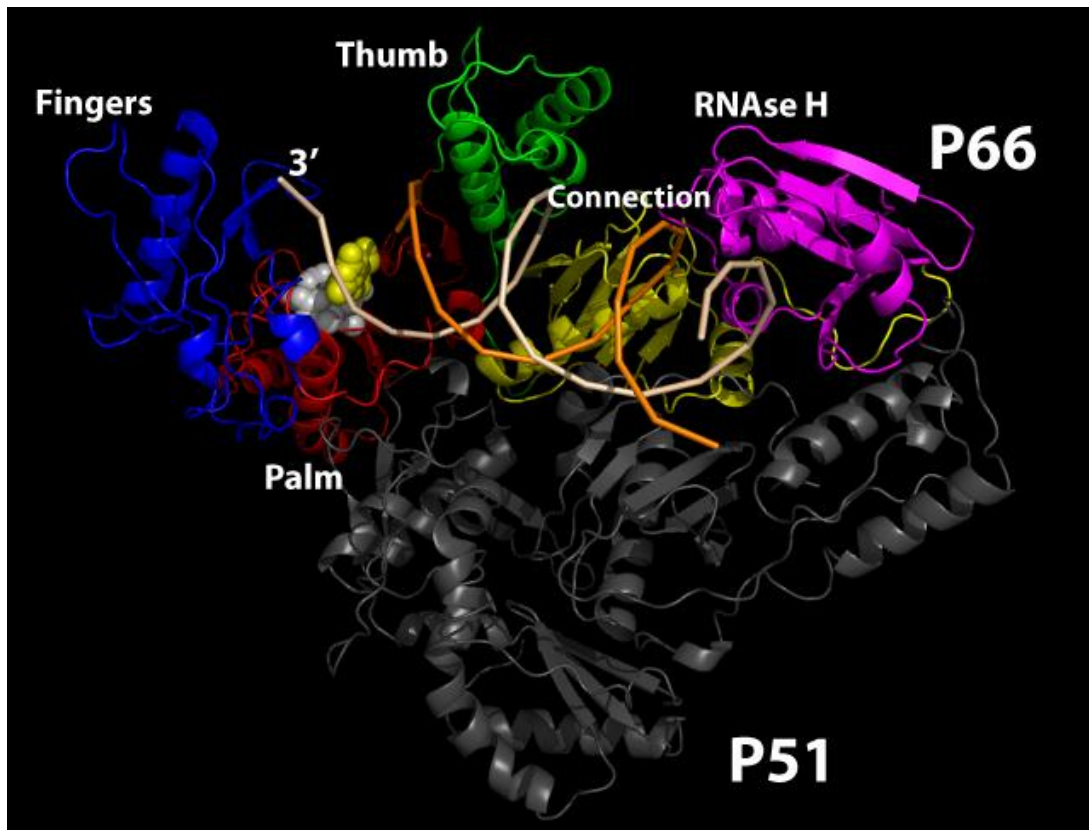


Figure 1.4: A structure of the HIV-1 RT heterodimer (p66/p51). The ribbons and coils represent the polypeptide backbones of the RT catalytic complex. The subunits p66 and p51 are indicated. P66 is associated with subdomains fingers; palm; thumb and connection, and RNase H in purple (Huang et al, 1998).

In both subunits, the individual subdomains fold similarly, except for their spatial arrangement (Huang, Zhang et al. 1998). In the p66, the polymerase active site is located in the palm. A deep template-binding cleft, which helps position the template-primer, is formed by the most conserved parts of the fingers and palm together with two helices of thumb subdomain (Freed 2001; Sarafianos, Das et al. 2004). One part of the palm acts as a DNA primer grip by positioning the primer terminus at the polymerase active site, and it also translocates the template primer after polymerization (incorporation of nucleotides) (Jacobo-Molina, Ding et al. 1993; Ding, Das et al. 1998). A proper binding or positioning is essential for the subsequent cleavage of RNA by RNase H (Sarafianos, Das et al. 2001; Julias, McWilliams et al. 2002; Julias, McWilliams et al. 2003).

1.2.2.2 Reverse Transcription

Following infection, all retroviruses including HIV-1 convert their RNA genomes into double-stranded DNA during reverse transcription, which is catalyzed by the reverse transcriptase enzyme. The process of reverse transcription is illustrated in **Figure 1.5**.

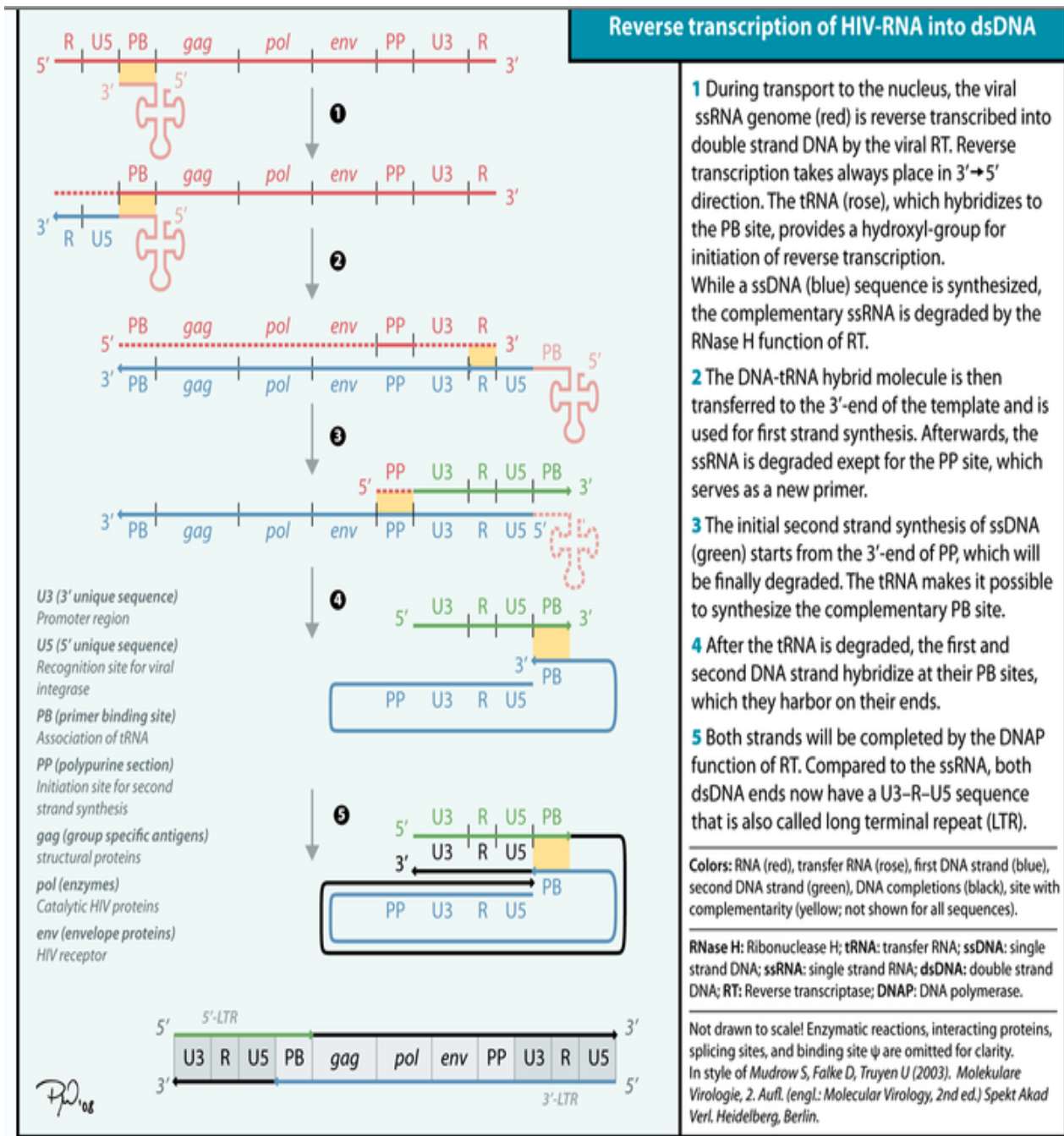


Figure 1.5: A schematic representation of reverse transcription after entry of HIV-1 RNA genome into a host cell cytoplasm (Mudrow and Falke, 2003).

Reverse transcription is initiated at the 3'-end of a cell-derived tRNA^{Lys,3} molecule that acts as a primer by binding its last 18 nucleotides to HIV-1 RNA sequence. The sequences are called the primer-binding site (PBS), and are complementary to these nucleotides. The tRNA^{Lys,3} primes the synthesis of HIV-1's single-stranded cDNA, by the RNA-primed RNA-dependent DNA polymerase activity (RDDP) of RT, upto the 5' end of the RNA genome generating a DNA-tRNA hybrid molecule. This hybrid molecule is called minus-strand strong-stop DNA. In the meantime, the RT ribonuclease H (Rnase H) activity hydrolyzes the viral RNA, allowing the transfer of the DNA-tRNA strand to the 3'-end of the template (HIV genomic RNA) to hybridize with the repeat sequence (R) (**Figure 1.5**, Step 1). Following that, the RT DNA-primed RDDP elongates the DNA strand for synthesis of the first DNA strand. Again, the Rnase H degrades the single-stranded RNA (ssRNA) but leaving only the purine-rich sequence called the polypurine tract (PPT) to serve as a primer for the second strand synthesis (**Figure 1.5**, Step 2). The second strand synthesis is initiated at the 3'-end of the HIV genomic RNA (template) by RNA-primed DNA-dependent DNA polymerase activity (DDDP) through elongation of the PPT primer. At the same time the Rnase H degrades the PPT, followed by the tRNA allowing the second strand to be transferred through interaction of the complementary PBS sequences (**Figure 1.5**, Step 3 and 4). The synthesis of both strands is then completed by the DDDP activity as well as the strand-displacement activity generating a final product carrying U3-R-U5 LTR at both dsDNA ends (**Figure 1.5**, Step 5) (Harrich, Ulich et al. 1996; Freed 2001; Mudrow and Falke 2003; Sluis-Cremer and Tachedjian 2008). Therefore, it is this product, the viral genomic DNA, that is inserted into the host cell chromosome during integration catalyzed by HIV-1 integrase enzyme (Sluis-Cremer and Tachedjian 2008).

1.2.3 Treatment of HIV-1

Since the discovery of HIV-1, 26 years ago, there are more than 20 anti-HIV drugs licensed for the treatment of HIV-1 infection. These drugs are intended to inhibit retroviral infectivity and replication. They are classified on the basis of the target with which they interact during HIV-1 replication. In these intensive efforts of anti-HIV drug research and development, the reverse transcriptase was an early target, followed

by the proteolytic enzyme, viral protease, which cleaves the viral polyprotein precursor into mature structural and functional proteins (De Clercq 2009).

Globally, the national antiretroviral therapy (ART) policy is guided by World Health Organization (WHO) to minimize HIV drug resistance (<http://www.who.int/hiv/pub/guidelines/adult/en/index.html>). In South Africa, the national antiretroviral (ARV) treatment programme started in April 2004. This treatment programme consisted of two different regimens, namely, the first line and the second line. The first-line regimen comprised stavudine (d4T), lamivudine (3TC) and efavirenz or nevirapine (NVP) with Kaletra (KLT), lopinavir boosted with ritonavir (LPV/r) for children and infants (<http://www.doh.gov.za/index.html>). The second-line regimen is used when the first-line regimen fails, and it consists of two NRTIs namely, zidovudine (AZT) and didanosine (ddI), and one PI (LPV/r). It is meant to minimize cross-resistance particularly caused by the first-line regimen (Sungkanuparph 2007). The national programme for the prevention of mother-to-child transmission (pMTCT) of HIV-1 was implemented in September 2001. The programme supplied single-dose nevirapine (SD-NVP) to women at delivery and infants at birth (<http://www.doh.gov.za/index.html>). Thus far, an estimate of 70% HIV-1 positive people (children, men and women) are benefiting from the national antiretroviral rollout program, with 90% national treatment coverage on pregnant women (UNAIDS, 2010).

The HAART strategy involving combinations of these classes (NRTI, NNRTI, PI) of drugs was implemented to combat resistance mutations. Its efficacy is more prominent in the Western countries where subtype B is prevalent (Brenner, Turner et al. 2003). In contrast to developing countries, it is because ARV treatment is mostly initiated at an acute stage on HIV infection when the CD4 cells, in which HIV is found, count is >350 cells/ μ l. Thus, the higher the CD4 count, greater are the chances of slowing down HIV replication in the body and the more effective treatment is. Additionally, an effective treatment is indicated by undetectable viral load (<50 RNA copies/ml). Subtype C accounts for the majority of this infection in South Africa (van Harmelen, Shepard et al. 2003).

In the developed countries, the antiretroviral drugs have been remarkably successful in suppressing the HIV-1 replication, even though not completely, and as a result

reduced mortality and morbidity. The suppression is not complete, but the plasma HIV-1 RNA levels are maintained below the detection limits (<50-400 copies/ml) of commercially available assays such as genotyping assay. These countries are achieving these results in large numbers unlike the developing countries because they have unlimited number of anti-HIV drugs from several classes other than the NRTIs and NNRTIs. In the developing countries the emergence of drug resistance to this limited number of drugs has been a serious hindrance to treatment successes particularly due to high replication and mutation rate of HIV (Freed 2001; De Clercq 2009). Therefore, monitoring of treatment in developing countries is essential in order to guide with a selection of effective drugs which can minimize HIV drug resistance. In South Africa the ARV treatment is monitored by CD4 counts and measuring of viral load (VL) (detection limit, <50 copies.ml) at least every six months (<http://www.doh.gov.za/docs/hiv aids-progressrep.html>). A high viral load signals ARV failure which may be due to the presence of drug resistant HIV, lack of adherence or poor drug interactions. An increasing viral load is followed by a decreasing CD4 count and a subsequent development of HIV-related opportunistic infections such as pulmonary TB, severe fungal and bacterial infection (WHO, 2006). This stage of the infection is referred to as AIDS.

South Africa has launched the new guideline on the 1st of April 2010. The previous (2004-2010) and new treatment guidelines are shown in **Table 1.1**.

Table 1.1: The previous and new HIV-1 treatment guidelines of HAART used in South Africa.

Regimen	Drugs		Age group
	Previous Guideline	New Guideline	
1	d4T+3TC+EFV	TDF+3TC/FTC+EFV/NVP d4T+3TC+EFV AZT+3TC+LPV/NVP	Adults
	d4T+3TC+Lopinavir/r	ABC+3TC+LPV/r ABC+3TC+EFV	< 3 year-olds
	d4T+3TC+NVP	sdNVP+AZT (during labour) TDF+FTC (after delivery)	Mothers/pregnant women
2	AZT+ddI+Lopinavir/r	TDF+3TC/FTC+LPV/r AZT+3TC+LPV/r	Adults
	AZT+ddI+NVP	AZT+ddI+LPV/r ABC+3TC+LPV/r	< 3 year-olds

3TC – Lamivudine; ABC - Abacavir; AZT – Zidovudine; d4T – Stavudine; ddI – Didanosine; EFV – Efavirenz; FTC - Emtricitabine; Lopinavir/r – Lopinavir boosted with Ritonavir; NVP – Nevirapine; TDF – Tenofovir.

1.2.3.1 Mechanisms of inhibition of HIV-1 replication by NNRTIs

The major role of the NNRTIs is to block HIV-1 replication by binding to the binding pocket, in the palm of p66, distal to the active site of the RT. Thereby it interferes with the precise positioning of the 3'-end of the template-primer and the incoming nucleotide. Following binding to the p66, an NNRTI breaks the hydrogen bond between Lys103 and Tyr188 side chains to form a hydrophobic binding pocket close to the template-primer binding site. This pocket is made up of Pro95, Leu101, Lys103, Val179, and Tyr181 of p66 (**Figure 1.6** and **Figure 1.7**) (Rodriguez-Barrios and Gago 2004).

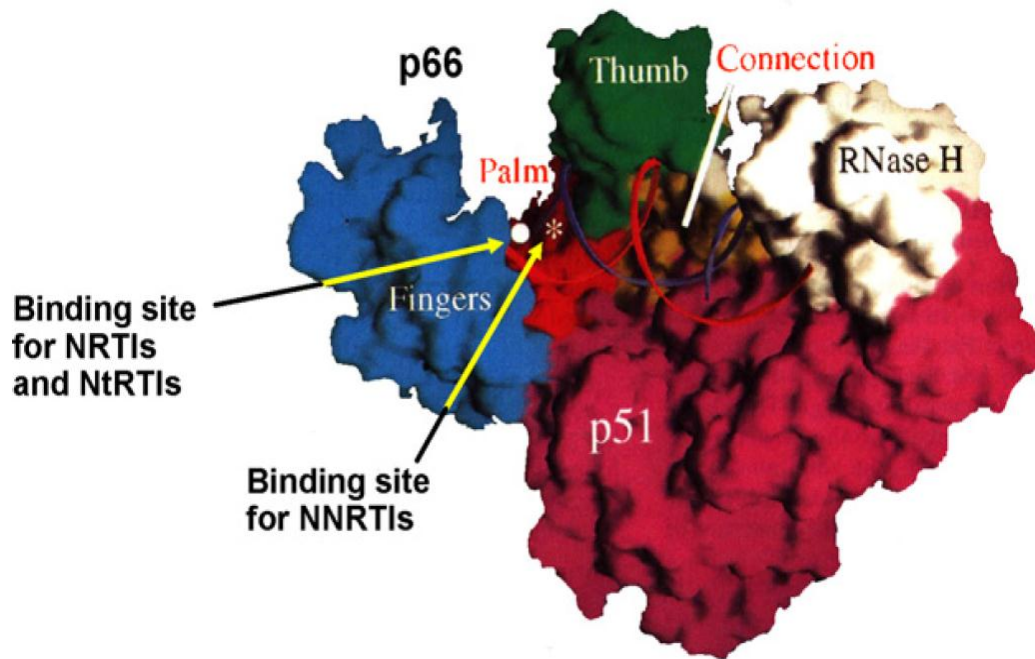


Figure 1.6: A structure of HIV-1 reverse transcriptase (RT) enzyme showing the binding sites for NRTIs, NtRTIs, and NNRTIs (De Clercq, 2009).

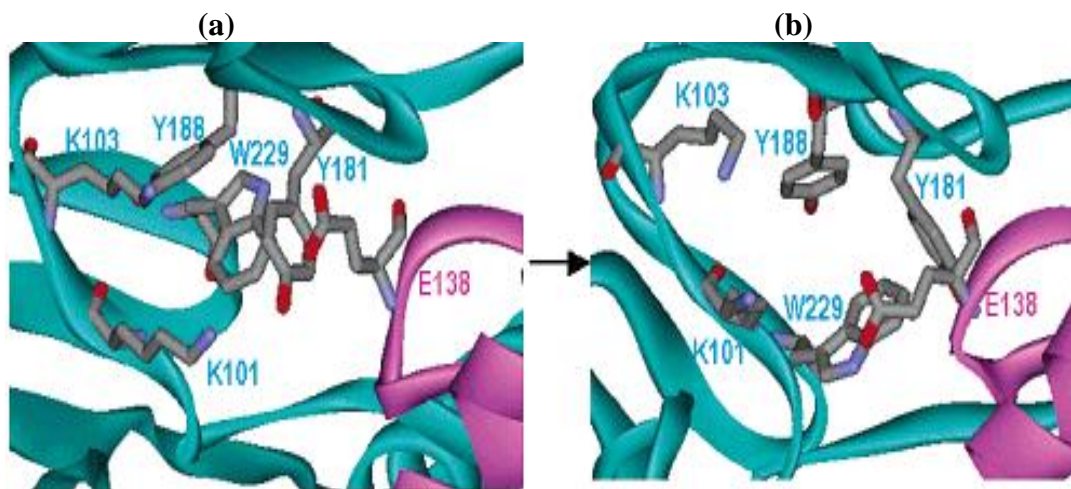


Figure 1.7: Structure of the p66/p51 heterodimer showing the closed and opened conformation of the hydrophobic binding pocket. (a) The p66 and p51 subunit showing a closed state of the conformation of a hydrophobic binding pocket. (b) Shows an open conformation (Rodriguez-Barrios and Gago, 2004).

1.2.4 Development of HIV-1 drug resistance mutations

The current recommended antiretroviral drug combinations completely suppress the HIV-1 replication in patients. Nevertheless, a rapid turnover ($\sim 10^9$ viral particles per day) of virions carrying resistance-associated mutations (viral quasispecies) facilitated by selection pressure from antiretroviral drugs, natural occurring diversity, or transmission of drug resistance reduce their efficacy (Bergroth, Sonnerborg et al. 2005; Couto-Fernandez, Silva-de-Jesus et al. 2005; Metzner, Rauch et al. 2005; Johnson, Li et al. 2008; Bergroth, Ekici et al. 2009; Menendez-Arias 2009). In addition to its high recombination frequency, HIV-1 produces about 10^{-4} to 10^{-5} mutations per nucleotide in every replication cycle in every infected individual. These mutations develop in the viral genes coding for structural proteins that are targeted by the current drugs and are involved in the binding or the activity of the antiretroviral drugs. As a result of these, the majority of HIV-infected patients fail therapy and they have to switch from one treatment regimen to the other (Menendez-Arias 2009).

Development of inhibitor-specific mutations is the substitutions of amino acids as a result of specific nucleotide changes, which could be in the HIV-1 proteins such as the reverse transcriptase, protease, envelope or integrase. They are known as NRTI resistance mutations, NRTI multi-drug resistance mutations, NNRTI resistance mutations, protease resistance mutations, integrase resistance mutations and entry resistance mutations. The amino acids are the residues in the active site regions on the inhibitors. Majority of licensed antiretroviral drugs, the nucleoside inhibitors (NRTIs), nucleotide inhibitors (NtRTIs) and the non-nucleoside inhibitors (NNRTIs), are targeting the DNA polymerase activity of the HIV-1 RT. Mutation(s) in the viral RT make it impossible for the enzyme to bind these RT inhibitors (e.g. lamivudine, 3TC and emtricitabine, FTC), conferring either high-, (M184V), or low-level of resistance to specific ARV drug(s), subsequently decreasing the viral fitness or replication capacity (Sarafianos, Das et al. 1999; Gao, Boyer et al. 2000; Menendez-Arias, Martinez et al. 2003; Menendez-Arias 2009). In contrast, other compensatory mutations, such as K103N (NNRTI resistance mutation), counteract these effects, thus enhancing the viral replication capacity (Menendez-Arias, Martinez et al. 2003). Other resistance-associated mutations in the RT influence the nucleotide discriminatory ability of RT from differentiating between the normal substrate, dNTP

with 3'-OH, and nucleoside analogue inhibitors which do not harbor the 3'-OH (Menendez-Arias 2009).

Understanding the molecular mechanisms whereby mutations give rise to drug resistance will help with the design of effective novel drugs and the selection of suitable drug combinations that are able to combat a large spectrum of HIV-1 mutated variants (Das, Sarafianos et al. 2007; Ren and Stammers 2008). Structural studies using X-ray crystallography are helping in this regard to reveal the effects of these mutations on the drug-binding sites, for example NNIBP (size, shape, and chemical environment) in NNRTIs, and the adaptability of potent inhibitors (Das, Sarafianos et al. 2007). The NNRTI class, which encompasses a wide range of chemically diverse compounds, gives rise to a different spectrum of resistance mutations which include the loss of important interactions such as the hydrophobic, electrostatic, stacking, or van der Waal, in binding the drug(s) to viral RT (Menendez-Arias 2009). Therefore, there are differences in the conformation of the drug-binding pocket depending on a compound. Common observed NNRTI resistant mutations in both clinical trials and therapeutic use include Leu100Ile (L100I), Lys103Asn (K103N), Val106Ala/Met (V106A/M), Val108Ile (V108I), Tyr181Cys/Ile (Y181C/I), Tyr188Cys/Leu/His (Y188C/L/H), Gly190Ser/Ala (G190S/A), or Pro225His (P225H), or combinations. The positions associated with these mutations in the polymerase active site of HIV-1 RT are shown in **Figure 1.8** (<http://hivdb.stanford.edu>).

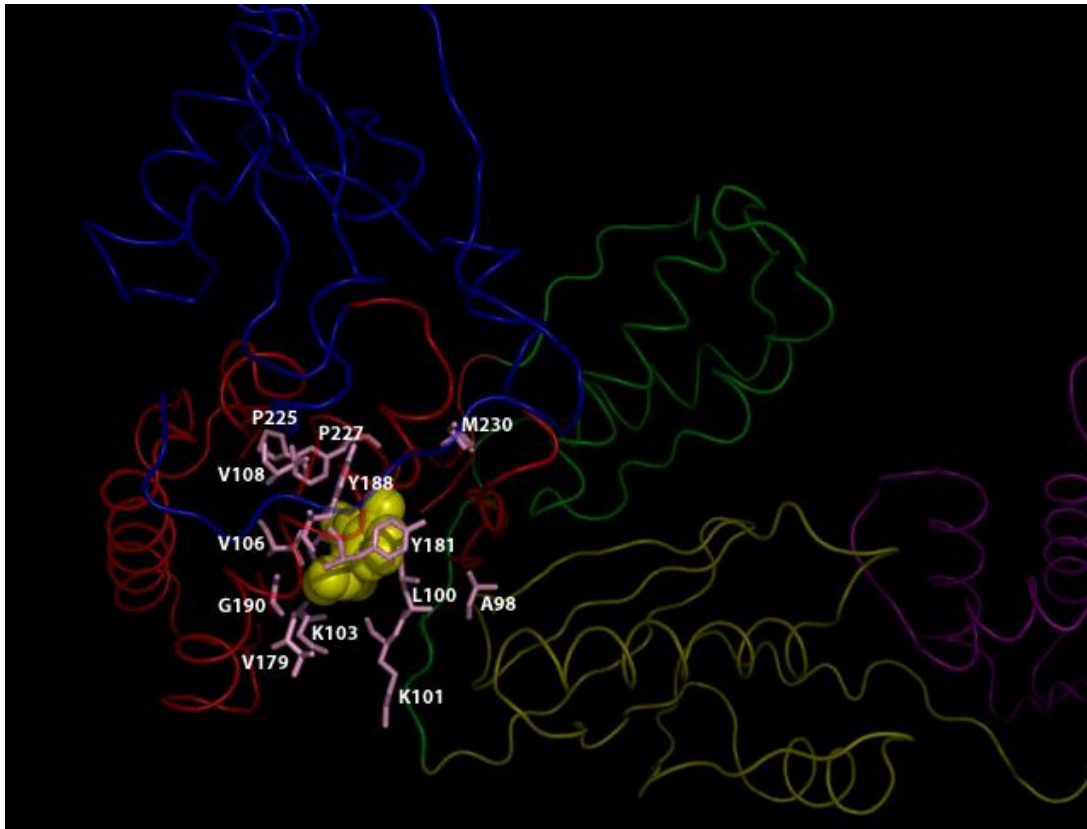


Figure 1.8: The structure of polymerase active site of HIV-1 RT showing sites for the NNRTI-associated resistance mutations in the non-nucleoside inhibitor binding pocket (NNIBP). The subdomains palm; thumb; fingers and connection are also shown. The solid molecule-like structure is nevirapine bound to the NNIBP (<http://hivdb.stanford.edu>).

1.2.4.1 K103N and Minor Drug-Resistant Variants

K103N is the most frequent and studied NNRTI mutation in patients treated with nevirapine (a first generation compound) or efavirenz (a second generation compound), (Ren, Milton et al. 2000; Das, Sarafianos et al. 2007; Johnson, Brun-Vezinet et al. 2008). It confers a high-level of resistance to these drugs, as well as a cross-resistance to all NNRTIs at varying levels, thus resulting in treatment failure. The mutation is caused by a single base substitution in the lysine residue at codon 103 (Lys103) of the RT gene, situated at the outer edge of the NNRTI binding pocket (NNIBP) (Hsiou, Ding et al. 2001; Rodriguez-Barrios, Perez et al. 2001). The substitution is a change of the adenine (A), third base in this codon (AAA), to either cytosine (C) or thymidine (T) (AAA to AAC/T).

The primary mechanism of resistance by K103N mutation in the HIV-1 RT involves a greater stabilization of the closed conformation (unliganded) of RT, unlike in the wildtype RT, which create an energy barrier to binding NNRTIs thereby reducing the binding potency. The loss of interactions between RT and inhibitor is challenging in terms of drug development, as this affects inhibitor entry from many chemically diverse compounds of the NNRTI class. This stronger stabilization involves additional hydrogen bonds between Asn103 and Tyr188 side chains, with extra interactions of two neighbouring water molecules (Hsiou, Ding et al. 2001). In addition, an alternative resistance mechanism by K103N involves the coordination of sodium ion (significant quantity of sodium ions in the host cells) with both side chains, thus inhibiting the binding of an NNRTI (Das, Sarafianos et al. 2007). However the newer second generation of NNRTI drugs are able to break this stronger hydrogen bond at the expense of more energy, e.g., TMC125 (etravirine) and TMC278 (not yet licensed) (Rodriguez-Barrios and Gago 2004).

The absence of drug-associated selection pressure causes the drug-resistant viruses to decline with time after discontinuation of the relevant drug(s), and these small populations of viruses are known as minor drug-resistant variants (Johnson, Li et al. 2008). According to genotypic assays for testing resistance, minor drug resistant variants is a population comprising less than 20-25% of the total virus in a patient (Bergroth, Sonnerborg et al. 2005; Balduin, Oette et al. 2009). Single-dose NVP for PMTCT is a proper example for suboptimal regimen that allows a selection of drug-resistant strains, and commonly carrying the prevalent K103N, which decline with time since the treatment is temporary. In addition to that, NVP has a long half-life meaning it remains longer in the blood even after its termination. Therefore, it continues to promote the generation of more K103N variants. Moreover, the K103N slightly reduces the viral replication capacity, to prevent the wildtypes from dominating them completely when NVP and EFV are discontinued. However, they may replicate at low copy number or rate (Balduin, Oette et al. 2009). When a treatment with either or both of these drugs is resumed, the K103N variants dominate the viral population, and are then called the majority population. With the use of highly sensitive detection methods, higher prevalence of K103N minor populations has been observed relative to major populations (Metzner, Rauch et al. 2005; Balduin, Oette et al. 2009). The emergence of K103N mutation is a major problem especially

in the developing countries where NVP is widely used and a majority of the world's HIV-1 infected individuals reside. Although NVP is used in such countries in babies and mothers for PMTCT, there was no significant difference observed in terms of K103N prevalence among men and women (Balduin, Oette et al. 2009). This is due to transmission, which clearly explains the high prevalence of K103N minorities. And minor populations of drug-resistance variants have been detected in the early phase of therapy failure (Grant, Hecht et al. 2002; Little, Holte et al. 2002; Violin, Cozzi-Lepri et al. 2004; Metzner, Rauch et al. 2005).

1.2.5 Detection methods for drug-resistant mutants of HIV-1

With the widespread use of anti-HIV drugs in many parts of the world and rapid emergence of drug resistance mutations, transmission of drug-resistant HIV-1 is becoming more common. Drug resistance is a major health concern globally, considering that only one mutation is required to make HIV-1 fully resistant to lamivudine (3TC), efavirenz or nevirapine; and that a single pattern of mutations causes cross-resistance to one class of drugs. In the developed countries, drug resistance testing is now considered the standard-of-care in the management of anti-HIV treatment failure for optimizing treatment therapy in individuals. Currently, the testing is recommended when a person has just been diagnosed with HIV, when a patient is about to start anti-HIV treatment for the first time, in women who are pregnant, and children (www.aidsmap.com). HIV Genotyping and phenotyping drug resistance tests are the two main methods for the management of antiretroviral therapy, which have contributed much knowledge regarding HIV-1 resistance patterns (Hirsch, Brun-Vezinet et al. 2000).

1.2.5.1 Genotyping methods

Genotyping is based on DNA sequencing that detects specific mutations in the HIV genes that are linked with resistance to anti-HIV drugs by using commercial assay kits or in-house (home-brew) techniques (Hirsch, Brun-Vezinet et al. 2003). Commercial assay kits and in-house techniques showed a high concordance in blinded, multicenter comparison for quality assurance of genotyping, with TRUGENE (Bayer, Tarrytown, New York, USA) as the most sensitive, followed by ViroSeq (Celera Diagnostics ViroSeq™ HIV-1 Genotyping System), then in-house assays (Hirsch, Gunthard et al.

2008). Commercial assay kits used for genotyping are ViroSeq and TRUGENE, which come with amplification and sequencing primers, and genotyping software. For the in-house assays amplification and sequencing primers are custom-designed. Genotyping (direct sequencing or sequencing of clones) is the most preferred as it is used widely in developed countries to provide resistance mutation profiles for reverse-transcriptase inhibitors, protease inhibitors, entry inhibitors and integrase inhibitors. It has a faster turn-around time, and is less complex in contrast with phenotyping (Vercauteren and Vandamme 2006). However, it cannot detect mutants that comprise less than 20% of the virus population.

A major challenge lies in the interpretation of reports for genotyping since they lack consensus, mainly due to the HIV-1 diversity and the large number of drug-resistant mutations (Daar 2007; Shafer, Rhee et al. 2008). Sequencing technologies used (ViroSeq, TRUGENE or in-house techniques) are not accountable for the level of variation encountered between laboratories, but rather laboratory-related. This implies laboratories must perform accurate genotyping with appropriately trained operators, certification, and where periodic proficiency testing is done. Resistance testing laboratories are therefore advised to take part in quality assurance programs (Schuurman, Brambilla et al. 2002; Hirsch, Brun-Vezinet et al. 2003; Hirsch, Gunthard et al. 2008).

Other problems with genotyping are that amplification of specimens with <500-1000 HIV-1 RNA copies/mL, and testing of other subtypes other than B, because majority of genotypic algorithms are built based on data from subtype B viruses (Hirsch, Gunthard et al. 2008). Algorithms differ in their interpretation of the expected drug activity (Ross, Boulme et al. 2005; Ross, Boulme et al. 2005).

1.2.5.2 Phenotyping methods

Phenotyping method is a cell culture-based assay that measures the concentration of a drug required to reduce replication of the virus (Hirsch, Gunthard et al. 2008). Virtual phenotyping uses genotypic algorithms to interpret drug resistance, in which a genotypic data for plasma HIV-1 RNA of a candidate gene is compared to a large database comprising paired phenotypes and genotypes (Bachelier, Jeffrey et al. 2001; Beerenwinkel, Daumer et al. 2003; Mazzotta, Lo Caputo et al. 2003; Perez-Elias, Garcia-Arota et al. 2003). This linkage then assigns the generated “virtual phenotype”

fold-changes in drug susceptibility. The main limitation to Virtual phenotyping is the predictive power which is determined by the number of matched datasets available. The matches are derived from pre-selected codons, not from the whole nucleotide sequence (Hirsch, Gunthard et al. 2008).

1.2.5.3 Sensitive detection methods

The era of relying on *in vitro* cell culture for routine laboratory diagnosis of virus infections is over. Currently, molecular methods are preferred for the detection and characterization the most common and frequent etiological agents in humans. According to a blinded, multicenter comparison of ten methods for the detection of K103N minor drug-resistant variants, two out of three real-time PCR-based assays called allele-specific RT-PCR (ASPCR) assays, and the Ty1/HIV-1 RT hybrid system (TyHRT) were the most sensitive (Metzner, Bonhoeffer et al. 2003; Nissley, Halvas et al. 2005; Halvas, Aldrovandi et al. 2006; Palmer, Boltz et al. 2006). One of the ASPCR assays quantified mutant down to 0.1%, and the other one quantified down to 0.4% (Metzner, Bonhoeffer et al. 2003; Nissley, Halvas et al. 2005; Palmer, Boltz et al. 2006). The third ASPCR assay was less sensitive, which could be due to differences in primer design or the number of samples analyzed (Kutyavin, Afonina et al. 2000). TyHRT was the second most sensitive method as it quantified K103N mutant down to 0.4% (Nissley, Halvas et al. 2005; Halvas, Aldrovandi et al. 2006). TyHRT is a phenotypic assay that assesses drug susceptibility by determining the effects of reverse transcriptase inhibitors on hybrid elements derived from the *Saccharomyces cerevisiae* Ty1 retrotransposon carrying reverse transcriptase derived from HIV-1 RT (Nissley, Halvas et al. 2005).

1.2.6 Real-time polymerase chain reaction (Real-time PCR)

Real-time PCR is a quantitative PCR (qPCR) which is characterized by the ability to detect and quantify specific nucleic acid sequences, and determine sequence variations (Houghton and Cockerill III 2006). Addition of sequence detection chemistry to PCR technology enabled the detection of amplicon as it accumulates in “real” time, during each PCR amplification cycle (Higuchi, Fockler et al. 1993; Bustin and Mueller 2005; Houghton and Cockerill III 2006). During amplification the amount of fluorescence emitted by the PCR chemistry is proportional to the increasing PCR product. In the conventional PCR the results or the accumulated PCR

products are analyzed at the end of PCR amplification (www.appliedbiosystems.com). Real-time PCR was developed in the mid 1990s (Walker 2002), whereas the PCR technology (conventional) was discovered in 1983 by Kary Mullis (Saiki, Scharf et al. 1985).

1.2.6.1 TaqMan[®] probes

Most studies find the TaqMan[®] chemistry to be more sensitive and specific for detection in real-time PCR, hence, accuracy is of higher importance in real-time quantification PCR. Introduction of fluorogenic-labeled probes that employ the 5' nuclease activity of the *Taq* DNA polymerase improved the real-time PCR. Such probes enabled the detection of only specific PCR products. A detection probe binds complementarily with a gene of interest to confirm the specific identification of a target gene (Mackay, Arden et al. 2002; Watzinger, Ebner et al. 2006). TaqMan regular hydrolysis and TaqMan-MGB (modified hydrolysis probes) are better suited for variable nucleotide sequences between pathogen strains, rather than hybridization probes. TaqMan probes are either fluorogenic or non-fluorogenic. The fluorogenic probes have a fluorescent quencher dyes such as TAMRA, black-hole quencher (BHQ) or QSY-7 at the 3' end and a fluorescent reporter dye called FAM at the 5' end. Non-fluoregenic probes, which are called the MGB (minor groove binder), are without any dye at the 3' end, but are labelled with a fluorescent reporter dye called FAM at the 5' end (Applied Biosystems Chemistry Guide, Part #4348358 Rev. E). The TaqMan-MGB probes are more advantageous as they have minor groove binding molecules attached at the end of the probe to enhance the binding of DNA, and they have shorter oligonucleotide sequences (Whiley and Sloots 2006). A demonstration of how the TaqMan sequence detection using fluorescent probes works in real-time PCR is illustrated in **Figure 1.9**.

It is described by the following steps: (1) Polymerization - a probe is intact with the reporter dye molecule (R) and the quencher dye (Q) attached to the 5' and 3' ends; (2) Strand displacement - the quencher significantly reduces the fluorescence emitted by the reporter dye through a non-irradiative process of fluorescence resonance energy transfer (FRET); (3) Cleavage - once the target sequence is present in a reaction, the probe anneals downstream from one of the primer sites and is cleaved by the 5' nuclease activity of Taq DNA polymerase during every extension cycle. This separates the reporter dye from the quencher; (4) Polymerization completed - as the

primer extension continues to the end of the template strand, the probe is removed from the target strand, thus allowing the reporter dye to emit a detectable fluorescence signal (www.appliedbiosystems.com). FRET is a process in which the fluorescent energy is transferred between permissive molecules which have emission and absorption spectra that overlap, and they are situated 10-100 Å apart (Stryer and Haugland 1967)

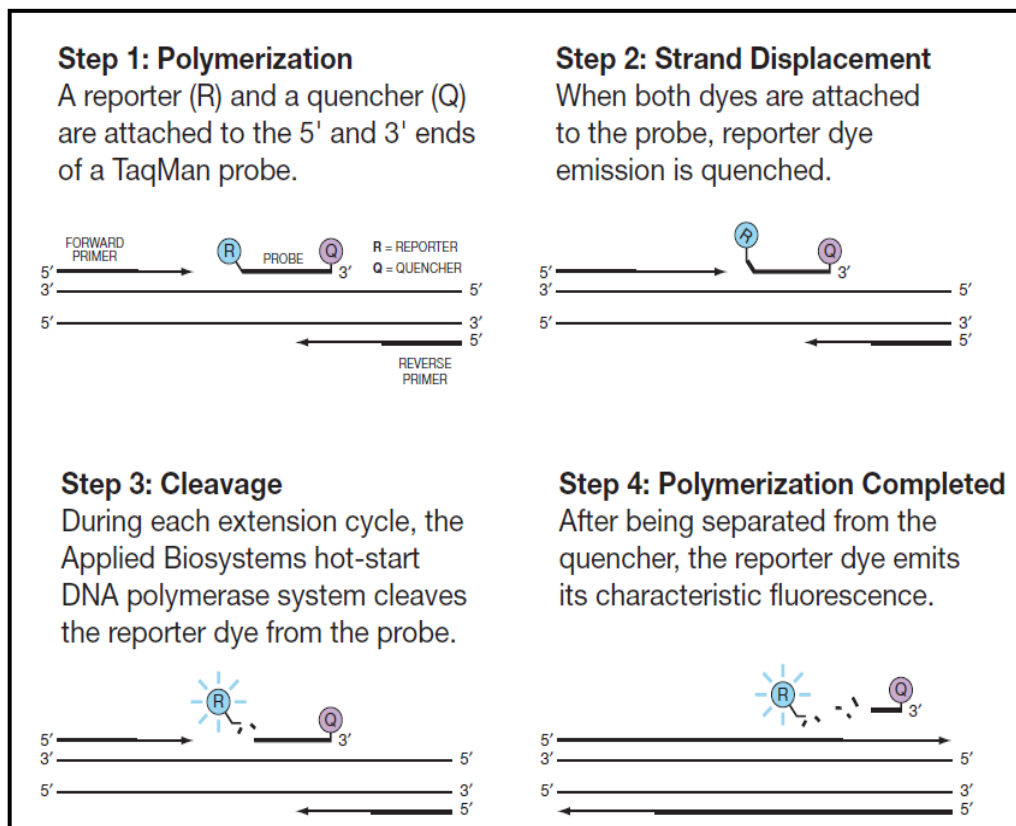


Figure 1.9: The principle of TaqMan sequence-specific detection chemistry. (www.appliedbiosystems.com).

1.2.6.2 Absolute quantification

Types of real-time PCR assays include the relative quantification which uses the comparative Ct (threshold cycle) method, allelic discrimination, plus/minus and the absolute quantification which uses a standard curve (www.appliedbiosystems.com). The latter assay type will be employed in this study. In absolute quantification, a nucleic acid standard curve of the gene of interest is required to determine or calculate

the absolute quantity (number of copies) of a specific nucleic acid target sequence in an unknown sample (VanGuilder, Vrana et al. 2008) (www.appliedbiosystems.com). It is used to quantify the exact viral copy number of the target nucleic acid (RNA or DNA) which are then associated with the stage of a disease. The absolute quantity (concentration) of the standard, a sample with known concentration used to construct a standard curve, must be determined by some independent means. Standards for real-time PCR assays are often quantified by direct measurement of nucleic acid concentration. These could be either plasmid DNA or in vitro transcribed RNA. In the case of HIV-1, the concentration of the complimentary DNA (cDNA) of HIV-1 RNA or the RNA itself is commonly quantified spectrophotometrically at 280 nm (Palmer, Wiegand et al. 2003).

The samples with valid concentration values in terms of the A260/A280 ratio for their UV absorbance at wavelengths of 260 nm and 280 are then diluted by accurate volumetric means to the final concentration series for the set of standards. When this ratio is greater than 1.8, it is indicative of the purity of the samples. The commonly used instrument for spectrophotometric measurements is the NanoDrop® spectrophotometer (NanoDrop Technologies, Wilmington, DE). It can measure concentrations ranging from 2 to 3700 ng/µl with the highest accuracy, requiring only a microliter of the sample to be loaded to an instrument's detector. By using the molecular weight of the DNA or RNA, the measured concentration is then converted to the copy numbers. DNA can be used as a standard for absolute quantification of RNA. The achieved dilution series of standards is run in a real-time PCR assay parallel with the test or unknown specimens, thereby generating the standard curve from which the concentrations of the target specimens will be extrapolated (<http://www.appliedbiosystems.com>).

1.2.6.3 Data analysis

The sequence detection system (SDS) software and the real-time PCR instrumentation acquire fluorescence data as amplicon accumulates (www.appliedbiosystems.com). Data are usually collected only once per PCR cycle at the same temperature (Wittwer, Herrmann et al. 1997). In that case, it is best collected during the extension of primers to make new PCR product (Reynisson, Josefsen et al. 2006). The fluorescence detected over a number of PCR cycles performed is then presented graphically in an

amplification plot that can be displayed in a linear or logarithmic (**Figure 1.10**) form. Baseline, threshold and C_t value are the three important parameters that determine the accuracy and reproducibility of real-time quantitative PCR assays (<http://www.appliedbiosystems.com>).

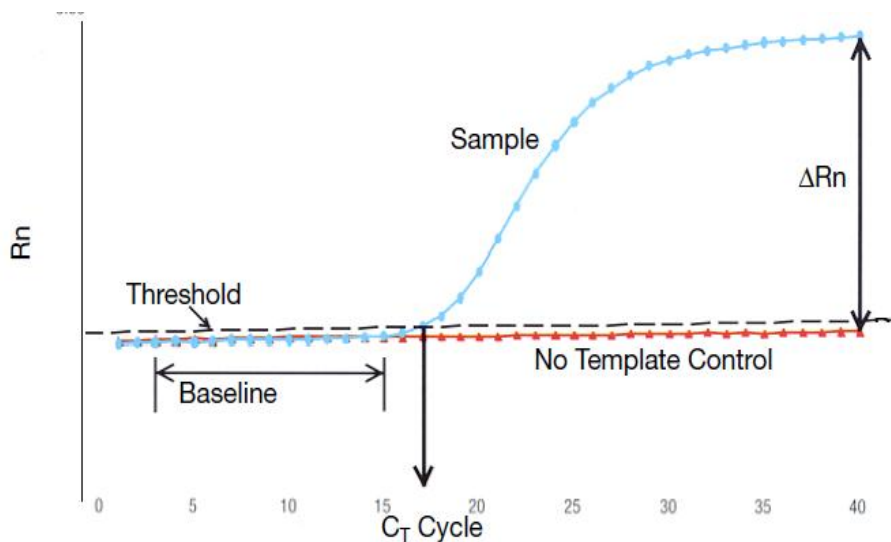


Figure 1.10: An amplification plot/curve showing the kinetic analysis of fluorescent changes during a real-time PCR run. (www.appliedbiosystems.com).

Baseline is the little change in fluorescence signal in the first few cycles performed. The sequence detection software generates an amplification curve by subtracting a normalized reporter (R_n) from the baseline, which is ΔR_n ($\Delta R_n = R_n - \text{baseline}$). The dots on the amplification curve represent an increase in fluorescence above the baseline, which is directly proportional to the amount of PCR product produced. ΔR_n is the amount of fluorescence signal generated by the set of PCR conditions used. Normalizer reporter is the ratio of the fluorescence emission intensity of the reporter dye to the fluorescence emission intensity of the passive reference dye. Then, algorithm finds the point on the amplification plot at which the ΔR_n value crosses the threshold. Threshold is the line whose intersection with the amplification plot defines a threshold cycle (C_t). Threshold cycle is the fractional cycle number at which the fluorescence emission passes the background threshold (www.appliedbiosystems.com). The higher the starting copy number of a target nucleic acid, the smaller the threshold cycle (Bustin and Mueller 2005).

Data acquisition at the end of the amplification reaction (plateau phase) poses problems because amplicon accumulation is more likely to be influenced by PCR inhibitors, poor reaction conditions, or excess amplicon. Moreover, there is no precise relationship between the initial template and the final amplicon at the end-point (Mackay 2007).

1.2.6.4 Applications of real-time PCR

Real-time PCR is being used increasingly in novel clinical diagnostic assays and research applications as the state-of-the-art technology for doing detection (diagnosis of hereditary and infectious diseases), characterization (genotyping) and quantification (microbial load) experiments of microbial nucleic acids (Mackay 2004; Bustin and Mueller 2005). The use of real-time PCR as a method for the quantitative detection (real-time quantification PCR) of DNA and RNA viruses is becoming increasingly prominent. The efficacy of antiretroviral therapeutic regimens on the viral reservoirs in HIV-1 patients is increasingly being evaluated through the quantification of the HIV-1 proviral DNA. The proviral DNA load (viral load) serves as specific marker for the early diagnosis of perinatal HIV-1 infection (Hatzakis 2004; Halfon 2006; Sarrazin 2006; Malnati, Scarlatti et al. 2008). Development of real-time PCR assays for gene expression studies by measuring the mRNA levels is significantly increasing. Nonetheless, microarray is still a method of choice in gene expression studies of whole-genome but real-time quantitative PCR is the gold standard for fast and easy confirmation of microarray results (Canales, Luo et al. 2006). High-throughput, automatization and accurate viral load measurements make real-time quantification PCR (real-time qPCR) suitable for use in the routine clinical diagnostic setting (Malnati, Scarlatti et al. 2008). Moreover, the facts that the method is less laborious; it reduces costs as no post-amplification steps, such as radioactive labelling and hazardous reagents in the conventional PCR, are required; it guides with the selection of intervention therapy; it can be performed on crude cellular extracts and provide crucial information such as the staging (acute and chronic) of the viral infections and the disease progression make it more fitting for resource-limited countries. (Koralnik 1999; Shiramizu, Gartner et al. 2004; Blackard 2005; Shiramizu 2005; Perrin 2006; Malnati, Scarlatti et al. 2008).

1.3 Motivation for study

South Africa is still the country that is most heavily struck by the AIDS epidemic with around 5.7 million people infected as estimated by UNAIDS in 2009. It has set up the largest antiretroviral treatment programme in the world with an estimate of 1000 000 people benefiting towards the end of 2009 (UNAIDS, 2010). In most studies, selective-polymerase chain reaction (SPCR) analysis detected resistant variants for the most common resistance mutations, such as K103N, V106M/I, M184V and Y181C, comprising of 0.1 to 20% of viral population in patient samples which were identified as wild-type by the conventional genotyping. These minor populations have a significant impact on virologic failure. Coupling of SPCR to the real-time PCR technology has improved resistance testing by making it more sensitive, accurate, less time-consuming, high-throughput and reproducible technique to assess drug-resistance variants in minor populations.

Therefore, the purpose of this study is:

1. To develop rapid and sensitive selective real-time PCR (SPCR) assays to detect minor HIV-1 resistant variants harbouring K103N which are not detected with more expensive and time-consuming genotyping methods,
2. To evaluate the method using constructed plasmid standards,
3. To screen 40 previously-genotyped patient samples. These samples were collected before the new HIV treatment regimens were in effect.

Chapter 2

2.1 Materials and Methods

Procedures carried out in this study are described herein. Briefly, two selective real-time PCR (SPCR) assays to enable the detection of K103N HIV-1 minor variants are being developed. They are total viral (non-specific) copy SPCR and K103N-SPCR assays, and use primers and TaqMan probes. K103 wild-type and K103N mutant plasmid standards with AAA and AAC/T codon, respectively, at 103 amino acid position of the HIV-1 reverse transcriptase (*RT*) will be constructed using the site-directed mutagenesis. The presence of the mutations will then be confirmed by cloning and sequencing. Once the assays are validated and optimized, 40 previously genotyped samples from patients (40) infected with HIV-1 subtype C will be screened for K103N minor resistance variants in the reverse transcriptase gene. The methodology and research approach are illustrated in a step-wise manner as follows:

1. To investigate HIV-1 *RT* diversity
 - Subtype C *RT* sequences were downloaded from the Los Alamos National Library HIV database to investigate the diversity in the *RT*.
 - Selection of primers and probes for both SPCR assays from literature review.
 - Comparison of the oligonucleotides with the sequences from the database to aid with the selection of primers and probes which accommodate polymorphisms.

2. Cloning and construction of mutant and wildtype standards
 - Two HIV-1 RNA samples from the department were amplified by RT-PCR and nested PCR
 - The resulted DNA was sequenced by genotyping and cloned into pGEM T-Easy vector
 - Site-directed mutagenesis was performed on the clones to induce K103 wildtype (AAA) codon, and both K103N mutant (AAC or AAT) codons.
 - Induced mutations were verified by sequencing

3. Optimization and Validation of total copy SPCR and K103N-specific SPCR assay on real-time PCR system
 - Testing the reactivity of primers and probes for each SPCR assay on all constructed standards
 - Optimization of primers for each assay
 - Optimization of probes for each assay
 - Construction of standard curves for each assay using a set of common mutant standards
 - Evaluation of discriminatory ability of a set of primers and probes for K103N-specific SPCR assay on all standards
 - Evaluation of the accuracy of both SPCR assays on wildtype-plus-mutant plasmid mixtures

4. Detection of K103N minor variants in patient samples
 - HIV-1 DNA was detected and quantified in 40 nested PCR products of previously genotyped patient samples using the optimized and validated total copy SPCR assay
 - HIV-1 DNA harbouring the K103N mutation was detected and quantified in the same 40 PCR products using the optimized and validated K103N-specific SPCR assay.

2.1.1 Patient samples

Patient samples used in the study were obtained from the HIV-1 database at the Division of Medical Virology at Tygerberg Academic Hospital, University of Stellenbosch and NHLS. We routinely screen patients for HIV-1 drug resistance at this division. HIV-1 status of patients is confirmed by the division before performing resistance testing. For this test, the samples are directly sequenced using population based (bulk) sequencing and followed by profiling the HIV-drug resistance mutation with the Stanford University HIV Drug Resistance interpretation algorithm Version 4.3.7 (available on <http://hivdb.stanford.edu>).

This study was approved by the Human Research Ethics Committee of the Stellenbosch University on the **20th of May 2008**, and the project number assigned is N08/03/069.

2.1.2 Analysis of known RT gene sequences in Los Alamos HIV database

2.1.2.1 Multiple alignments of RT gene sequences from Los Alamos HIV database

Total of 495 sequences were downloaded from the Los Alamos HIV database (<http://www.hiv.lanl.gov>) in 2008. Multiple alignments were generated using ClustalX (Thompson© et al., 1997), and viewed with BioEdit Sequence Alignment Editor v7.0.9.0 (Hall 1999). The diversity or sequence variations in the reverse transcriptase (*RT*) gene at amino acid position 103 was noted in the generated multiple alignments to aid in the construction of plasmid-derived standards or controls, and the design of primers and probes for the development of a real-time PCR-based assay, selective-polymerase chain reaction (SPCR), to detect K103N resistance mutation.

2.1.3 Construction of plasmid-derived DNA standards to use in the SPCR assays

2.1.3.1 RNA isolation of patient samples

Two samples, STV139166 and STV128864 known to carry the K103N resistance mutation were selected to use as controls in the study. HIV-1 RNA was extracted from plasma of each sample with the QIAamp® UltraSens™ Virus Kit (Qiagen GmbH, Hilden, Germany) according to the manufacturer's protocol. Briefly, the QIAamp® UltraSens™ technology lyses 1 mL plasma samples to concentrate viral RNA, which is applied to a QIAamp® spin column. RNA selectively binds to the QIAamp® membrane as contaminants and enzyme inhibitors pass through. The pure viral RNA is then eluted, aliquoted and stored at $-70\text{ }^{\circ}\text{C}$ for further analysis.

2.1.3.2 RT-PCR and PCR of the HIV-1 *RT* gene

The purified HIV-1 RNA was reverse-transcribed and amplified in one step reverse transcription-polymerase chain reaction (RT-PCR) using a forward primer MJ3 (Jung, Agut et al. 1992; Plantier, Dachraoui et al. 2005) and a reverse primer MJ4 (Jung,

Agut et al. 1992; Plantier, Dachraoui et al. 2005). This was followed by a separate polymerase chain reaction for nested amplification of the RT-PCR product, cDNA, using a forward primer A35 (Larder, Kellam et al. 1991) and a reverse primer NE135 (Larder, Kellam et al. 1991). This is illustrated below in **Figure 2.1**.

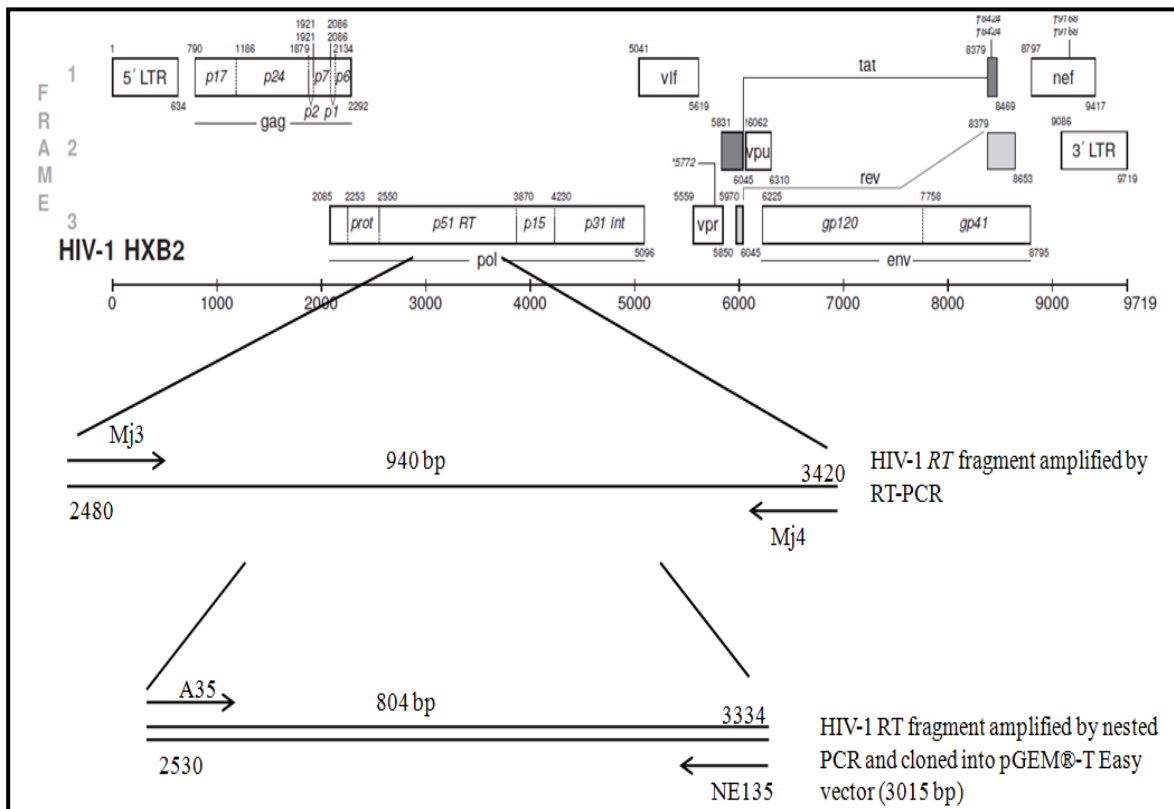


Figure 2.1: The schematic diagram showing the reverse transcription-polymerase chain reaction (RT-PCR) and the polymerase chain reaction (PCR) of the selected HIV-1 RT region which encompasses the amino acid position 103 associated with K103N resistance mutation. The arrangements of the primers to amplify this region are also shown based on the HIV-1 HXB2.

The method for one-step RT-PCR was adapted from Plantier et al (2005). (Plantier, Dachraoui et al. 2005) Briefly, RT-PCR was performed on stored purified viral RNA for samples STV139166 and STV128864. The reverse primer MJ4 and the forward primer MJ3 listed in **Table 2.1** were used in order to obtain the RT fragment of these samples. Access RT-PCR system (Promega, Madison, Wisconsin, USA) was used. A 50 μ L reaction mixture was prepared with AMV/*Tfl*, dNTPs Mix (0.2 mM each), 2 mM $MgSO_4$, 0.1U/ μ L AMV RT, 5 U/ μ L *Tfl* DNA Polymerase, forward and reverse

primer each at a final concentration of 40 picomoles (pmol), nuclease-free water, and 10 μ L RNA in 0.2-ml thin-walled PCR[®] tubes (QSP, Porex Bioproduct Inc., California, USA). The reaction was performed on the GeneAmp[®] 9700 PCR system (Applied Biosystems, Foster City, California, USA). Cycling conditions were hot start at 65°C for 30 seconds, RT at 48°C for 50 minutes, one cycle of denaturation at 94°C for 2 minutes, followed by 40 cycles of 94°C further denaturation for 20 seconds, 55°C annealing of primers for 30 seconds and 68°C extension for 90 seconds.

Table 2.1: Primers used in RT-PCR and Nested PCR.

Primer Name	Sequence (5'-3')	T _m (°C)	HXB2 nucleotide position Start-Stop
^a MJ4	CTGTTAGTGCTTTGGTTTCCTCT	54.8	3420-3399
^a MJ3	ATGAGGACCTACACCTGTCA	54.3	2480 to 2499
^b NE135	CCTACTAACTTCTGTATGTCATTGACA GTCCAGCT	61.4	3334 to 3300
^b A35	TTGGTTGCACTTTAAATTTCCCATTA GTCCTATT	58.9	2530 to 2564

^a – Jung et al., 1992

^b – Larder et al., 1991

The RT-PCR products were further amplified by nested amplification using reverse primer NE135 and forward primer A35. GoTaq[®] Flexi DNA Polymerase (Promega Corporation, Madison, Wisconsin, USA) was used to make the reaction mixture. It was prepared with GoTaq Flexi buffer, 0.2 mM of each dNTP, 1.5 mM of MgCl₂, 2.5 U/ μ l Taq DNA Polymerase, the forward and the reverse primer were each at a final concentration of 40 picomol, and nuclease-free water to a final volume of 50 μ L in 0.2-ml thin-walled PCR[®] tubes (QSP, Porex Bioproduct Inc., California, USA). The GeneAmp[®] 9700 PCR system (Applied Biosystems, Foster City, California, USA) was used at a ramp speed of 9600, with the following cycling conditions: 94°C for two minutes; 40 cycles which include denaturation at 94°C for 30 seconds, annealing of primers at 55°C for 30 seconds as well as primer extension at 68°C for 90 seconds, and followed by one cycle of final extension at 68°C for five minutes.

2.1.3.3 Agarose gel electrophoresis of PCR products

All nested PCR products sized 804 bp were analyzed by agarose gel electrophoresis. A gel was prepared with 0.8% agarose (WhiteSci, Whitehead Scientific (Pty) Ltd., Burgos, Spain) in TAE buffer (0.04 M Tris hydrochloride (Roche, Berlin, Germany), 0.001 M EDTA (Sigma-Aldrich, Saint-louis, USA). A 0.5 µg/ml Ethidium bromide (Promega, Madison, Wisconsin, USA) was added to the gel to trace the DNA. After the gel was set, 8 µL of each PCR product was mixed with 2 µL of Blue/Orange 6X Loading Dye (Promega Corporation, Madison, Wisconsin, USA) and ran on the gel in parallel with 1 kb DNA ladder (Promega Corporation, Madison, Wisconsin, USA) which acts as their molecular size marker. The ultra violet (UV) light was used to visualize the DNA bands at 302 nm wavelength. Then the images were captured with the GeneSnap image acquisition software version 4.0.0 (Synoptics Ltd., Cambridge, UK).

2.1.3.4 Cloning

The product of the nested PCR was further cloned into a pGEM® T Easy vector to construct plasmid standards for the real-time selective-polymerase chain reaction (SPCR) assays.

Ligation with pGEM®-T Easy vector (3015 bp)

After electrophoresis, the PCR products were purified with QIAquick® PCR Purification Kit protocol (Qiagen GmbH, Hilden, Germany). The concentration of the purified PCR products was determined by the Nanodrop™ ND-1000 system (Nanodrop Technologies Inc., Delaware, USA). A 2X Rapid Ligation Buffer, included in the pGEM®-T Easy Vector system II (Promega Corporation, Madison, Wisconsin, USA) was used to ligate a purified 804-bp HIV-1 *RT* fragments of both samples separately, as inserts, with a 3015-bp pGEM®-T Easy vector (**Figure 2.2**). Promega's Protocol for ligations (Part# TM042, Promega Corporation, Madison, Wisconsin, USA) was followed. A 40 ng (1 µL for sample 1 and 1.2 µL for sample 2) of each PCR product was used in the ligation reactions to reach a 3:1 vector to insert molar ratio required by the protocol.

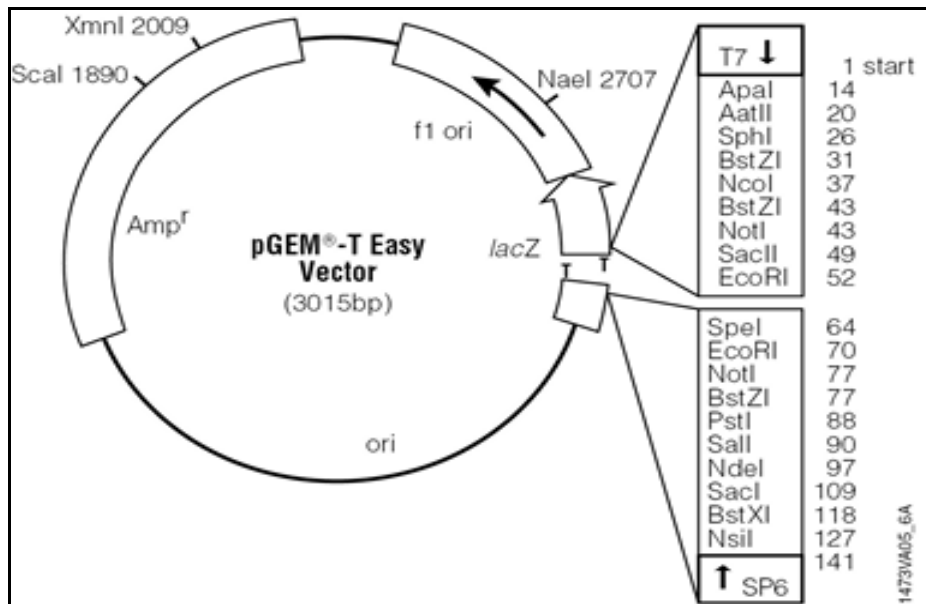


Figure 2.2: A structure of pGEM®-T Easy vector showing its multiple restriction sites within the multiple cloning sites (Technical Manual Part# TM042, Promega Corporation, Madison, Wisconsin, USA) (<http://www.promega.com>).

Transformation using the JM109 High efficiency competent cells

Following incubation, the two ligation reactions of our respective samples were transformed into JM109 high-efficiency competent bacterial cells (Promega Corporation, Madison, Wisconsin, USA) according to Promega's „Protocol for Transformations Using the pGEM®-T Easy Vector Ligation Reactions' (Part# TM042, Promega Corporation, Madison, Wisconsin, USA). Modifications to the protocol include transferring 5 μ L instead of 2 μ L of each ligation reaction into a sterile 1.5-mL microcentrifuge tube, and adding 90 μ L instead of 50 μ L of the JM109 bacterial cells to each tube. Following that, the LB plates were incubated in inverted position overnight in a 37°C walk-in incubator, to allow the colonies to develop. The LB plates contained Amp/X-gal/IPTG ([100 μ g/ml]/ [20 μ l/ml]/100 μ l/ml).

Culturing of colonies

White colonies which grew on the plates were aseptically picked with a pipette the following day and each was inoculated in a 15-ml centrifuge tube containing 3 ml of LB (Luria-Bertani) (Fluka Biochemika, Buchs, Switzerland) medium containing 100 μ g/ml ampicillin (Invitrogen Corporation, Paisley, UK) prepared according to

Promega's protocol (Technical Manual Part# TM042, Promega Corporation, Madison, Wisconsin, USA). Six (6) colonies for each sample were cultured. The cultures were incubated overnight at 37°C in a Labcon® shaking incubator (Labmark, Roodepoort, RSA) at speed of 157 rpm.

Screening for recombinant clones

To preserve the transformed bacterial cells, 150 µL of sterile glycerol (15%) was added to 850 µL of the stock cultures (85%), and frozen away at -20°C for future use. The plasmid DNA was extracted according to Promega's Standard DNA Purification protocol (Technical Manual Part# TM253) using the PureYield™ Plasmid Midiprep system (Promega Corporation, Madison, Wisconsin, USA). Briefly, the bacterial cells were lysed and applied to a silica-membrane column in which DNA binds to the binding membrane. The vacuum is applied to the column to purify DNA of substantial amounts of protein, RNA and endotoxin contaminants with Endotoxin Removal Wash. A purified plasmid DNA is then eluted with 600 µL of nuclease-free water (Promega Corporation, Madison, Wisconsin, USA). DNA concentration was measured using the Nanodrop™ ND-1000 system (Nanodrop Technologies Inc., Delaware, USA).

The plasmid DNA was later subjected to restriction digestion with the restriction enzyme *EcoRI* (Promega Corporation, Madison, Wisconsin, USA) in Buffer H (90 mM Tris-HCl, 10 mM MgCl₂, 50 mM NaCl, pH 7.5) (Promega Corporation, Madison, Wisconsin, USA). The reaction was incubated at 37°C for four hours. Agarose gel electrophoresis was used to verify the presence of an insert as described.

2.1.3.5 DNA sequencing

Cycle Sequencing Reactions

Recombinant clones were sequenced using sequencing primers listed in **Table 2.2**. A 500-ng DNA of each clone was added in a separate reaction with each of these primers. The reactions were prepared with the BigDye™ Terminator V3.1 Cycle Sequencing Mix (Applied Biosystems, Foster City, California, USA) and Half-dye Buffer (Bioline USA Inc., Randolph, Miami, USA). Then the cycling reactions were run on the GeneAMP® 9700 PCR system (Applied Biosystems, Foster City,

California, USA) at a ramp speed of 9700. The cycle method used is as follows: 25 cycles which included a heat-denaturation at 95°C for 10 seconds, primer annealing at 45°C for five seconds and elongation at 60°C for 4 min. These sequencing extension products were analyzed on the ABI prism[®] 310 Genetic Analyzer (Applied Biosystems, Foster City, California, USA) to generate data trace files.

Table 2.2: Sequencing primers used for plasmid clones.

Primer name	T _m (°C)	Sequence (5'-3')	HXB2 nucleotide position Start-Stop
Pol3D	45	CAG TAC TGG ATG TGG G ^a	2869-2884
Pol3rev	50	CTG AAA AAT ATG CAT CCC CC ^a	2901-2882
ABB20-3F	50	ATC AGT ACA ATG TGC TTC CA ^b	2980-2999
HIV-AK12	50	TGG TGT YTC ATT RTT TRY ACT AG ^c	2969-2947
HIV-AK11	50	GTA CCA GTA AAA TTA AAR CCA G ^c	2571-2592

^a, Susan Engelbrecht, personal communication

^b, John Hachett, personal communication

^c, Plantier et al, 2005

Sequence analysis of pGEM[®]-T Easy plasmid clones

Raw data trace files were read and edited using Sequencher version 4.6 (Gene Codes Corporation, Michigan, USA). Initially, the sequences were trimmed of poor quality ends, and then overlapping fragments, elongated with varying primers, were assembled to form a contig. The correct consensus *RT* sequences were exported in a FASTA format to be analyzed for drug resistance-associated mutations.

2.1.4 Site-directed mutagenesis

2.1.5.1 Mutagenic primer design

Mutagenic primers were manually designed according to the requirements in Stratagene's protocol for mutagenic oligonucleotide primers. The primers should be between 25 and 45 bases in length, and with a melting temperature (T_m) of ≥78°C. Briefly, the mutagenic primer design was based on the sequences of each generated plasmid, which span nucleotides 2844-2877 of the HXB2 HIV-1 *RT*. They were designed to replace amino acid lysine (AAA, K103), a wildtype, with asparagine

(AAC/T, K103N), a mutation, or vice versa, at codon 103 and simultaneously with the substitution of amino acid valine (GTA, V106), a wildtype, with methylene (ATG, V106M), a mutation, at codon 106 in these plasmid clones. The mutation V106M was meant to be investigated in this study to but due to time constrain further attempt to do so were discontinued. The primers were designed such that the mutations were situated in the middle of the mutagenic primers with 10-15 nucleotides at both ends. The primers contained one or two C and/or G bases at both ends. They are listed in **Table 2.3**.

Table 2.3: Site-directed mutagenesis primers used on four of the generated plasmid clones.

Primer name	T _m (°C)	Sequence (5'-3')	HXB2 nucleotide position Start - Stop
MS3-N103K-V106M(F)	55.3	GGT TAA AAA AGA ATA AGT CAA TGA CAG TAT TGG	2946-2978
MS3-N103K-V106M(R)	55.3	CCA ATA CTG TCA TTG ACT TAT TCT TTT TTA ACC	2978-2946
MS1-V106M(F)	49.3	GAA CAA ATC AAT GAC AGT ACT AG	2947-2970
MS1-V106M(R)	49.3	CTA GTA CTG TCA TTG ATT TGT TC	2970-2947
MS9-N103K-V106M(F)	53.9	GGA TAA AAA AGA AAA AAT CAA TGA CAG TAC TAG	2946-2978
MS9-N103K-V106M(R)	53.9	CTA GTA CTG TCA TTG ATT TTT TCT TTT TTA TCC	2978-2946
MS10AK1-N103K(F)	47.3	GAT AAA AAA GAA AAA ATC AGT GAC	2947-2970
MS10AK1-N103K(R)	47.3	GTC ACT GAT TTT TTC TTT TTT ATC	2970-2947

The nucleotides in red are the mutations implemented in these primers as compared with the sequences of plasmids so they can be used to induce the desired mutations. F – Forward, R – reverse.

2.1.4.2 Mutant strand synthesis and *Dpn* I Digestion of the amplification products

Eight forward and reverse mutagenic primers (**Table 2.3**) were used to induce the desired mutations in the *RT* sequence of the four plasmids using QuikChange® Lightning Site-Directed Mutagenesis Kit (Stratagene, La Jolla, Canada) according to the manufacturer's protocol. In contrast to other kits, the QuikChange® Lightning Kit

induces a site-specific mutation in almost any double-stranded plasmid; therefore we needed not to convert our plasmids into single-stranded DNA prior to site-directed mutagenesis.

The mutagenesis protocol uses 125 ng of each oligonucleotide primer. The higher or lower concentrations of primers could have inhibitory effects on the site-directed mutagenesis. To apply this amount to the reactions nanograms (ng) of oligos had to be converted to picomoles (pmol). The following equation was applied to calculate the desired concentration for the primers:

$$\text{X pmoles of oligo} = \frac{\text{ng of oligo}}{330 \times \text{of bases in oligo}} \times 1000$$

The mutant strand synthesis reaction was done according to Stratagene's protocol. Each reaction was prepared with 5 µl of 10 × reaction buffer, 100 ng plasmid DNA, appropriate amount of each mutagenic primer pair as calculated using the formula above, 1 µl of dNTP mix (0.2 mM of each dNTP), 1.5 µl of QuikSolution, nuclease-free water (Promega Corporation, Madison, Wisconsin, USA) to a final volume of 50 µl, and then 1 µl of QuikChange® Lightning Enzyme.

The PCR reaction was performed on the GeneAMP® 9700 PCR system (Applied Biosystem, Foster City, California, USA) using the standard 9700 ramp speed. The cycling conditions were, 95°C for 2 minutes; 18 cycles of DNA denaturation at 95°C for 20 seconds, primer annealing at 55°C for 30 seconds, and extension at 68°C for 140 seconds; followed by a final extension step at 68°C for 5 minutes. Following the thermal cycling, 2 µl of *Dpn* I restriction enzyme was added to each amplification reaction, and then immediately incubated at 37°C for 5 minutes to digest the methylated parental plasmids (the unmutated), leaving the desired mutated ones intact.

2.1.4.3 Transformation of XL10-Gold® ultra-competent cells

After the site-directed mutagenesis, the plasmids had to be transferred to bacteria to obtain enough plasmid DNA for screening and further analysis. The plasmids were

transformed into XL10-Gold® ultracompetent cells (Stratagene, La Jolla, USA), which are included in the kit. Modification to the protocol included the use of SOC medium (Sigma-Aldrich, Saint-Louis, USA) medium for transformation instead of NZY⁺ broth. Briefly, the XL10-Gold ultracompetent cells were thawed on ice. For each sample reaction to be transformed, a 45 µl of the ultracompetent cells was aliquoted to sterile 14-ml polypropylene round-bottom tubes (Becton Dickinson, Franklin Lakes, USA) on ice. Two-microliter of the β-mercaptoethanol mix, provided with the kit, was added to the 45 µl of cells, and the cells were incubated on ice for 2 minutes. Two-microliter of the *Dpn* I-treated DNA samples was transferred to separate aliquots of the ultracompetent cells. The transformation reactions were gently mixed and incubated on ice for 20 minutes. The tubes were heat-shocked in a 42°C water bath for 30 seconds and the samples were immediately transferred on ice and incubated for 2 minutes. A preheated SOC medium (0.5 ml) was added to each tube the tubes were incubated at 37°C for 1 hour with shaking at 200 rpm in Labcon® shaking incubator (Labmark, Roodepoort, RSA). For each sample, 20 and 100 µl of each transformation reaction, were plated on LB agar plates containing the 100 µg/ml ampicillin (Invitrogen Corporation, Paisley, UK). The transformation plates were incubated at 37°C for 16-24 hours.

2.1.4.4 Confirmation of the presence of the desired mutations by sequencing

To screen the colonies for the desired mutations, 4 colonies were tested for each sample. Briefly, 4 colonies from each sample were picked and inoculated in 3-mL LB medium containing 100 µg/ml ampicillin. The 16 tubes were incubated in a Labcon® shaking incubator (Labmark, Roodepoort, RSA) overnight at 150 rpm and 37°C to allow the cultures to grow. After 16 hours the mutated plasmids were extracted from the cultures of XL10-Gold® ultracompetent cells using QIAprep® Spin Miniprep Kit (Qiagen GmbH, Hilden, Germany) according to manufacturer's protocol.

To confirm if the 16 plasmid clones are carrying the intended mutations, cycle sequencing reactions were performed as previously described. Primer HIV-AK12 (**Table 2.2**) and HIV-cm237R2500 (5'-GTA CTG ATA TCT AAT CCC TGG -3') were used. The latter primer starts at nucleotide (nt) position 2987 and stops at 2967 of the HIV-1 HXB2, and has a melting point (*T_m*) of 50°C. Following sequencing,

the resulting raw data were read and edited with Sequencher version 4.8 (Gene Codes Corporation, Michigan, USA). Furthermore, the multiple sequence alignments of the consensus C, HIV-1 HXB2, the constructed plasmids and their parental plasmids were constructed by Geneious version 4.5.5 (<http://www.geneious.com>) to view and ensure that the intended mutations at amino acid positions 103 and 106 were successful.

2.1.5 Development of primers and probes for the selective real-time polymerase chain reaction (SPCR) assays

Sets of primers and probes used in Johnson et al, 2005 and Johnson et al., 2007 for the detection of K103N minor resistance variants were multiple-aligned with the constructed plasmid standards using Geneious version 4.5.5 (<http://www.geneious.com>) to ensure sequence complementarities (Johnson, Li et al. 2005; Johnson, Li et al. 2007). The two sets of primers and probes from the former were found suitable for the total copy and the K103N-specific SPCR assays in terms of sequence complementarities and their consideration for HIV-1 nucleotide polymorphisms. They are shown in **Table 2.4**.

Table 2.4: Primers and probes used for total copy and K103N-specific SPCR assays.

Probe/Primer Name	Sequence (5'-3')	HXB2 nucleotide position Start-Stop	T _m (°C)
^a 1P TaqMan® Probe	FAM ^b -TGG GGG ATG CAT ATT TTT CAG TTC CTT TAG ATG A –TAMRA ^c	2879-2913	56.1
^a 2P TaqMan® Probe	FAM ^b -TGG GAG ATG CAT ATT TTT CAG TTC CTT TAG ATG A-TAMRA ^c	2879-2913	56.8
^a C-103N.1F Primer	CCC AGT AGG RTT AAA RAA GGA C	2838-2860	52.4
^a C-103N.2F Primer	CCC AKC RGG GTT RAA AGA GGA C	2838-2860	58.8
^a C-103NT.3F Primer	CCC AGC AGG RTT AAA AVA GGA T	2838-2860	55.5
^a ComFWD Primer	CTT CTG GGA AGT TCA ATT AGG AAT ACC	2808-2835	55.3
^a 103/com.C3R	CAT TGT TTA TAC TAG GTA TGG TGA ATG C	2962-2934	54.1

^a – Johnson et al., 2005

^b – FAM is a fluorescent reporter dye

^c – TAMRA is a non-fluorescent quencher

Multiple sequence alignment was generated with all 2008 HIV-1 subtype C *RT* sequences to view the extent of sequence similarities and mismatches at the binding sites of these primers and probes. The total copy SPCR assay amplifies all the HIV-1 present in a sample, whereas the K103N-SPCR assay amplifies only the HIV-1 harbouring the K103N resistance mutation. Both assays use common reverse primer called 103/com.C3R and two TaqMan® detection probes, namely 1P and 2P. They only differ by forward primers. In the total copy assay only one forward primer called ComFWD is employed, whereas the K103N-specific assay has three specific forward primers namely, C-103N.1F, C-103N.2F and C-103NT.3F. 1P and 2P are labelled with 6-carboxyfluorescein (FAM) as the reporter or fluorophore at a 5' end and TAMRA as the fluorophore quencher at a 3' end. Schematic diagram in **Figure 2.3** roughly illustrates the position of these primers and probes in the RT gene of HIV-1 HXB2.

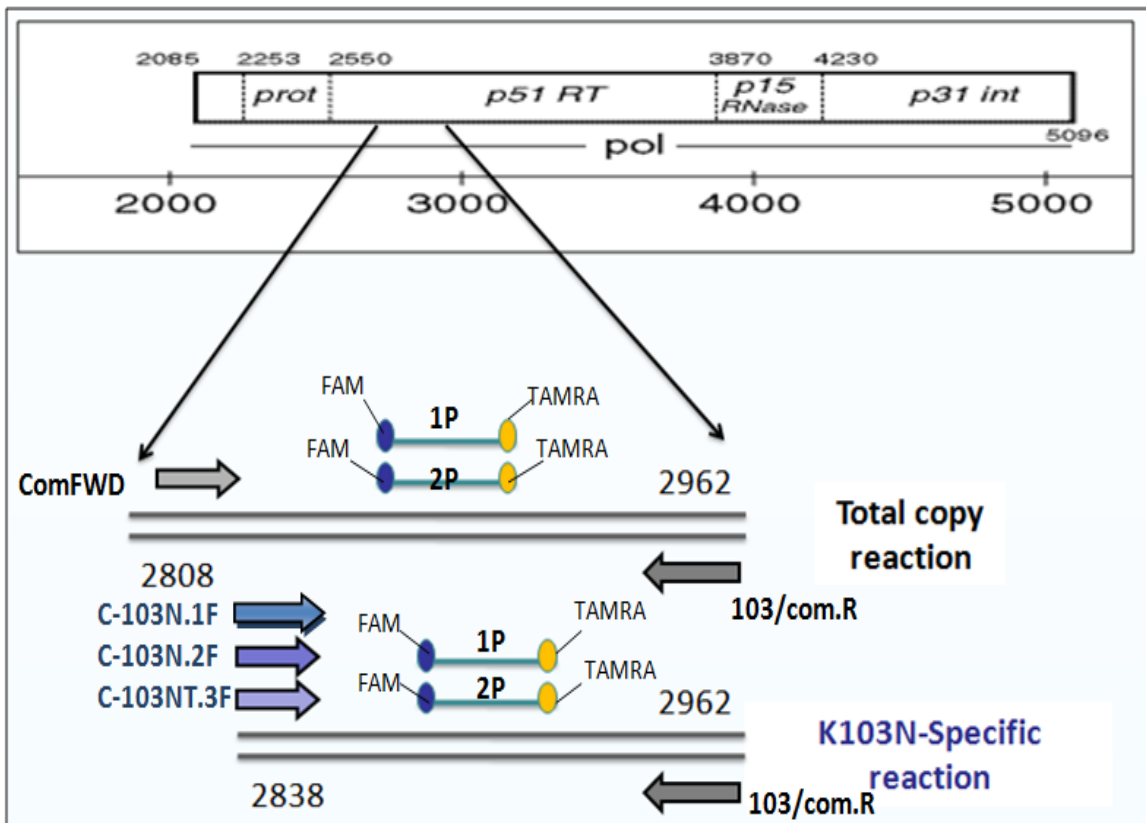


Figure 2.3: A schematic representation showing the positioning of primers and probe for the total copy and the K103N-specific SPCR assays on the HIV-1 HXB2.

Probe hybridization to a complementary target followed by 5'-3' exonuclease hydrolysis causes release of the fluorophore (FAM) (Holland, Abramson et al. 1991). All oligonucleotides were custom synthesized by IDT (Whitehead Scientific (Pty) Ltd) with standard purification.

2.1.6 Preparation of plasmid DNA standards/controls

The concentrations of all 12 plasmid DNA standards constructed by site-directed mutagenesis (and the others as original clones) were measured using a Nanodrop™ ND-1000 spectrophotometer (Nanodrop Technologies Inc., Delaware, USA). Ten-fold serial dilutions from 10^9 to 1 copy/ μl of each plasmid DNA was made to use as standards/controls in the two real-time SPCR assays.

A mass of one DNA copy per μl was calculated from the determined concentration of each plasmid DNA sample using the following formula:

$$\frac{\text{(Size of DNA bp)} (644 \text{ g/mol bp})}{6.023 \times 10^{23} \text{ copy}} \rightarrow \text{Molarity of each nucleotide base}$$

According to this calculation 1 copy of DNA per μl is equivalent to 4 attograms (4×10^{-18} grams) of plasmid DNA. In that case, 4 nanograms will have 10^9 copy/ μl . Initially, each plasmid stock was diluted to a concentration of 4 ng DNA per μl which corresponds with 10^9 copies of DNA per μl . In summary, for each set 900 μl of nuclease-free water was added into ten 1.5-ml Eppendorf tubes. Then a 100 μl of the respective diluted plasmid stock was transferred into a 1.5-ml Eppendorf tube with nuclease-free water (Promega Corporation, Madison, Wisconsin, USA). The tube was mixed by vortexing. For each subsequent dilution, 100 μl was transferred from the previous dilution into another tube with 900 μl of nuclease-free water. Each plasmid dilution was then divided into small aliquots of 100 μl and stored at -20°C . Each aliquot was thawed and used not more than three times.

2.1.7 General conditions and execution of real-time SPCR assays

All the reactions were prepared on Standard 96-well plates (Applied Biosystems, Foster City, California, USA) to a total volume of 25 μl . Each reaction per well,

among other reagents, contained 12.5 µl of TaqMan[®] Gene Expression Master Mix (Applied Biosystems, Forster City, California, USA). Optical caps (Applied Biosystems, Forster City, California, USA) were used to close the wells. All the experiments were done at least three times, each run included a no-template control (NTC) in triplicates and each standard or sample was run in duplicate on the 7900HT Real-Time PCR System (Applied Biosystems, Foster city, California, USA). Data were captured and analyzed by using SDS[®] 2.3 (Sequence Detection System) software (Applied Biosystems, Foster city, California, USA). The thermal cycling conditions for every real-time PCR or SPCR assay throughout this study are shown in **Table 2.5**, and they will be used unless stated otherwise.

Table 2.5: Thermal cycling conditions for the real-time SPCR assays.

Instrument: 7900HT Fast Real-Time PCR System				
Method: Absolute Quantification				
Cycling Conditions: Standard				
Cycle Steps		Number of cycles	Temperature (°C)	Time
Stage 1	AmpErase [®] UNG activation	x 1	50	2 minutes
Stage 2	AmpliTag Gold [®] DNA Polymerase activation	x 1	95	10 minutes
Stage 3 PCR	Denaturing	x 40	95	15 seconds
	Annealing		60	1 minute
	Extension		60	1 minute

2.1.8 Testing the reactivity of primers and probes for total viral copy SPCR assay

The primers and probes (**Table 2.4**) for the total viral copy SPCR were tested for their reactivity on all 12 constructed plasmid standards/controls at low and high concentrations of 5×10^3 and 5×10^6 DNA copy/µl. The master mix included total copy forward primer ComFWD, a common reverse primer 103/com.C3R and a mixture of

probe 1P and 2P at 75% and 25% proportions respectively. The highest final concentrations of 900 nM and 250 nM for each primer and probe were used, respectively, as recommended by Applied Biosystems' protocol for 'Preparing the PCR Master Mix' (Part# 4364014Rev. C, Applied Biosystems, Foster City, California, USA). The PCR reaction setup of the experiment for testing the reactivity on each plasmid standard is shown in **Table 2.6**.

Table 2.6: Total copy reaction setup for testing the reactivity of total copy primers and probes.

Total copy reaction	
Reagents	Final concentration [nM]
TaqMan Gene Expression Master mix	12.5µL/reaction
ComFWD primer	900
103/com.C3R primer	900
75% 1P 25% 2P } Probe mix	250
Nuclease-free water	Up to 25µL
Template: plasmid standard	5x10 ⁴ DNA copies/µl
Total volume of reaction: 25 µL	

2.1.9 Optimization of primers for total viral copy SPCR assay

Forward and reverse primers for total viral copy reaction were optimized by adjusting their working concentrations. Briefly, ComFWD and 103/com.C3R were used in each reaction at 50 nM, 300 nM and 900 nM with 75%1P and 25%2P probe mixture at a constant concentration of 300 nM. The ratios for forward to reverse primer were alternated using these concentrations. A K103N-mutant plasmid standard MS15-3 (harbouring AAA codon at amino acid position 103 containing 5 000 DNA copy/µl) was used as a template in each reaction. A concentration ratio of the forward to reverse primer that yielded the minimum threshold cycle (Ct) in each experiment was considered optimal.

2.1.10 Optimization of probes for total viral copy SPCR assay

The optimal working probe concentration for the total viral copy SPCR assay was determined with varying concentrations of 50 nM, 100 nM, 150 nM, 200 nM, 250 nM and 300 nM for the mixture of 75% 1P and 25% 2P. ComFWD (900 nM) and 103/com.C3R (900 nM) primers were used at their determined optimal working concentration and kept constant, in each reaction. AAC-mutant standard MS15-3 at 5 000 DNA copies/ μ L was used as a template. The probe concentration that yielded the minimum threshold cycle (Ct) was considered the optimal.

2.1.11 Construction of standard curve for total viral copy SPCR assay

To determine the reportable linear dynamic range of the total viral copy SPCR assay 5×10^7 to 5×10^0 DNA copy/ μ l serial dilution of MS15-3 was used to construct a standard curve. SDS v2.3 software (Applied Biosystems, Forster City, California, USA) generated a standard curve. The software analyses detected fluorescence data from the real-time instrument and presents it in the form of a standard curve, amplification plot or curve. Optimal concentrations determined above for ComFWD primer (900 nM), 103/com.C3R primer (900 nM), and the two probes (1P and 2P at 300 nM) were used in the PCR master mix setup. In addition to NTC, of two K103 wild-type (MS9-3 and MS10-2) and one K103N mutant (MS10-4) controls were included in two replicates at concentrations of 5×10^0 and 5×10^6 DNA copy/ μ l for each. The reactions were run for 55 cycles.

2.1.12 Testing the reactivity of primers and probes for K103N-SPCR assay

Reactivity testing for K103N-specific primers was divided into five experiments using C-103N.1F, C-103N.2F, C-103NT.3F individually, or mixed. Each experiment was done on all 12 plasmid standards containing 5×10^4 DNA copy/ μ l, individually. Despite the common reagents such as the reverse primer 103/com.C3R and a mixture of 1P and 2P at 75% to 25% ratio in all their master mixes, the experiments differed with K103N specific primers. Experiment 1 included primer C-103N.1F, Experiment 2 included primer C-103N.2F, Experiment 3 included C-103NT.3F, Experiment 4 included a mixture of C-103N.1F and C-103NT.3F (50:50), and Experiment 5 is for testing the reactivity of a mixture of all three K103N-specific primers with 47% C-103N.1F, 33% C-103N.2F and 20% C-103NT.3F. The reaction setup of these experiments is summarized in **Table 2.7**. The highest final concentrations of 900 nM

and 250 nM for each primer and probe were used, respectively, as recommended by Applied Biosystems' protocol for 'Preparing the PCR Master Mix' (Part# 4364014Rev. C, Applied Biosystems, Forster City, California, USA).

Table 2.7: PCR master mix setup for five experiments using all three K103N specific forward primers.

Reagents	Exp* 1	Exp* 2	Exp* 3	Exp* 4	Exp* 5
TaqMan [®] Gen Ex Master Mix ^a	X	X	X	X	X
Probe [1P+2P]	X	X	X	X	X
C-103N.1F	X			X	X
C-103N.2F		X			X
C-103NT.3F			X	X	X
Template: standard	50 000 DNA copies				
Nuclease-free water	Up to a final volume of 25 µL				

* Experiment

^aTaqMan[®] Gene Expression Master Mix

X – Means the corresponding reagent is included in the reaction mix.

2.1.12.1 Design of additional K103N-specific primer and its reactivity testing

Another specific primer named C-103N.3FC was designed similar to C-103NT.3F, but the last nucleotide of codon 103, thymine (T), was replaced by cytosine (C). This new primer was tested likewise as the only forward primer on all 12 standards (50 000 DNA copy/µL). The experiment was run for 50 cycles.

2.1.13 Optimization of primers for K103N-SPCR assay

The K103N-SPCR assay was optimized by individually adjusting the forward and the reverse primers to optimal working concentrations. This means that two experiments were performed with a common reverse primer 103/com.C3R, but with different individual specific forward primers. This is to determine the optimal proportion or concentration each primer will be required to achieve its full effectiveness, and this will also guide when the primers are used as a mixture. Experiment 1 included

forward C-103NT.3F and Experiment 2 included forward primer C-103N.3FC. Each primer was used with the reverse primer in each reaction. The ratios for forward to reverse primer were alternated at concentrations 50 nM, 300 nM and 900 nM with 75% 1P and 25% 2P probe mixture at a constant concentration of 300 nM. In Experiment 1 a mutant plasmid standard MS3-4 (AAT) was used as a template, whereas mutant standard MS15-3 (AAC) was used in Experiment 2. Each standard contained 5×10^5 DNA copies per μl . The primer concentration ratio that yielded the minimum threshold cycle (Ct) in each experiment was considered the optimal.

2.1.14 Optimization of probes for K103N-SPCR assay

Optimal working probe concentration for the K103N-SPCR assay was determined by varying the concentration of a probe mixture of 75% 1P and 25% 2P and keeping all the primers constant. Probe concentrations used were 50 nM, 100 nM, 150 nM, 200 nM, 250 nM and 300 nM. Two experiments were performed, namely, Experiment 1 which used C-103NT.3F forward primers with MS3-4 (AAT) as the template, and Experiment 2 which used C-103N.3FC with MS15-3 (AAC) as the template. This is because each primer is specific for a different codon of the K103N mutation. In that case, this is to determine the optimal probe concentration at which each of these primers will work effectively. All the primers including 103/com.C3R reverse primer were used at their optimal working concentration of 900 nM. The templates were used at 10^5 DNA copy/ μL each. The probe concentration that yielded the minimum threshold cycle (Ct) was considered the optimal.

2.1.15 Construction of standard curve for K103N-SPCR assay

To determine a reportable linear dynamic range of the K103N-SPCR assay 10^7 to 1 DNA copy/ μl serial dilutions of K103N-mutant standard MS15-3 (AAC) were used to construct a standard curve with SDS[®] v2.3. Optimal concentrations determined above for the specific forward primer mixture (50% C-103N.3FC plus 50% C-103NT.3F at 900 nM), 103/com.C3R (900 nM), and a mixture of the two probes (75% 1P plus 25% 2P at 300 nM) were employed in the master mix setup of the reactions. Other controls included were 10^6 and 1 copy/ μL of MS9-3 (Wt), MS10-2 (Wt) and MS10-4 (Mut) as wild-type and mutant controls. The experiment was run for 55 cycles.

2.1.16 Evaluation of the discriminatory ability of K103N-SPCR assay

The discriminatory ability of the K103N-specific SPCR assay was assessed on each of the 12 plasmid standards at low (5×10^3) and high (5×10^6) DNA copies. The specific forward primer mixture (50% C-103N.3FC and 50% C-103NT.3F) and the universal reverse primer 103/com.C3R were used at a concentration of 900 nM. The probe mixture (75% 1P and 25% 2P) was used at 300 nM. The PCR cycles were repeated 50 times. The assay was run together with known standards to generate a curve. Then the unknowns were compared to this standard curve in order to interpolate their absolute quantity such as the DNA copies from the generated standard curve.

2.1.17 Evaluation of the accuracy of both SPCR assays

The accuracy for both SPCR assays was evaluated in the wild-type/mutant (Wt/Mut) plasmid mixture experiment. This was investigated by independently assessing the total viral copy SPCR assay and the K103N- SPCR assay on a panel of K103-wildtype (MS10-2, AAA) and K103N-mutant (MS15-3, AAC) plasmid mixtures. A 10-fold serial dilution of the mutant standard at 5×10^6 to 5×10^0 DNA copy/ μ l was added to a constant background of 5×10^7 DNA copy/ μ l of the wild-type standard. This was prepared by adding 10 μ l of mutant to 90 μ l of wildtype. In all experiments, the primers were used at a concentration of 900 nM and a mixture of two probes, 1P and 2P, at 300 nM. Other controls included were 5×10^6 and 10^0 DNA copy/ μ l of pure MS15-3 as the K103N mutant control, and 5×10^7 and 5×10^0 DNA copy/ μ l of pure MS10-2 a K103 wild-type control, with each concentration in duplicates. Each assay was run together with the 10-fold serial dilutions of its validated standard curve. The PCR cycle was repeated 55 times.

The detection limit of K103N variants by the SPCR assays was calculated using the formula from Paredes et al, 2007:

% of K103N detection limit = $[\text{input of K103N-mutants MS15-3 at } 5 \times 10^3 \text{ DNA copy}/\mu\text{L detected by K103N-SPCR assay}] / (\text{Input of MS15-3 total viral copies at } 50\,005\,000 \text{ DNA copy}/\mu\text{L detected by total copy SPCR assay})] \times 100$. It was found to be equal to to 0.01%.

2.1.18 Detection of K103N minor variants in patient samples

2.1.18.1 Total viral copy SPCR assay on patient samples

The optimized total viral copy SPCR assay was used to detect and quantify HIV-1 in the nested *RT* PCR products of 40 HIV-1 subtype C patient samples. The 40 samples were run along a 10-fold (10^7 -1 DNA copy/ μ L) serially diluted MS15-3 mutant standard (K103N) to construct a valid standard curve. Real-time PCR cycling conditions stated in **Table 2.5** were followed, but using 55 cycles. Fluorescence data (Ct) and the amount of viral DNA (copy/ μ l) detected in each 40 samples were interpolated from the standard curve.

2.1.18.2 K103N-SPCR assay on patient samples

The optimized K103N-SPCR assay was used to detect and quantify the minor variants of both K103N codons (AAT and AAC) in the nested *RT* PCR products from 40 HIV-1 subtype C patient samples in which resistance mutations were previously analyzed by population sequencing. The 40 samples were run along a 10-fold (10^7 -1 DNA copy/ μ L) serially diluted MS15-3 mutant (K103N) plasmid standard that generated a valid standard curve. Real-time PCR cycling conditions stated in **Table 2.5** were followed, but using 55 cycles. Fluorescence data (Ct) and the amount of viral DNA (copy/ μ l) detected in each 40 samples were interpolated from the standard curve.

Chapter 3

3.1 Results

3.1.1 Patient samples

Clinical information and demographics of the patients are supplied in **Table 3.1**. All the patients are infected with HIV-1 subtype C. There are 25 females (62.5%) and 15 males (37.5%), with average age of 26. Assignment of NRTI and NNRTI drug resistance mutations was done using the Stanford University HIV Drug Resistance database (<http://hivdb.stanford.edu/pages/algs/HIVdb.html>). The RT (reverse transcriptase) sequences of the patient samples were compared to HIV-1_{HXB2} (<http://hiv-web.lanl.gov>).

3.1.2 Analysis of RT gene sequences in the Los Alamos HIV database

3.1.2.1 Multiple alignments of the RT gene sequences from Los Alamos HIV database

Part of the generated multiple sequence alignments of the all 2008 subtype C HIV-1 *RT* sequences, 494 in total, is depicted in **Appendix B**. Codon 103 at nucleotide position 307-309 is very diverse, but with many wildtype codons such as AAA and AAG. It harbours either one of the following codons in the prevalence order; AAA, AAG, AAC, AGA, AAM, AGC, GAA, AAS. Neither of the sequences has AAT at codon 103. Therefore, the prevalence ratio for AAC to AAT was 100% to 0%, respectively.

3.1.3 Construction of plasmid-derived standards for the SPCR assays

3.1.3.1 RT-PCR and PCR amplification of HIV-1 *RT* gene

Both pre-nested (RT-PCR) and nested PCR amplifications for samples STV139166 and STV128864 were successful and negative controls showed that the PCR reagents were not contaminated. Nested PCR generated 804-bp amplicons spanning the *RT* gene, and these were verified on a 0.8% agarose gel (**Figure 3.1**) with reference to a

1-kb DNA molecular marker. The concentrations of the purified nested PCR products for the samples determined by Nanodrop™ ND-1000 system (Nanodrop Technologies Inc., Delaware, USA) were 39.1 ng/μL and 37.1 ng/μL, respectively.

Table 3.1: Clinical information and demographics of patient samples.

STV #	Age	Gender	Treatment	NNRTI mutations
297883	9	Female	3TC,AZT,NVP	NONE
294855	<1	Male	3TC,d4T,KLT	NONE
294773	9	Male	3TC,d4T,EFV	NONE
294771	7	Male	3TC,d4T,EFV	NONE
293935	11	Male	3TC,EFV,d4T	NONE
290766	5	Female	3TC,d4T,KLT, Cotri ^a	NONE
288044	47	Female	ddI,d4T, Alluvia	NONE
286813	31	Female	KLT,ddI,AZT	NONE
286808	35	Female	3TC,KLT,d4T	NONE
286807	45	Female	3TC,AZT,EFV	NONE
286803	39	Female	KLT,ddI,AZT	NONE
284540	2	Female	3TC,d4T,KLT	NONE
288667	4	Male	3TC,d4T,ABC	NONE
288668	4	Female	3TC,KLT,d4T	NONE
291336	40	Female	ddI,d4T	NONE
291337	33	N/A*	3TC,d4T,EFV	NONE
294770	2	Male	3TC,KLT,d4T	NONE
296155	6	Male	3TC,d4T,KTL	NONE
285739	67	Male	KLT,ddI,AZT	K103N
288042	63	Female	3TC,d4T,EFV	K103N
288043	41	Male	3TC,d4T,EFV	K103N
289783	44	Female	KLT,AZT,ddI	K103N
290767	12	Male	3TC,d4T,EFV	K103N
292197	48	Female	3TC,EFV,d4T	K103N
294767	48	Male	3TC,AZT,EFV	K103N
284246	8	Male	3TC,d4T,EFV	K101E,V106M,G190A
288041	42	Female	AZT,3TC,KLT	K101E,V106M,G190A
275180	2	Male	3TC,KLT,ABC,INV,Cotri ^a	NONE
285742	41	Female	3TC,KLT,SQV,TDF	Y181C
292196	32	Female	KLT,AZT,ddI, Cotri ^a	E138A
286812	36	Female	3TC,d4T,EFV	V90I,K103N,V108I
275181	4	Male	3TC,d4T,KLT	NONE
296685	2	Female	3TC,KLT,d4T	E138S
289781	37	Female	3TC,d4T,EFV	V106M,Y188C
294769	13	Female	3TC,EFV,d4T	V106M.Y188L
293934	12	Female	3TC,d4T,KLT	NONE
294772	34	Female	3TC,d4T,EFV	NONE
295251	36	N/A*	3TC,EFV,d4T, Cotri ^a	NONE
293936	56	Male	3TC,EFV,d4T, Cotri ^a	V106M,G190A,F227L
297431	30	Female	TDF,EFV,3TC	V106M,G190A,F227L

N/A*, Not available; Cotri, Cotrimoxazole; AZT, Zidovudine; ABC, Abacavir; ddI, didanosine; 3TC, lamivudine; d4T, stavudine; NVP, nevirapine; IDV, indinavir; SQV, saquinavir; KLT, Kaletra (Lopinavir/ritonavir); EFV, efavirenz.

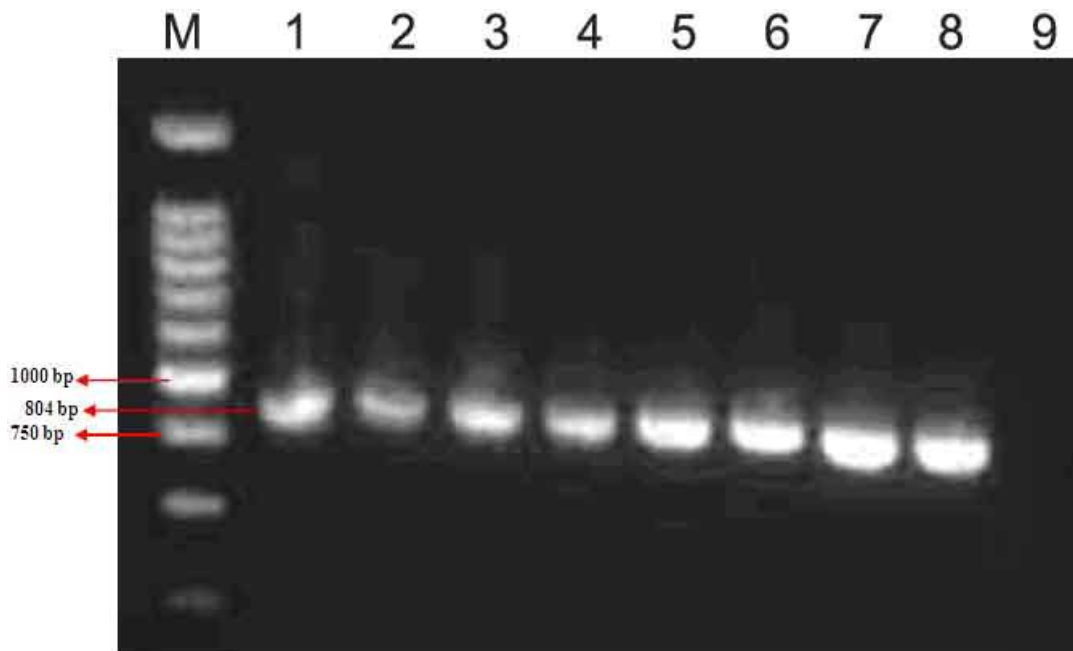


Figure 3.1: A 0.8% agarose gel image of 804-bp amplicons for samples STV139166 and STV128864 after RT-PCR and nested PCR amplification. Lanes 1-4 belong to samples STV128864 and lanes 4-8 to sample STV139166. Lane M is the molecular marker, 1-kb DNA ladder, and lane 9 is the negative control.

3.1.3.2 Transformation using JM109 High efficiency competent cells

A transformation efficiency of 1×10^8 cfu/ μ g DNA was achieved. Approximately 80 white and 15 blue colonies were observed on each of the two LB/ampicillin/IPTG/X-gal control plates on which a 100 μ L of the transformation culture with uncut plasmid was streaked. This proves that the JM109 cells used here were highly competent. The LB/ampicillin/IPTG/X-gal control plates, on which the JM 109 cells alone were streaked, had no colonies indicating that the ampicillin was active and it was not contaminated with plasmid. The LB/IPTG/X-gal control plates with no ampicillin, and streaked with the JM109 reaction was crowded with white colonies indicating that the JM109 cells were viable.

3.1.3.3 Screening for recombinant clones

The arrangement of the purified plasmid DNA is shown in **Figure 3.2** with reference to a 1-kb DNA ladder as the molecular marker. Lanes 2 and 3 for sample STV139166 shows that these clones do not have an insert because their bands moved faster than

the others which are circular or supercoiled like the pGEM®-T Easy vector.

Therefore, these clones were excluded for further analysis. The negative control, N (-), which has all PCR reagents including the primers except for template, shows that the PCR reactions were not contaminated.

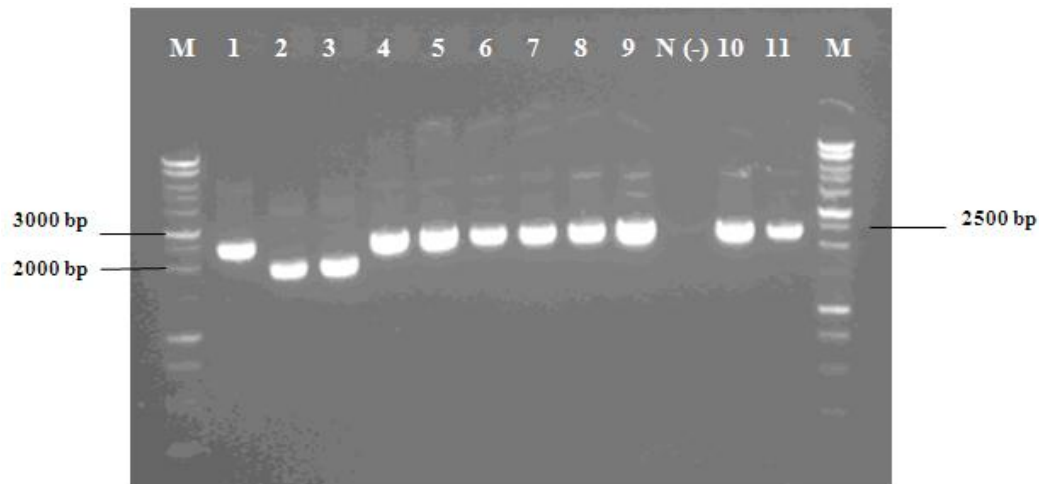


Figure 3.2: A 0.8% agarose gel image of some of the purified pGEM®-T Easy plasmid clones. Lane M represents the 1-kb DNA marker, lane 1-8 are plasmids from sample STV139166, lane 9-11 are for sample STV128864, and lane N(-) is a negative control.

An agarose gel image of pGEM®-T Easy plasmid DNA after enzyme digestion with the restriction enzyme *EcoRI* is shown in **Figure 3.3**. This is to verify if the insert is of the correct size. According to the agarose gel electrophoresis, the plasmid clones in lanes 2, 4, 10 and 13, which are uncut and supercoiled, have the correct insert of size 804 bp. This is because their cut plasmid DNA, which follows after each one of them, shows to have the desired insert of 804 bp and the linearized pGEM®-T Easy vector individually.

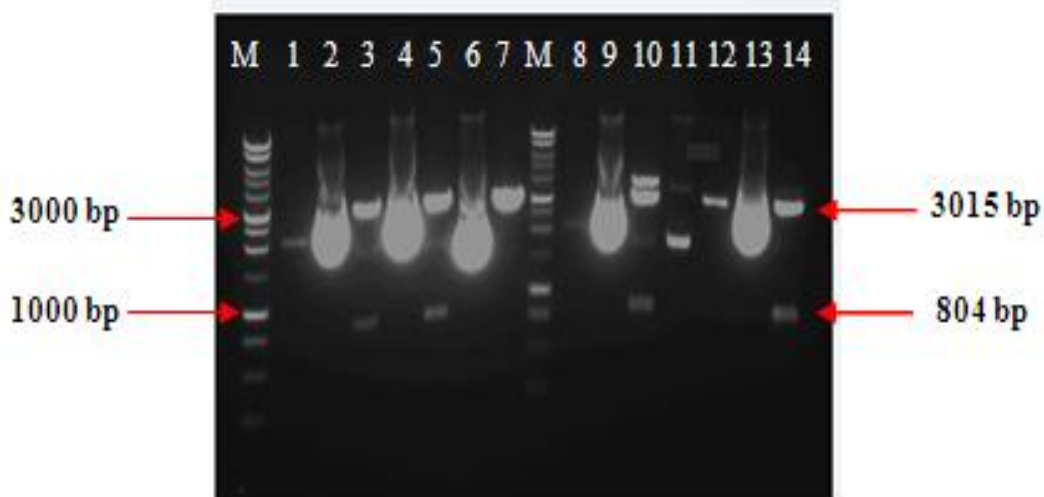


Figure 3.3: A 0.8% agarose gel photo of the pGEM®-T Easy recombinant plasmid clones after a restriction digestion with *EcoRI*. Lanes M represent the 1-kb DNA molecular marker, Lanes 1 and 8 are the plasmid control (pGEM®-T Easy vector). Lanes 2, 4, 6 and lanes 9, 11, 13, represent the uncut plasmid DNA of samples STV139166 and STV128864, respectively. Lanes 3, 5, 7 and lanes 10, 12, 14 represent the cut plasmid DNA of samples STV139166 and STV128864, respectively.

3.1.3.4 Sequence analysis of pGEM®-T Easy plasmid clones

The *RT* sequences of pGEM®-T Easy plasmid clones are shown in **Appendix C**, as supplementary results. The plasmid clones are listed in **Table 3.2**, with their codon at amino acid position 103 of the *RT*. They are all harbouring the K103N resistance mutation which is encoded by codon AAC or AAT.

3.1.4 Site-directed Mutagenesis

3.1.4.1 Mutagenesis of selected recombinant plasmids

The site-directed mutagenesis performed on four recombinant plasmids (MS3-A, MS9-A, MS10-A and MS15-A) is summarized in **Table 3.3**. During site-directed mutagenesis, MS1-V106M (F)/(R) primer set only changed valine(Val) to methylene (Met) at amino acid position 106 of the plasmid clone MS15, thereby generating a plasmid with V106M mutation. MS3-N103K-V106M (F)/(R) primer set replaced the amino acid lysine (Lys) in plasmid clone MS3 with asparagine (Asn) at position 103,

by inducing AAT transversion, another codon encoding K103N mutation, from AAC codon. Unlike codon AAC, which also encodes K103N, AAT is very uncommon. The primer set simultaneously substituted valine (Val) with methylene (Met) at position 106, causing a V106M mutation. MS9-N103K-V106M (F)/(R) and TV10AK1-N103K (F)/(R) primer sets replaced amino acid asparagine in plasmid MS9 and MS10 with lysine at position 103, respectively, generating AAA transversion (K103 wildtype). Simultaneously, MS9-N103K-V106M (F)/(R) primer set substituted valine (Val) in the same plasmid with methylene (Met) at position 106 to induce V106M mutation. The purpose of these primers was to generate sufficient standards with varying codons with regard to wildtype K103 and mutant K103N at amino acid positions 103 for the optimization of the K103N-specific SPCR assay.

Table 3.2: pGEM®-T Easy plasmid clones and their codon at amino acid position 103 of HIV-1 *RT*.

Sample	Plasmid Clone	Sequence length (bps)	K103N
STV# 139166	MS1	1729	AAC
	MS2	1784	AAC
	MS1-A	529	AAT
	MS2-A	619	AAT
	MS3-A*	617	AAC
	MS6-A	269	AAT
STV# 128864	MS9	1632	AAC
	MS9-A*	631	AAC
	MS10-A*	699	AAC
	MS11-A	721	AAC
	MS12-A	689	AAC
	MS14-A	614	AAC
	MS15-A*	648	AAC
	MS17-A	622	AAC

*Plasmid DNA used for site-directed mutagenesis.

Table 3.3: A summary of site-directed mutagenesis and the mutated plasmids generated.

Parental Plasmids & Genotype	Mutagenic primers	K103/N	V106/M	Mutated plasmids generated
<u>MS15-A</u> Asn (103)=K103N [AAC] Val (106) = V106 [GTG]	TV1-V106M (F) TV1-V106M (R)	Mutagenesis was not intended.	Val > Met = V106M (GTG > ATG)	MS15-3 MS15-4
<u>MS3-A</u> Asn (103) =K103N[AAC] Val (106) = V106 [GTG]	TV3-N103K-V106M (F) TV3-N103K-V106M (R)	Asn > Asn = K103N (AAC > AAT)	Val > Met = V106M (GTG > ATG)	MS3-1 MS3-2 MS3-4
<u>MS9-A</u> Asn (103) =K103N[AAC] Val (106) = V106 [GTG]	TV9-N103K-V106M (F) TV9-N103K-V106M (R)	Asn > Lys = K103 (AAC > AAA)	Val > Met = V106M (GTG > ATG)	MS9-2 MS9-3 MS9-4
<u>MS10-A</u> Asn (103) =K103N[AAC] Val (106) = V106 [GTG]	TV10AK1-N103K (F) TV10AK1-N103K (R)	Asn > Lys = K103 (AAC > AAA)	Mutagenesis was not intended.	MS10-1 MS10-2 MS10-3 MS10-4

3.1.4.2 Sequence analysis of site-directed mutagenesis-generated plasmid clones

All the mutated plasmids generated by site-directed mutagenesis were also sequenced and their sequences were compared with the consensus sequences of the four parental plasmids (MS3-A, MS9-A, MS10-A and MS15-A) in a multiple alignment. This was to verify if the desired mutations were successfully induced. The multiple sequence alignment is shown in **Figure 3.4**.

3.1.5 Primers and probes used for two real-time SPCR assays

According to the generated multiple sequence alignments of all 2008 subtype C HIV-1 RT sequences (shown in **Appendix C**) the greatest sequence diversity was found from RT nt 292-1326. This region encompasses a sequence where the K103N-specific forward primers C-103N.1F, C-103N.2F and C-103N.3F (nt 288-309), the two probes, 1P and 2P (nt 332-365), and the universal reverse primer 103/com.C3R (nt

385-412) were derived from (Johnson, Li et al. 2005). The region spanning nt 293 and further upstream to 5' end of the *RT* is more conservative and encompasses ComFWD, a forward primer that is meant to amplify or target any HIV-1 in a sample. A multiple sequence alignments of all primers and probes, 14 pGEM® T-Easy recombinant plasmid clones, Consensus C, and HIV-1 HXB2 as a background sequence, are displayed in **Appendix C**.

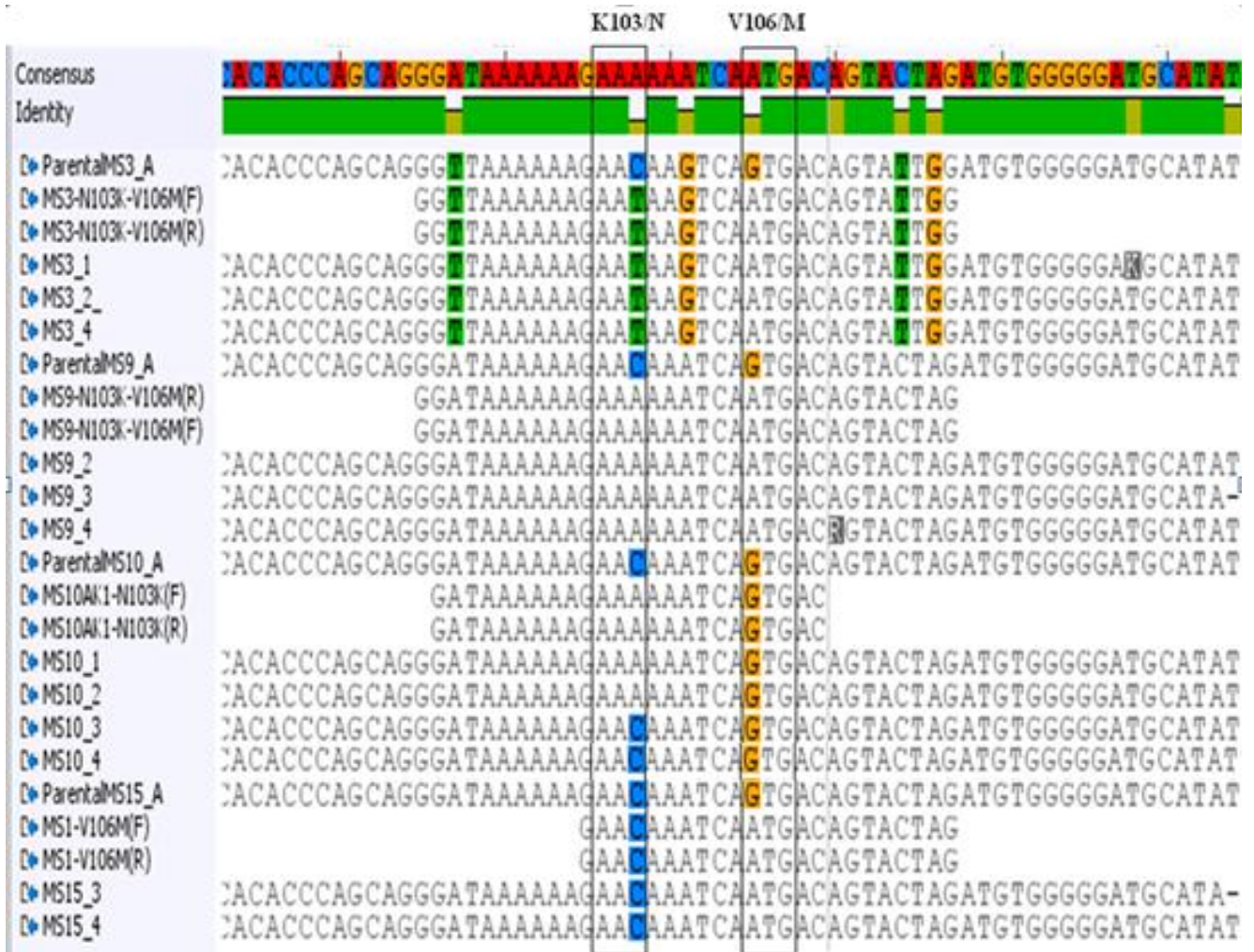


Figure 3.4: A multiple sequence alignment of *RT* Consensus C, consensus *RT* sequences of the four parental plasmids (pGEM® T-Easy) and all 12 mutated plasmid clones generated using Geneious version 4.5.5 (<http://www.geneious.com>). As in this order in the figure, it is parental plasmid (template for site-directed mutagenesis), mutagenic forward primer, mutagenic reverse primer (reverse complement), then the clones after site-directed mutagenesis. The first column labeled K103/N shows how

mutagenesis occurred at codon position 103. The second column labeled V106/M shows how mutagenesis occurred.

3.1.6 Total viral copy SPCR assay

3.1.6.1 The reactivity of total viral copy primers and probes

After three runs of the total viral copy experiment the total copy primers ComFWD (forward primer) and 103/com.C3R (reverse primer) were able to amplify all the 12 plasmid standards at 5 000 (**Figure 3.5 (a)**) as well as at 5 000 000 DNA copies/ μ l (**Figure 3.5 (b)**). The reactions were not contaminated as three replicates of the no-template controls (NTCs - negative controls) were not amplified. The probes are working effectively as indicated by the amplification curves (fluorescent signals) in **Figure 3.5** generated for all these plasmid standards.

The threshold cycle (Ct) values after three runs, including the representative amplification plots in **Figure 3.5**, for testing the reactivity of the total copy primers and probes on 12 plasmid standards are supplied in **Table 3.4**. A successful amplification of all K103 wild-type and K103N-mutant plasmid controls with Ct ranges of 26-30 for 5×10^3 and 17-20 for 5×10^6 DNA copy/ μ l indicate that the primers and the probes are ideal for annealing to various HIV-1 subtype C sequences. A significant difference in Ct observed with the plasmid standards at 5 000 DNA copy/ μ l is due to the presence of different nucleotide sequences with varying binding affinity for total copy primers found when the same standard is being used across the three runs.

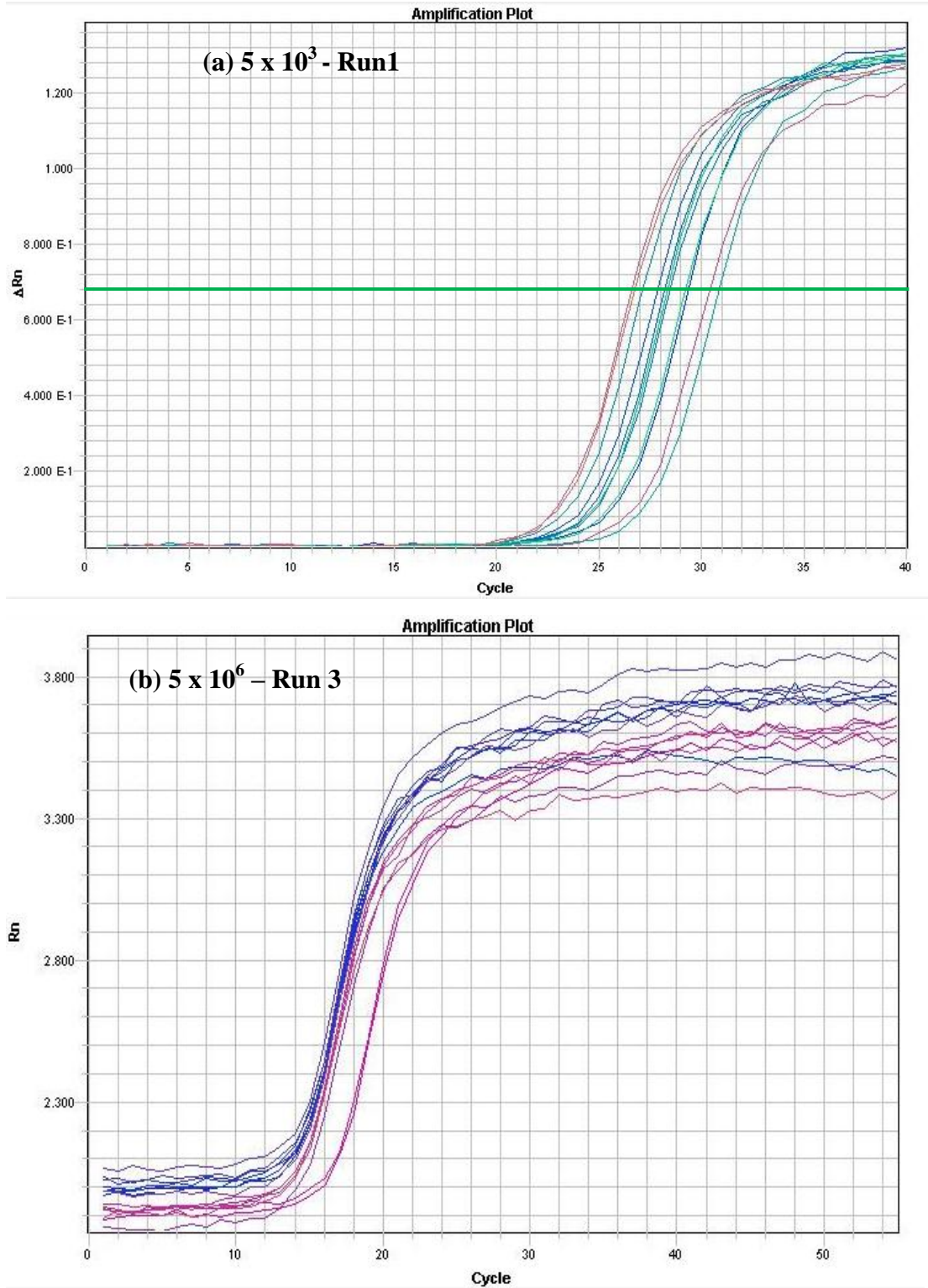


Figure 3.5: Representative amplification plots showing the amplification curves of all 12 plasmid standards for testing the reactivity of total copy primers and probes. (a) Run 1 - all 12 plasmid standards at 5 000 DNA copy/ μ l with Ct values ranging from 26-31. (b) Run 3 - all 12 plasmid standards at 5 000 DNA copy/ μ l with Ct ranging from 17-20.

Table 3.4: Mean threshold cycle (Ct) values after three runs of the total copy experiment for testing the reactivity of total copy primers and probes on all 12 standards at low and high DNA copy numbers.

Plasmid standard	K103/N	DNA copy/ μ l, 5×10^3				DNA copy/ μ l, 5×10^6			
		Ct ₁	Ct ₂	Ct ₃	Average Ct	Ct ₁	Ct ₂	Ct ₃	Average Ct
MS3-1	AAT	27.58	27.53	29.40	28.00	18.16	19.27	19.	19.12
MS3-2	AAT	26.59	26.03	28.20	27.73	19.80	18.60	20.97	20.64
MS3-4	AAT	28.55	27.90	28.40	28.70	20.74	19.68	18.92	19.50
MS9-2	AAA	28.00	29.70	28.76	28.82	19.62	19.48	18.90	19.52
MS9-3	AAA	28.42	27.89	29.45	28.76	18.50	19.78	20.42	19.96
MS9-4	AAA	28.75	29.79	29.20	29.44	18.32	17.24	20.98	18.85
MS10-1	AAA	29.42	31.28	28.88	29.86	19.00	18.98	20.94	19.64
MS10-2	AAA	26.93	26.99	29.28	27.73	18.54	20.18	20.20	19.64
MS10-3	AAC	27.96	28.98	29.75	28.95	18.95	19.15	18.65	18.98
MS10-4	AAC	31.02	31.74	29.70	30.82	20.54	18.70	19.63	19.72
MS15-3	AAC	27.23	28.98	29.75	28.65	20.70	17.01	19.34	18.62
MS15-4	AAC	30.52	27.89	30.75	29.46	19.96	20.03	17.94	19.31
NTC		N/A	N/A	N/A	N/A	N/A	N/A	N/A	N/A
NTC		N/A	N/A	N/A	N/A	N/A	N/A	N/A	N/A
NTC		N/A	N/A	N/A	N/A	N/A	N/A	N/A	N/A

NTC - No-template control; N/A - No Amplification; Ct₁ – mean Ct for Run 1; Ct₂ – Mean Ct for Run 2; Ct₃ – Mean Ct for Run 3.

3.1.6.2 Total viral copy primer optimization

Three runs of the experiment to adjust the total copy primer concentrations using titrations of 50 nM, 300 nM and 900 nM concentrations revealed that 900:900 forward primer to reverse primer concentration ratio of ComFWD and103/com.C3R, respectively, was found to be the optimal. This is because it yielded the lowest Ct values after three runs for the total copy reaction. The reactions were not

contaminated as three replicates of no-template controls (NTCs - negative controls) were not amplified. The results of the experiment are shown in **Table 3.5**. A significant difference in Ct observed with the plasmid standards at 5 000 DNA copy/ μ l is due to the presence of difference nucleotide sequences, with varying binding affinity for total copy primers, found in a common standard across the runs.

Table 3.5: Mean Ct values after three runs for the titration experiment using the total copy primers on the AAC-mutant standard MS15-3 at 5 000 DNA copies/ μ l.

[ComFWD]:[103/com.C3R] [nM]	Mean Ct ₁	Mean Ct ₂	Mean Ct ₃	Average Ct
50:50	37.45	37.78	39.46	38.92
50:300	33.36	32.12	31.06	32.18
50:900	33.00	34.25	30.05	33.10
300:50	35.40	29.90	32.60	32.30
300:300	28.80	32.75	29.05	29.85
300:900	30.05	31.40	27.45	29.20
900:50	31.32	33.46	30.82	32.60
900:300	27.50	32.86	28.12	29.38
900:900	27.60	31.30	29.28	28.76
No-template control (NTC)	N/A	N/A	N/A	N/A
No-template control (NTC)	N/A	N/A	N/A	N/A
No-template control (NTC)	N/A	N/A	N/A	N/A

N/A – No amplification; Ct₁ – Ct for Run 1; Ct₂ – Ct for Run 2; Ct₃ – Ct for Run 3.

3.1.6.3 Total viral copy probe optimization

The results following three runs for the probe titration experiment in the total viral copy reaction using a mixture of 75% 1P and 25% 2P probes with MS15-3 (K103N) mutant plasmid standard as a template revealed that a mixture of the two probes offers the optimal sequence detection in real-time when each probe is at a concentration of 300 nM, and provided that the total copy forward primer ComFWD and the universal reverse primer 103/com.C3R are at a constant concentration ratio of 900:900 (nM). It was therefore chosen because it yielded a minimum threshold cycle value compared to the rest of the concentrations (50 nM, 100 nM, 150 nM, 200 nM and 250 nM) used. Moreover, it yielded a smaller range, unlike the others, thus showing to be reliable.

The reactions were not contaminated as three replicates of the no-template controls (NTCs - negative controls) were not amplified. The results are provided in **Table 3.6**.

Table 3.6: Mean Ct values after three runs of the probe titration experiment with total copy primers (900:900 nM; forward: reverse) on the AAC-mutant standard MS15-3 at 5×10^3 DNA copy/ μ l.

[1P+2P] nM	Mean Ct	Mean Ct	Mean Ct	Average Ct
50	33.78	32.85	27.20	31.22
100	26.90	30.85	33.14	29.19
150	32.29	27.02	31.15	29.78
200	29.44	32.78	26.99	29.38
250	30.88	32.05	27.02	29.40
300	27.40	27.70	28.18	27.76
NTC	N/A	N/A	N/A	N/A
NTC	N/A	N/A	N/A	N/A
NTC	N/A	N/A	N/A	N/A

[1P+2P] – 75% Probe 1 plus 25% Probe 2; NTC – No-template control; N/A – No amplification; Ct₁ – Ct for Run 1; Ct₂ – Ct for Run 2; Ct₃ – Ct for Run 3.

3.1.6.4 Standard curve for total viral copy SPCR assay

Over eight standard curves were constructed in the total copy SPCR reaction with serial dilutions (5×10^7 to 5×10^0 DNA copy/ μ l) of MS15-3 K103N-mutant standard. The average Ct values of the linear dynamic range from the fluorescence data of eight runs is shown in **Table 3.7**. The reactions from the chosen eight runs were not contaminated as three replicates of the no-template controls (NTCs - negative controls) were not amplified. In addition, two K103-wild-type and one K103N-mutant controls included in two replicates for each at 5×10^0 and 5×10^6 copy/ μ l were MS9-3 (WT), MS10-2 (WT) and MS10-4 (MUT). They were amplified with the same efficiency (approximately) as the MS15-3 standard at the same DNA copy numbers in all eight assay runs, thus validating the accuracy of the assay (data is supplied in **Table 3.8**). SDS 2.3 software collected these fluorescence data from the linear phase

of the exponential PCR so that a broad dynamic range of the amplicon, which is directly proportional to the fluorescence emitted, can be detected.

Table 3.7: Threshold cycle (Ct) data after the construction of a standard curve with K103N-mutant standard MS15-3 (AAC) from eight (8) runs using total viral copy SPCR assay. Data for negative controls (NTCs), K103-wild-type and K103N-mutant controls is also included.

DNA copy/ul (MS15-3)	Ct ₁	Ct ₂	Ct ₃	Ct ₄	Ct ₅	Ct ₆	Ct ₇	Ct ₈	Average Ct
5	37.56	N/A	N/A	38.84	N/A	41.03	41.25	N/A	39.14
5	37.96	N/A	N/A	38.48	N/A	41.16	41.25	N/A	39.71
50	34.04	35.14	35.94	35.21	35.92	37.38	38.64	N/A	36.04
50	34.01	34.92	35.98	35.21	35.60	37.56	38.01	N/A	35.90
500	30.36	31.98	32.18	32.33	32.49	33.61	35.26	35.68	32.99
500	30.20	32.06	32.75	32.24	32.49	33.91	34.47	35.79	32.99
5 000	27.28	28.93	29.88	28.66	28.87	30.72	31.94	32.97	29.91
5 000	27.31	28.93	29.88	28.66	28.61	30.84	31.67	32.93	29.85
50 000	23.83	25.54	26.39	25.12	25.65	27.62	28.94	30.24	26.67
50 000	23.02	25.50	26.22	25.02	25.65	27.6	28.75	30.34	26.51
500 000	19.68	21.39	22.53	21.97	22.17	24.91	25.03	26.73	23.05
500 000	19.99	21.23	22.53	21.90	22.10	25.02	25.29	26.84	23.11
5 000 000	16.72	18.03	19.01	18.51	18.42	21.03	21.33	22.85	19.49
5 000 000	16.96	18.10	18.79	18.61	18.34	20.97	21.52	23.01	19.54
50 000 000	N/A	14.40	14.90	15.05	14.67	16.10	16.50	17.68	15.61
50 000 000	N/A	14.48	14.94	15.05	14.88	16.15	16.53	17.71	15.68
3 NTCs	N/A	N/A	N/A	N/A	N/A	N/A	N/A	N/A	N/A
Wt MS9-3 (5x10 ⁰)	N/A	N/A	39.12	N/A	39.09	N/A	39.10	38.52	38.96
Wt MS9-3 (5x10 ⁶)	20.56	20.12	19.20	19.85	19.72	19.33	18.32	20.08	19.65
Wt MS10-2 (5x10 ⁰)	N/A	39.19	N/A	N/A	38.94	N/A	38.66	38.79	38.90
Wt MS10-2 (5x10 ⁶)	17.78	18.75	19.56	18.19	19.89	18.66	19.91	19.79	19.07
Mut MS10-4 (5x10 ⁰)	N/A	N/A	N/A	39.19	N/A	N/A	N/A	38.79	38.99
Mut MS10-4 (5x10 ⁶)	19.92	20.00	19.05	19.19	19.89	19.66	19.68	19.26	19.58

N/A – No amplification; NTC – No-template control; Ct₁ – Ct for Run 1; Ct₂ – Ct for Run 2; Ct₃ – Ct for Run 3; Ct₄ – Ct for Run 4; Ct₅ – Ct for Run 5; Ct₆ – Ct for Run 6; Ct₇ – Ct for Run 7; Ct₈ – Ct for Run 8.

The mean Ct linearly correlates with the DNA copy number over the range of $0\log_{10}$ to $7\log_{10}$ of the mutant (K103N) dilution series. Overall, a slope of -3.35 proves that amplification or PCR was 98.84% efficient. Amplification efficiency (E) is calculated from the slope with the following equation: $E = 10^{(-1/\text{slope})} - 1$ (Paredes, Marconi et al. 2007). It ranged from 90.59% to 97.99% across all eight runs, which is within the acceptable precision range of 90-110% (Burd 2010). The y-intercept reflects on the sensitivity or the lower detection limit of the assay by showing how many cycles are required to detect 1 DNA copy. An estimate of 40 cycles is required to detect 1 DNA copy using the total viral copy primer and probe set. The intra- and inter-assay precision is 99.84% and 99.54% and it is defined by the repeatability (R^2) and the reproducibility, respectively. The former reflects on the closeness of the replicate data points (concentration) to the regression line in each assay run, whereas the latter is average the former across eight assay runs. The intra-assay precision for each of the eight runs ranged from 98.33 to 99.96% (**Table 3.8**). This makes the total viral copy SPCR assay highly consistent (Muller, Stelzl et al. 2004). The standard curve with the average values (Ct) of all eight runs is shown in **Figure 3.6**.

Table 3.8: Assay efficiency and reproducibility results for the total copy SPCR standard curve experiment after 8 runs.

	Run 1	Run 2	Run 3	Run 4	Run 5	Run 6	Run 7	Run 8	Average
Slope	-3.57	-3.47	-3.49	-3.37	-3.49	-3.41	-3.45	-3.54	-3.35
Efficiency	90.59	93.99	93.59	97.99	93.36	95.64	94.92	91.78	98.84
Y-intercept	37.16	39.95	39.79	38.73	39.39	41.05	41.85	43.64	39.63
R^2 - repeatability	99.80	99.79	99.68	99.96	99.93	99.48	99.36	98.33	99.84
Cycles	50	55	55	55	55	55	55	55	
Reproducibility									99.54

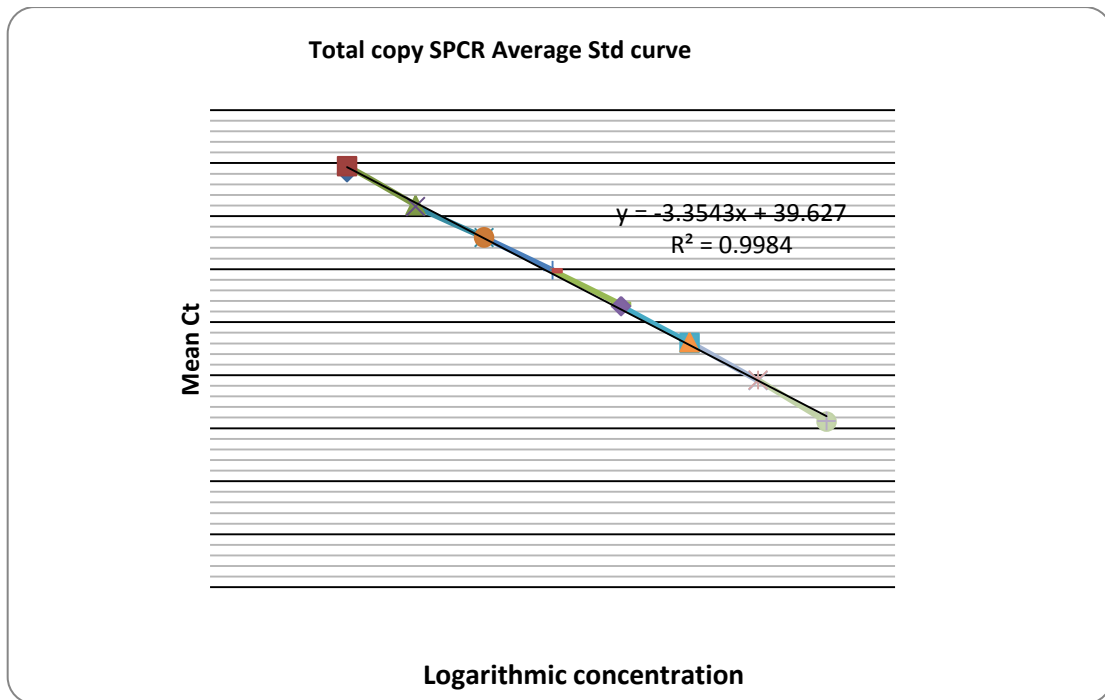


Figure 3.6: The average standard (std) curve for the total viral copy SPCR assay. The mean threshold values (Ct) are plotted on the y-axis and the mean logarithmic of the initial DNA copy number/ μL of the AAC-mutant standard MS15-3 on the x-axis are from eight runs with each dilution/point in duplicates. The standard curve forms a straight line over eight orders of magnitude. The equation on the plot stands for $y = mx + c$, which defines the linear regression, with „m’ representing the slope (-3.3493), „c’ as the y-intercept (39.627) and „R²’ stands for the repeatability of the assay.

3.1.7 K103N-SPCR assay

3.1.7.1 The reactivity of K103N-specific primers and probes

Among several experiments (Experiment 1-5) performed on 12 plasmid standards (50 000 DNA copy/ μl) with three specific forward primers C-103N.1F, C-103N.2F and C-103NT.3F, individually or in a mixture, amplification was found only in Experiment 3, 4 and 5. These are the experiments in which primer C-103NT.3F is present either alone (Experiment 3) or in a mixture with C-103N.1F (Experiment 4) or C-103N.1F and C-103N.2F (Experiment 5). In Experiment 3, C-103NT.3F amplified the K103N standards encoded by AAT (MS3-1, MS3-2 & MS3-4) at *RT* codon 103. In Experiment 4 and 5, it was still able to amplify the same standards when used in combination with C-103N.1F, or with both C-103N.1F and C-103N.2F, but with less

efficiency though. The probes are working as indicated by the fluorescent signals (on the amplification plots in all five experiments) generated during specific hybridization between the 5' FAM-labelled probes and the target. The reactions were not contaminated as three replicates for no-template controls (NTCs - negative controls) were not amplified. Amplification plots for Experiment 3, 4, and 5 on the 12 plasmid controls are shown in **Figure 3.7**.

The mean threshold cycle (Ct) values for Experiment 4 when C-103NT.3F was used in a mixture with C-103N.1F range from 33 to 36. This indicates C-103N.1F decreases the reactivity of C-103NT.3F with AAT standards, unlike when it is used alone, as shown above. Moreover, its reactivity in Experiment 5 decreases when used in a mixture with C-103N.1F and C-103N.2F, resulting in a mean threshold cycle (Ct) range of 31-33. It worked better in Experiment 3 when used alone as the only forward primer, yielding a mean Ct of 28-31. Three no-template controls (NTCs) included in each run were not amplified, showing that the reagents were not contaminated. Threshold cycle (Ct) values representing the reactivity of the K103N-specific primer and probe sets used in experiment 3, 4, and 5, are shown in **Table 3.9**.

3.1.7.2 New additional specific-primer and its reactivity

Since out of all three K103N-specific primers only C-103NT.3F was able to amplify some of the 12 standards which are encoded by codon AAT at 103, it was then decided to design another primer which was called C-103N.3FC which will target the prevalent codon AAC for K103N. This new primer was found specific for codon AAC after assessing it on all 12 plasmid standards (500 000 DNA copy/ μ l) in three runs. The results are represented by an amplification plot displaying amplification curves for all four AAC mutant plasmid standards (MS10-3, MS10-4, MS15-3 and MS15-4) in **Figure 3.8**.

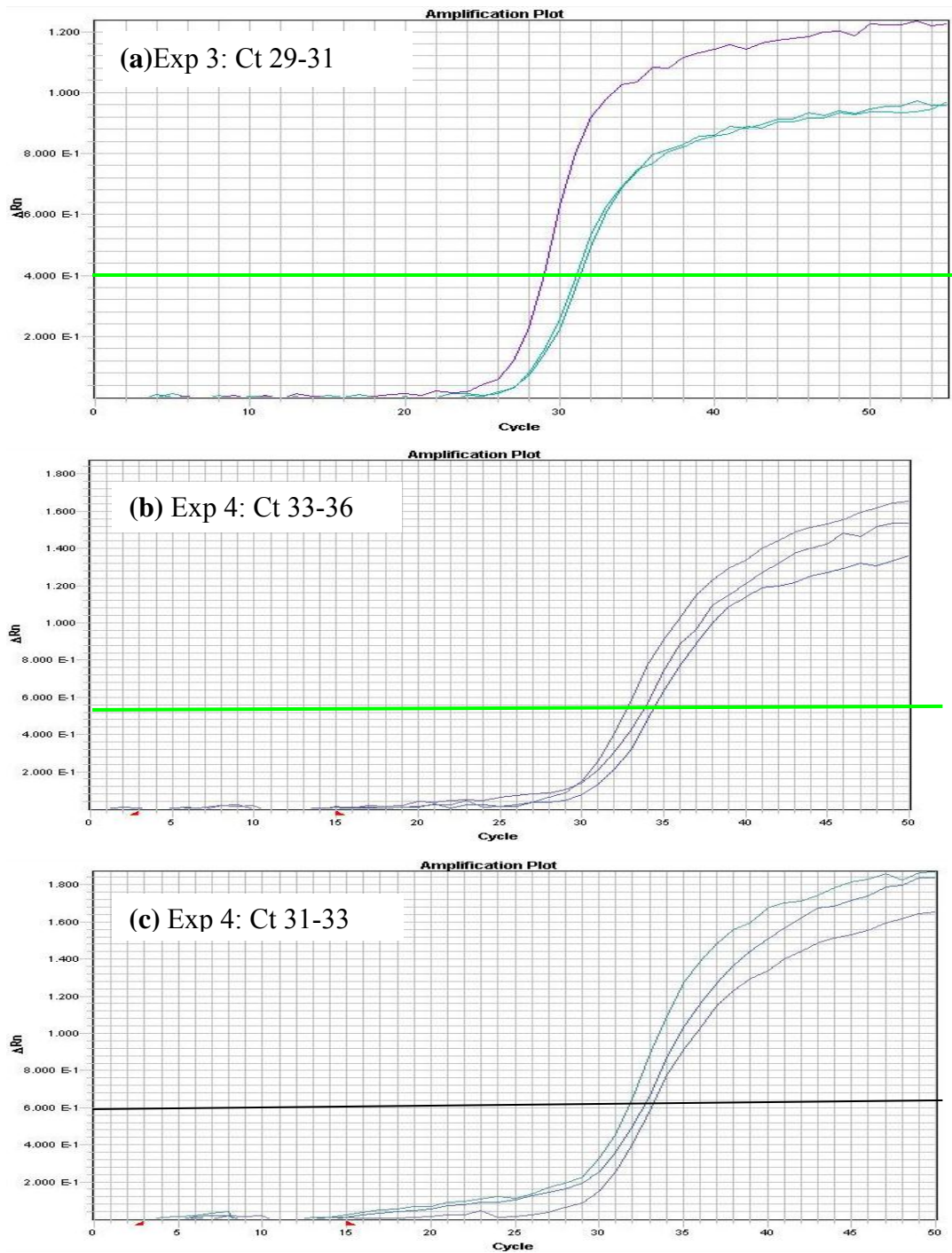


Figure 3.7: Representative amplification plots showing the reactivity of K103N specific primers and probes on three (3) plasmid standards. **(a)**, Exp 3: amplification curves for the three AAT-K103N standards generated with C-103NT.3F only. **(b)** Exp 4: amplification curves generated with a mixture of C-103N.1F and C-103NT.3F. **(c)** Exp 5: amplification plot generated with a mixture of C-103NT.3F, C-103N.1F and C-103N.2F.

Table 3.9: Threshold cycle (Ct) values from Experiments (Exp) 3, 4 and 5 for testing the reactivity of K103N-specific forward primers C-103NT.3F, C-103N.1F and C-103N.2F on four AAT-K103N plasmid standards at 5×10^0 DNA copy/ μ L.

AAT-K103N Plasmid standard	Exp 3			Exp 4			Exp 5			Exp 3	Exp 4	Exp 5
	Ct ₁	Ct ₂	Ct ₃	Ct ₁	Ct ₂	Ct ₃	Ct ₁	Ct ₂	Ct ₃	Ave. Ct	Ave. Ct	Ave. Ct
MS3-1	31.23	28.78	30.26	32.84	36.98	37.95	30.25	36.26	33.06	30.09	35.92	33.19
	31.23	28.78	30.27	32.85	36.98	37.95	30.26	36.26	33.07	30.09	35.93	33.20
MS3-2	31.26	29.40	26.89	32.45	36.38	31.95	28.78	29.80	33.62	29.18	33.59	30.73
	31.27	29.40	26.88	32.44	36.38	31.96	28.79	29.79	33.63	29.18	33.59	30.74
MS3-4	30.62	30.10	27.05	31.48	34.42	32.00	29.45	30.50	33.87	29.26	33.49	31.47
	30.63	30.11	27.06	31.48	34.41	32.02	29.46	30.48	33.88	29.27	32.64	31.27

Ct₁ – Ct for Run 1; Ct₂ – Ct for Run 2; Ct₃ – Ct for Run 3; Ave. Ct – Average Ct.

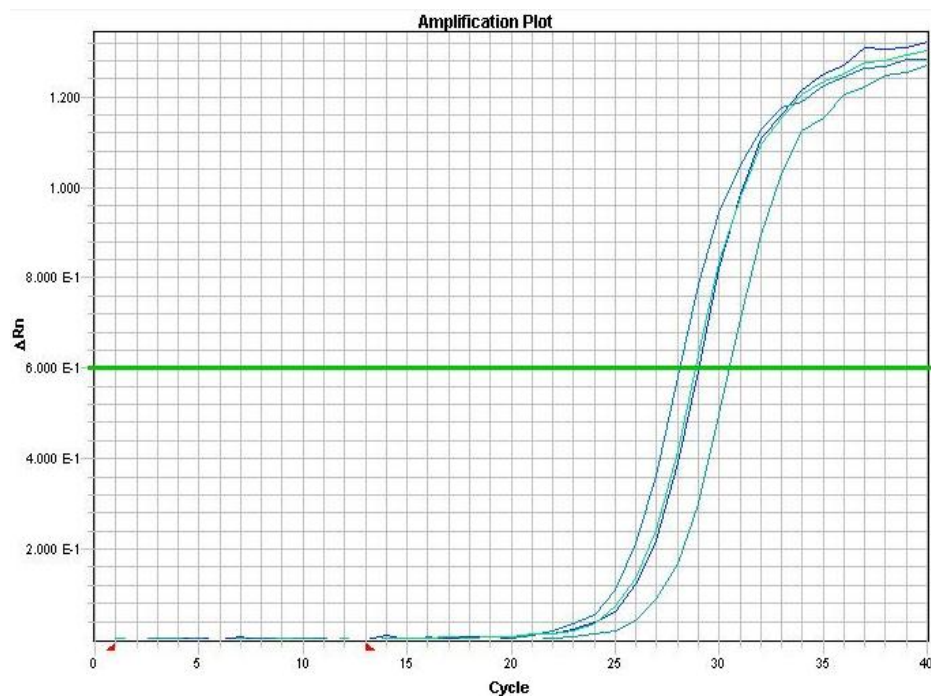


Figure 3.8: A representative amplification plot displaying amplification curves generated with the specific forward primer C-103N.3FC for all four AAC-K103N mutant standards.

The threshold cycle (Ct) values, for all four AAC-K103N plasmid standards (MS10-3), MS10-4, MS15-3, and MS15-4), range from 28 to 31 across all three runs with each reaction in duplicate. There was no amplification the three reactions of the no-template controls (NTCs) included. The results are provided in **Table 3.10**.

Table 3.10: Threshold cycle (Ct) values for all K103N-mutant standards encoding AAC in the reactivity experiment using new specific forward primer C-103N.3FC.

AAC-K103N Plasmid Standards	Ct ₁	Ct ₂	Ct ₃	Average Ct
MS10-3	28.01	27.02	29.64	28.00
	28.19	27.05	29.63	28.29
MS15-3	30.20	31.70	29.40	31.06
	30.23	31.69	29.47	30.46
MS10-4	28.55	28.02	31.38	29.01
	28.61	27.98	31.37	29.32
MS15-4	30.17	30.86	29.08	29.85
	30.18	30.86	29.10	30.05

Ct₁ – Ct for Run 1; Ct₂ – Ct for Run 2, Ct₃ – Ct for Run 3.

3.1.7.3 K103N-specific primer optimization

The experiments to adjust the K103N-specific primer concentrations using titrations of 50 nM, 300 nM and 900 nM concentrations revealed that 900:900 forward primer to reverse primer concentration ratio of C-103NT.3F and 103/com.C3R is the optimal. The titration experiments with C-103N.3FC, the newly designed specific primer, and the universal reverse primer 103/com.C3R also revealed that the 900:900 concentration ratio gives efficient amplification. This is because it yielded the lowest Ct values in two independent experiments. The reactions were not contaminated as three replicates of no-template control (negative control) were not amplified. The threshold cycle results for plasmid standard MS3-4 (AAT) as a template in the Experiment 1, and MS15-3 (AAC) used in Experiment 1, at 500 000 copy/μl, are shown in **Table 3.11**.

Table 3.11: Mean threshold cycle (Ct) values from two primer titration experiments using two K103N specific primers individually.

Forward: Reverse [nM]	Exp 1 (Run 1-3) [MS3-4] Mean Ct			Exp 2 (Run 1-3) [MS15-3] Mean Ct			Exp 1 Average Ct	Exp 2 Average Ct
	50:50	N/A	N/A	N/A	N/A	N/A	N/A	N/A
50:300	37.40	N/A	N/A	N/A	35.70	N/A	37.40	35.70
50:900	N/A	37.83	N/A	38.99	N/A	37.89	37.83	37.94
300:50	N/A	N/A	36.21	N/A	37.25	N/A	36.21	37.25
300:300	29.10	32.25	28.10	31.25	33.60	32.15	30.90	32.00
300:900	27.80	28.70	30.85	32.17	33.15	30.26	29.45	31.22
900:50	N/A	38.90	N/A	N/A	N/A	36.10	38.90	36.10
900:300	27.40	28.14	29.25	29.45	28.10	27.26	28.74	28.82
900:900	26.50	27.85	29.15	27.85	29.90	26.85	27.90	28.53

N/A – No amplification; Exp 1 - [C-103NT.3F]: [103/com.C3R];

Exp 2 - [C-103N.3FC]:[103/com.C3R]

3.1.7.4 K103N-specific probe optimization

The probe titration results from Experiment 1 using the K103N-specific primer C-103NT.3F with 5×10^5 DNA copy/ μ L of MS3-4 (AAT-K103N) as the mutant standard; Experiment 2 which used C-103N.3FC as the specific primer with 5×10^5 DNA copy/ μ L MS5-3 (AAC-K103N) standard revealed that a mixture of 1P and 2P at a 75:25 ratio offers optimal sequence detection when each probe is at a concentration of 300 nM. It was chosen since it yielded a minimum threshold cycle value compared to the rest of the probe concentrations used. The reactions were not contaminated as three replicates of the no-template control (negative control) were not amplified. The results are provided in **Table 3.12**.

Table 3.12: Mean threshold cycle (Ct) values from the probe titration experiments after using two K103N specific primers individually. In Experiment 1 C-103NT.3F was used on MS3-4 (AAT) and Experiment 2 C-103N.3FC was used on MS15-3 (AAC).

[1P+2P] nM	Exp 1 – MS3-4 Mean Ct (Run 1-3)			Exp 2 – MS15-3 Mean Ct (Run 1-3)			Exp 1 Average Ct	Exp 2 Average Ct
50	31.49	N/A	N/A	N/A	N/A	32.14	31.49	32.14
100	30.82	31.75	N/A	N/A	30.05	N/A	30.09	30.05
150	29.81	30.55	31.10	29.61	28.85	32.41	30.23	30.61
200	31.80	33.68	32.00	33.45	27.85	28.80	32.49	30.00
250	32.45	28.18	31.56	31.45	31.63	27.32	30.95	29.85
300	31.40	31.50	27.23	30.25	27.55	30.60	29.96	29.80

N/A – No amplification.

3.1.7.5 Evaluation of the discriminatory ability of K103N-SPCR assay

No cross-reactivity was observed between the K103 wild-types (AAA) and the K103N mutants (AAC or AAT) when comparing the Ct values of the three species (AAA, AAC, and AAT) in a K103N-specific experiment, with each standard at 5×10^6 DNA copy/ μ l. The results after three runs are represented by the amplification plots in **Figure 3.9** where the amplification curves for the K103N-mutant standards encoded by AAC are depicted in **(b)**, with mean Ct value of 30.65, whereas the rest of the wild-types ranged between 44 and 47 (**Table 3.12**). Amongst the mutants, the Ct values for the AAT mutant standards roughly ranged between 26 and 27, whereas all the AAC mutant standards ranged between 30 and 31. The reactions were not contaminated as the three replicates for the no-template controls (negative controls) were not amplified. The mean Ct values from the three runs of the discriminatory ability experiment on all 12 plasmid standards are shown in **Table 3.13**.

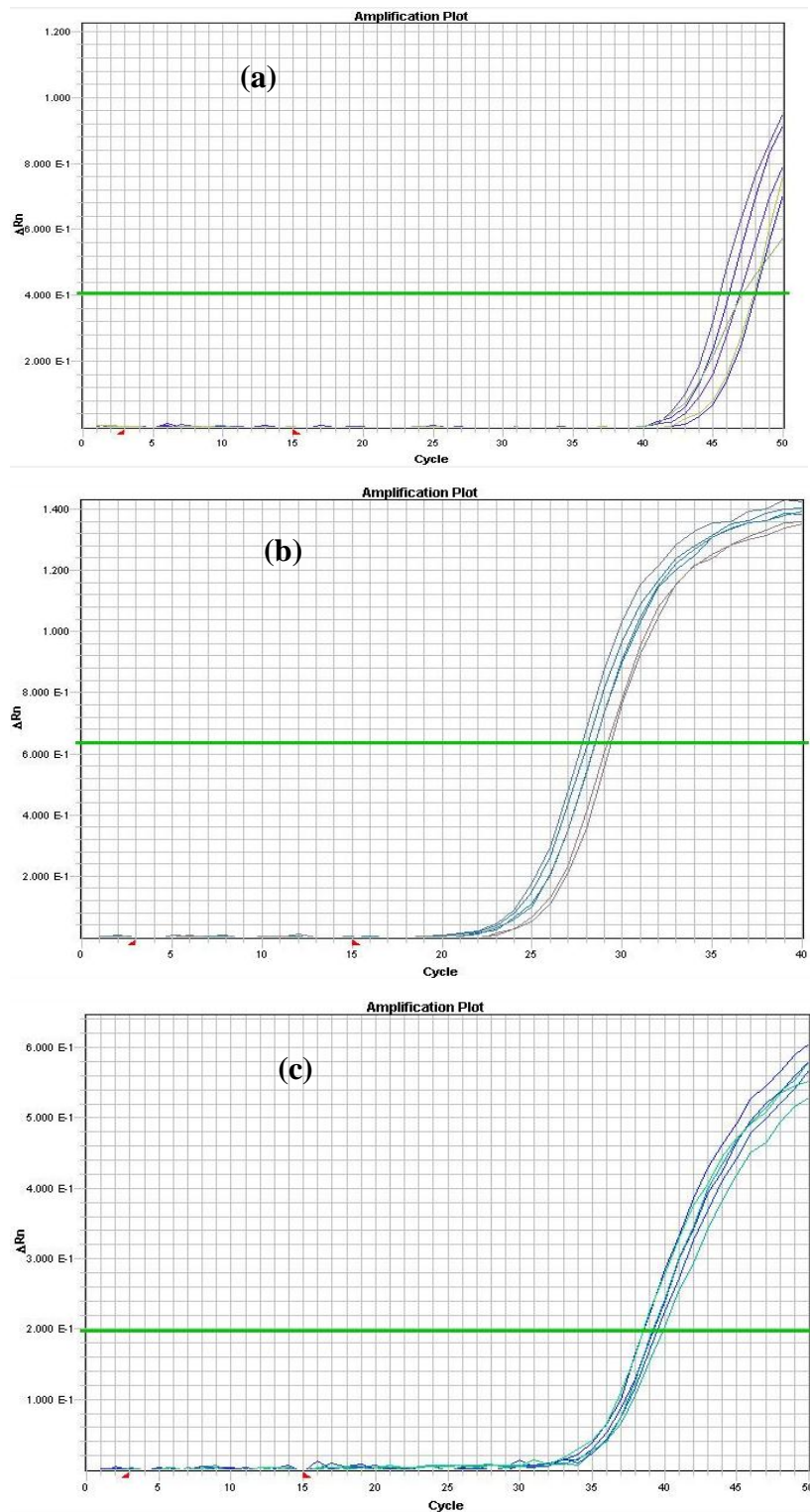


Figure 3.9: Amplification plots showing the discriminatory ability of five K103N specific primers on all 12 genetically varying standards. **(a)** Five WT-standards (MS9-2, MS9-3, MS9-4, MS10-1 & MS10-2) at 5×10^6 copy/ μ L. **(b)** and **(c)** Seven MUT-standards (AAC/T) (MS3-1, MS3-2, MS3-4, MS10-3, MS10-4, MS15-3 & MS15-4) at 5×10^6 copy/ μ L, and 5×10^3 copy/ μ L, respectively.

Table 3.13: Mean threshold cycle (Ct) values after assessing the discriminatory ability of a mixture of C-103N.3F and C-103NT.3FC on all 12 plasmid standards at low (5×10^3) and high (5×10^6) DNA copy/ μ l.

Plasmid standard	K103/N	Low copy number 5×10^3			High copy number 5×10^6			Average Ct	Average Ct
		Run 1	Run 2	Run 3	Run 3	Run 2	Run 3		
		Ct	Ct	Ct	Ct	Ct	Ct		
MS3-1	AAT	37.58	39.22	38.20	27.80	28.10	29.02	38.00	28.92
MS3-2	AAT	36.50	36.03	36.20	27.97	29.30	28.60	38.73	28.68
MS3-4	AAT	38.50	37.90	39.40	28.92	29.78	29.68	38.70	29.44
MS9-2	AAA	N/A	N/A	N/A	44.90	44.62	45.48	N/A	45.00
MS9-3	AAA	N/A	N/A	N/A	50.42	48.50	50.78	N/A	49.90
MS9-4	AAA	N/A	N/A	N/A	46.98	47.32	47.40	N/A	47.20
MS10-1	AAA	N/A	N/A	N/A	47.02	46.00	45.98	N/A	46.40
MS10-2	AAA	N/A	N/A	N/A	48.20	46.54	46.79	N/A	47.19
MS10-3	AAC	37.95	40.00	38.90	28.65	28.95	29.00	38.95	29.20
MS10-4	AAC	38.40	37.53	40.97	29.63	30.54	28.70	39.30	29.65
MS15-3	AAC	38.75	39.30	37.20	29.33	30.70	27.01	38.45	28.52
MS15-4	AAC	39.12	39.22	40.00	28.94	30.96	27.98	39.46	29.49

N/A – No amplification.

3.1.7.6 Standard curve for K103N-SPCR assay

Data obtained from eight runs of the K103N-SPCR assay while generating the standard curve using the serial diluted (5×10^7 to 5×10^0 DNA copy/ μ l) AAC-K103N mutant standard (MS15-3) is presented in **Table 3.14**. The reactions were not contaminated as the three replicates of no-template controls (negative controls) were not amplified. Three 5×10^0 DNA copy/ μ l replicates for MS9-3 and MS10-2 as wild-type controls were not amplified in all eight runs, whereas some of the three replicates at 5×10^6 DNA copy/ μ l for these controls were amplified with Ct values around those of the mutant standard MS15-3 at 5×10^0 DNA copy/ μ l concentration.

Table 3.14: Threshold cycle (Ct) values after eight runs for constructing K103N-SPCR standard curve using mutant standard MS15-3 (AAC).

MS15-3 DNA copy/ uL	Ct ₁	Ct ₂	Ct ₃	Ct ₄	Ct ₅	Ct ₆	Ct ₇	Ct ₈	Ave. Ct
5	N/A	N/A	49.43	N/A	49.81	N/A	N/A	49.75	49.66
5	N/A	N/A	49.43	N/A	48.51	N/A	N/A	49.73	49.22
50	N/A	N/A	44.05	N/A	46.20	44.64	N/A	46.66	45.39
50	N/A	N/A	45.43	N/A	46.68	43.69	N/A	46.58	45.60
500	40.71	41.17	40.02	41.17	43.71	42.00	41.45	44.50	41.84
500	41.96	42.32	40.58	42.32	43.71	41.95	41.45	43.67	42.25
5 000	36.85	38.99	37.01	38.99	39.00	38.92	40.00	40.05	38.73
5 000	37.01	38.06	36.01	38.06	39.00	39.05	40.55	40.19	38.49
50 000	33.86	35.08	34.91	35.08	35.38	36.33	37.77	37.02	35.68
50 000	34.03	35.24	34.80	35.24	35.00	36.10	37.36	37.89	35.71
500 000	30.23	31.08	31.19	31.08	32.11	32.98	33.67	34.00	32.04
500 000	30.05	31.08	32.42	31.08	32.26	33.65	34.13	34.24	32.36
5 000 000	27.02	27.77	27.9	27.77	28.22	29.42	30.31	30.80	28.65
5 000 000	26.95	27.33	28.12	27.33	28.57	29.19	30.62	30.80	28.61
50 000 000	N/A	24.13	23.79	24.13	24.70	24.92	25.68	25.73	24.73
50 000 000	N/A	24.19	25.43	24.19	24.60	24.92	25.52	25.89	24.96
3 NTCs	N/A	N/A	N/A	N/A	N/A	N/A	N/A	N/A	N/A
Wt MS9-3 (5)	N/A	N/A	N/A	N/A	N/A	N/A	N/A	N/A	N/A
Wt MS9-3 (5x10 ⁶)	N/A	N/A	50.90	N/A	47.78	N/A	52.06	N/A	50.25
WT MS10-2 (5)	N/A	N/A	N/A	N/A	N/A	N/A	N/A	N/A	N/A
Wt MS10-2 (5x10 ⁶)	N/A	N/A	52.56	51.19	48.89	N/A	N/A	N/A	50.88
Mut MS10-4 (5)	N/A	N/A	N/A	N/A	N/A	N/A	N/A	N/A	N/A
Mut MS10-4 (5x10 ⁶)	27.92	28.04	28.05	29.19	28.89	29.66	31.68	29.26	29.09

N/A – No amplification. Ct

The three replicates for 5×10^0 and 5×10^6 DNA copy/ μ l MS10-4 K103N-mutant control were amplified with similar efficiency to those of the mutant standard MS15-3. The K103N-SPCR assay efficiencies and reproducibility results from these eight runs are provided in **Table 3.15**. The resulted slope (m) of -3.44 indicates that amplification was 95.30% efficient, with the efficiencies of all eight runs ranging from 90.60 to 106.76%. Here, about 50 cycles are required to detect 1 DNA copy of

the K103N variant using K103N-specific primer and probe set. The precision which is described by the intra- (repeatability) and the inter-assay (reproducibility) run after all three assay runs is around 99.88% and 98.90%, respectively. Therefore, this makes the K103N-SPCR a highly consistent assay (Muller, Stelzl et al. 2004).

Table 3.15: Efficiency and reproducibility data from standard curve experiment using K103N-SPCR assay.

	Run 1	Run 2	Run 3	Run 4	Run 5	Run 6	Run 7	Run 8	Average
Slope	-3.55	3.57	-3.38	-3.45	-3.57	-3.17	-3.21	-3.39	-3.44
Efficiency	91.32	90.60	97.63	94.77	90.60	106.76	104.90	97.12	95.30
Y-intercept	48.06	49.10	48.14	51.17	52.15	48.23	49.32	50.57	49.16
R ²	99.31	99.63	98.50	99.58	99.51	98.66	96.81	99.17	99.88
Cycles	50.00	55.00	55.00	55.00	55.00	55.00	55.00	55.00	
Reproducibility									98.90

The average Ct linearly correlated with the mean DNA copy number over the range of $0\log_{10}$ to $7\log_{10}$ mutant and wild-type dilution series. The average standard curve representing eight runs for the K103N-SPCR assay generated with the serial dilutions (5×10^7 to 5×10^0 DNA copy/ μ l) of MS15-3 K103N-mutant standard is shown in **Figure 3.10**.

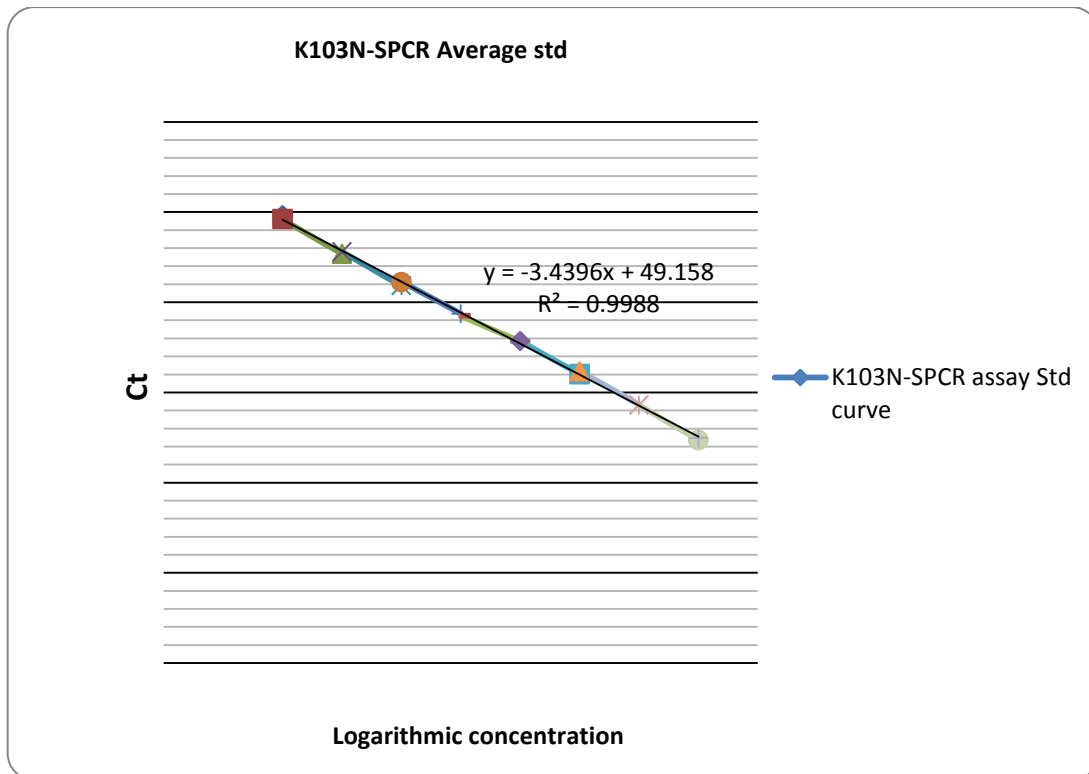


Figure 3.10: A plot of standard (std) curve for the K103N-SPCR assay using average Ct values of eight runs. Serial dilutions of MS15-3 K103N-mutant plasmid standard were used to construct the standard curve. On the x-axis is the mean DNA copy number based on logarithmic and on the y-axis is the mean threshold cycle (Ct). The squares along the lines represent the concentration of the serial diluted (5×10^7 - 5×10^0 DNA copy/ μ l) standard in duplicate. The standard curve forms a straight line over eight orders of magnitude. The equation, $y = mx + c$, defines the linear regression with 'm' representing the slope (-3.4396) which describes the amplification efficiency of the assay run and 'c' as the y-intercept (49.158) indicating the sensitivity or the lower detection limit of the assay. R^2 represents repeatability or the level of consistency of the assay in terms of the closeness of the replicate data to each other.

3.1.8 Accuracy of both SPCR assays

3.1.8.1 Accuracy of the total viral copy SPCR assay

Total viral copy SPCR reactions after three runs for the wild-type/mutant plasmid mixture experiment were not contaminated as three replicates for the no-template control (NTC - negative control) were not amplified. The three replicates for the

consensus/subtype C wild-type control containing 5×10^0 and 5×10^7 DNA copy/ μl of MS9-3 were amplified with the approximately same efficiency as the 5×10^0 and 5×10^7 DNA copy/ μl of MS15-3 K103N-mutant plasmid standard in all three assay runs. The mean Ct values for the standard curve are 39 and 16 at concentrations of 5×10^0 and 5×10^7 DNA copy/ μl , respectively (data not supplied). The average results of all three runs are represented in the amplification plot in **Figure 3.11**.

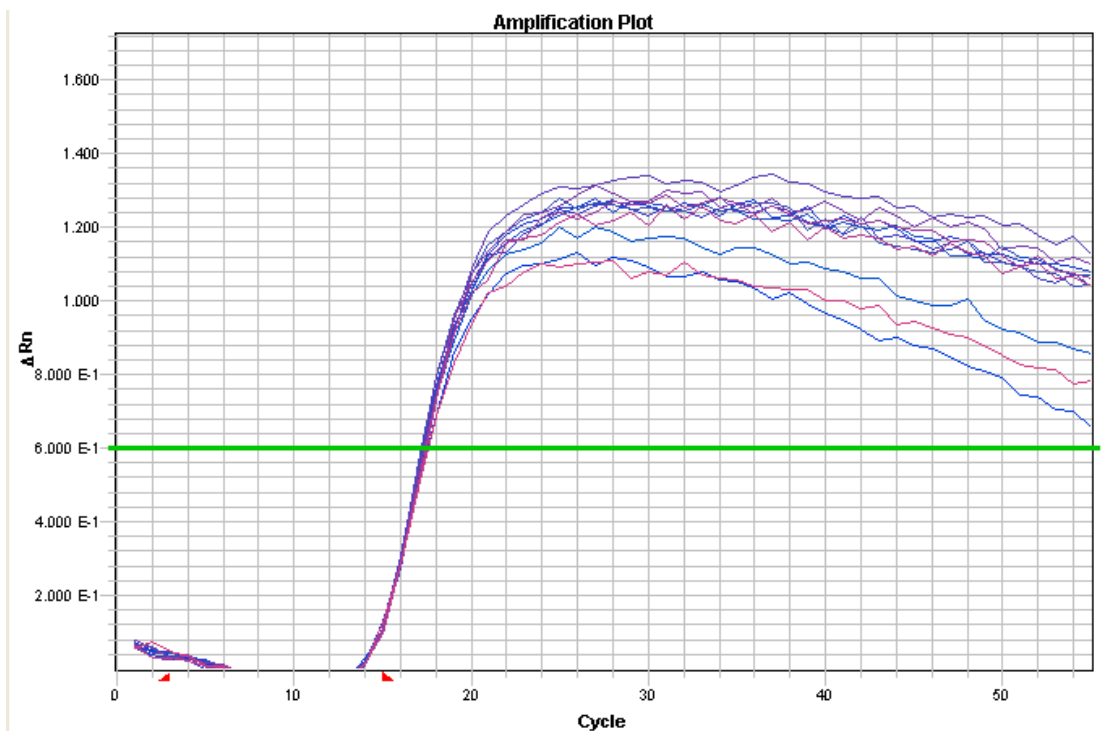


Figure 3.11: A representative amplification plot for Run 2 with Ct values of the wild-type/mutant plasmid mixture experiment in the total viral copy SPCR reaction. The total copy which is 5×10^6 - 0.5 DNA copy/ μl of MS15-3 K103N-mutant plus 5×10^7 DNA copy/ μl of MS10-2 K103-wild-type resulted in a mean threshold cycle of ~ 17 .

The Ct value of one of three runs (Run 2) for the total viral copy DNA (mutant plus wild-type) at all concentrations is approximately 17. This proves the accuracy of the total viral copy SPCR assay as the average concentration is in the order of 5×10^7 DNA copy/ μ l. However, there is overestimation as the quantity of the total viral copy detected by the assay is not the same as the input. Data is provided in **Table 3.16**. This could be due to pipetting errors, and this is reason why the average Ct is ~ 17 instead of 16 as in the pure standard curve for the total copy SPCR assay.

Table 3.16: Data of the results from the wild-type/mutant plasmid mixture experiment in the total copy SPCR reaction and the K103N-SPCR reaction.

Total DNA copies/ μ l	Ct ₁	Ct ₂	Ct ₃	Average Ct	Ave. Qty Detected
55 000 000	16.83	17.19	15.70	16.57	99 100 000
55 000 000	16.85	17.22	15.70	16.59	99 000 000
50 500 000	17.12	17.46	15.70	16.76	78 800 000
50 500 000	17.10	17.43	15.90	16.81	73 800 000
50 050 000	17.03	17.46	15.80	16.76	83 300 000
50 050 000	17.11	17.39	15.80	16.77	85 800 000
50 005 000	16.86	17.34	15.60	16.60	85 400 000
50 005 000	16.99	17.36	15.70	16.68	82 300 000
50 000 500	17.04	17.41	15.90	16.78	78 500 000
50 000 500	16.97	17.36	15.80	16.71	81 700 000
50 000 050	17.16	17.55	15.90	16.87	74 700 000
50 000 050	17.16	17.53	15.80	16.83	73 600 000
50 000 005	17.14	17.46	15.80	16.80	78 400 000
50 000 005	17.17	17.57	15.80	16.85	83 100 000
50 000 000.5	17.09	17.57	15.90	16.85	78 000 000
50 000 000.5	17.08	17.53	15.80	16.80	80 200 000

Ct₁ – Ct for Run 1: 26/04/10; Ct₂ – Ct for Run 2: 27-04-10; Ct₃ – Ct for Run 3: 05-08-10; Ave. Qty detected – average quantity of K103-wildtype MS10-2 plus K103N-mutant MS15-3 DNA copies/5 μ L.

3.1.8.2 Accuracy of the K103N-SPCR assay

K103N-SPCR reactions for the wild-type/mutant plasmid mixture experiment were not contaminated as three replicates for the no-template controls (NTCs - negative controls) were not amplified. Additionally, the three replicates for the consensus/subtype C wild-type control containing 5×10^0 DNA copy/ μ l of MS9-3 were

not amplified. However, the 5×10^7 DNA copy/ μl was amplified with the approximately same efficiency (Mean Ct of 49) as the 5×10^0 DNA copy/ μl MS15-3 plasmid standard in all three assay runs. The results of all three runs using the K103N-SPCR assay in the plasmid mixture experiment are plotted together with the pure K103N-SPCR standard curve (with MS15-3 as the standard) in **Figure 3.12**. Ct values for these plasmid mixture runs comply with or are similar to those of the pure K103N standard curve at each concentration point, especially from $6 \log_{10}$ (5×10^6 DNA copy/ μl) to $1 \log_{10}$ (5×10^1 DNA copy/ μl). This proves the accuracy of the K103N-SPCR assay since the addition of 10^7 DNA copy/ μl of a wild-type standard MS10-2 to the serially diluted MS15-3 K103N-mutant did not change the K103N standard curve substantially (Paredes, Marconi et al. 2007).

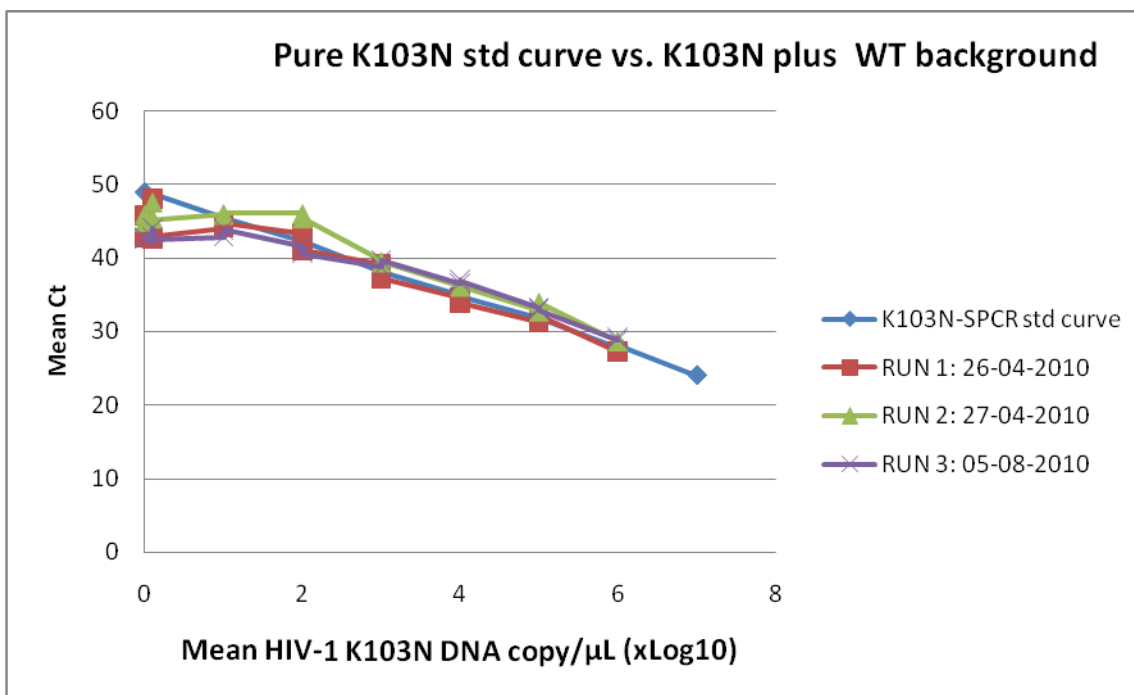


Figure 3.12: A representative of the accuracy of K103N-SPCR assay by comparing the three regression lines (Run 1-3) from three plasmid mixture runs with the K103N-SPCR assay standard curve using pure K103N-mutant standard. The standard curve was generated with serial dilutions (5×10^7 to 5×10^0 DNA copy/ μl) of pure MS15-3 K103N-mutant standard. The regression lines for Run 1-3 were generated with serial dilutions (5×10^6 - 5×10^0 DNA copy/ μl) of MS15-3 mutant plasmid standard plus a background of 5×10^6 DNA copy/ μl of MS10-2 wildtype plasmid standard.

However, the plasmid mixture Ct values at concentrations of $0\log_{10}$ (1 copy/ μl) to $0.5\log_{10}$ (0.5 copy/ μl) do comply with those of their counterparts in the pure K103N standard curve experiment. This shows poor accuracy of the assay as concentration decreases to lower than 5×10^0 to 1 DNA copy/ μl . Pipetting errors as well as contamination by the wild-type plasmid MS10-2 could be accountable for that because higher copies (quantity) more than the input MS15-3 mutant DNA at these concentrations were detected. The data for the wild-type/mutant plasmid mixture experiment using the K103N-SPCR assay are shown in **Table 3.17**.

Table 3.17: Data of results for the wild-type/mutant plasmid mixture experiment with 5×10^6 -0.5 DNA copy/ μl of MS15-3 K103N-Mut plasmid DNA added to a background of 5×10^6 DNA copy/ μl MS10-2 K103-Wt plasmid DNA in the K103N-SPCR reaction.

MS15-3 copies/ μl	Ct ₁	Ct ₂	Ct ₃	Average Ct	Ave. Qty Detected
5 000 000	27.43	28.67	29.10	28.40	4 386 667
5 000 000	27.31	28.66	28.90	28.29	4 710 000
500 000	32.22	33.96	33.00	33.06	223 333
500 000	31.33	32.76	33.20	32.43	329 667
50 000	33.94	36.13	37.00	35.69	43 967
50 000	34.69	36.20	36.60	35.83	35 067
5 000	37.31	39.42	39.70	38.81	5 343
5 000	39.20	39.57	38.80	39.19	4 123
500	41.13	45.43	40.60	42.39	1 051
500	43.33	46.04	41.70	43.69	505
50	44.77	46.04	43.90	44.90	123
50	44.17	45.91	42.90	44.33	214
5	42.79	44.94	42.60	43.44	301
5	45.78	45.91	42.80	44.83	221
0.5	42.65	45.43	42.80	43.63	282
0.5	48.12	47.63	44.10	46.62	85

Ct₁ – Ct for Run 1: 26-04-2010; Ct₂ – Ct for Run 2: 27-04-2010; Ct₃ – Ct for Run 3: 05-08-2010; Ave.

Qty – Average quantity of MS15-3 DNA copies detected per 5 μL .

3.1.8.3 The assay cut-off and mutation detection limit

A SPCR assay cut-off that differentiates the K103N-mutant and the K103-wild-type specimens was defined as the difference between the threshold cycle (Ct) of the total viral copy and the K103N-SPCR assay. This difference which is called delta Ct (ΔCt) ranges from 8.23 to 10.33 across the whole linear dynamic range and is provided in **Table 3.18**. Both the minimum (8.23) and the maximum (10.33) ΔCt were used as the assay cut-off. The minimum was chosen in order to avoid or exclude false positives, in other words it is used to buffer against non-specificity. In that case, any specimen with a delta Ct of 8.23 or lower indicates the presence of a K103N mutant virus. The maximum ΔCt of 10.33 was used as comparison because it is similar to a cut-off determined in a study by Johnson et al (2005) from which most of the primers and probes used in this study were taken. Johnson obtained a cut-off of 10.5 (Johnson, Li et al. 2005).

A detection limit of K103N variants by the SPCR assays was calculated from the results in **Table 3.16** and **Table 3.17** using the formule from Paredes et al, 2007:

$$\% \text{ of K103N detection limit} = \left[\frac{\text{detected quantity of K103N variants by K103N-SPCR assay when MS15-3 input is } 5 \times 10^3 \text{ copy}/\mu\text{L}}{\text{detected quantity of total viral copies by total copy SPCR assay when MS15-3 input is } 50\,005\,000 \text{ copy}/\mu\text{L}} \right] \times 100.$$

It resulted in a detection limit of 0.01%. These concentrations were chosen because they are the lowest concentrations at which the standard curve of pure mutant MS15-3 and the regression lines for wildtype/mutant plasmid mixture experiment showed to comply (**Figure 3.12**).

Table 3.18: Data of results for the total copy SPCR and the K103N-SPCR assay standard curves using a common K103N-mutant MS15-3 standard to determine the Δ Ct assay cut-off.

K103N-SPCR Assay		Total copy SPCR Assay		Mean ($Ct_{Total} - Ct_{K103N}$) Δ Ct
MS15-3 DNA copy/ μ l xLog ₁₀	8 runs Mean Ct	MS15-3 DNA copy/ μ l xLog ₁₀	8 runs Mean Ct	
0	49.00	0	39.90	9.10
0	49.00	0	39.89	9.11
1	45.30	1	35.18	10.12
1	45.30	1	34.97	10.33
2	42.18	2	32.99	9.19
2	42.20	2	32.99	9.21
3	38.01	3	29.78	8.23
3	38.01	3	29.57	8.44
4	34.91	4	26.54	8.37
4	34.80	4	26.51	8.29
5	31.85	5	22.99	8.86
5	31.85	5	23.00	8.85
6	27.90	6	19.36	8.54
6	28.12	6	19.41	8.71
7	24.00	7	15.61	8.39
7	24.00	7	15.68	8.32

3.1.9 Detection of K103N minor variants in patient samples

The assay cut-off of 8.23 detected 10 (25.64%) patients with the K103N resistance variants in the HIV-1 reverse transcriptase (one could not be amplified) whereas the cut-off of 10.33 detected 13 (33.33%), out of the 39 patients using both the total copy SPCR and the K103N-SPCR assays. Since genotyping detected K103N resistance variants in only six (60%) patients out of 10 or 13 detected by the SPCR assays, therefore it missed 40% (based on a cut-off of 8.23) or 53.85% (based on a cut-off of 10.33). Thus, these missed proportions are classified as the minor variants.

In contrast to genotyping, SPCR assays could not detect the K103N variants in patients STV289783 when using either 8.23 or 10.33 assay cut-off. However, this patient yielded some of the highest Δ Ct values compared to a majority of the patients. It could be a false positive detected by the population-based genotyping. All three

replicates of the no-template controls (NTCs) in the three runs were not amplified, showing that all the reactions were not contaminated. Data of the results after three runs of detecting the K103N minor variants in 40 previously genotyped (population sequencing) patient samples using the optimized and validated total copy SPCR and K103N-SPCR assays are shown in **Table 3.19**.

Table 3.19: Data from three runs after detecting minor resistance variants of K103N in 40 patient samples using SPCR assay cut-offs of 8.23 and 10.33.

STV #	K103N Genotyping Results	Mean ΔCt_1	Mean ΔCt_2	Mean ΔCt_3	Average ΔCt	ΔCt 8.23 Cut-off K103N	ΔCt 10.33 Cut-off K103N
297883	NONE	13.12	14.21	13.18	13.50		
294855	NONE	12.69	13.41	12.83	12.98		
294773	NONE	13.84	11.14	16.33	13.77		
294771	NONE	10.20	11.03	9.71	10.31		Positive
293935	NONE	11.34	11.19	11.64	11.39		
290766	NONE	11.98	12.73	12.47	12.39		
288044	NONE	9.61	13.90	13.80	12.44		
286813	NONE	12.53	15.11	18.02	15.22		
286808	NONE	6.53	6.65	6.29	6.49	Positive	Positive
286807	NONE	11.23	13.67	12.82	12.57		
286803	NONE	7.99	8.14	7.67	7.93	Positive	Positive
284540	NONE	15.20	17.80	17.61	16.87		
288667	NONE	20.63	17.70	22.45	20.26		
288668	NONE	12.19	13.57	16.24	14.00		
291336	NONE	11.14	12.32	18.90	14.12		
291337	NONE	N/A	N/A	N/A	N/A		
294770	NONE	16.80	16.64	14.14	15.86		
296155	NONE	8.63	9.14	11.24	9.67		Positive
285739	K103N	2.77	0.43	0.35	1.18	Positive	Positive
288042	K103N	3.94	4.62	1.51	3.36	Positive	Positive
288043	K103N	4.50	4.22	3.11	3.94	Positive	Positive
289783	K103N	12.87	13.65	12.79	13.10		
290767	K103N	2.54	0.11	0.29	0.98	Positive	Positive
292197	K103N	6.75	6.78	5.39	6.31	Positive	Positive
294767	K103N	5.19	3.75	4.22	4.39	Positive	Positive
284246	NONE	21.81	10.31	N/A	16.06		
288041	NONE	19.12	23.76	N/A	21.44		
275180	NONE	10.81	11.50	10.27	10.86		
285742	NONE	15.39	16.69	14.84	15.64		
292196	NONE	8.54	9.71	8.67	8.97		Positive
286812	K103N	0.78	14.29	2.48	5.85	Positive	Positive
275181	NONE	11.66	12.23	10.32	11.40		
296685	NONE	10.91	12.48	10.61	11.33		
289781	NONE	10.51	11.17	10.40	10.69		
294769	NONE	10.97	11.20	10.94	11.04		
293934	NONE	20.53	30.38	25.09	25.33		
294772	NONE	4.71	2.86	14.99	7.52	Positive	Positive
295251	NONE	12.14	14.63	14.35	13.71		
293936	NONE	12.10	11.60	13.78	12.49		
297431	NONE	11.26	11.92	10.74	11.31		

Ct_1 - Ct for Run 1; Ct_2 - Ct for Run 2; Ct_3 - Ct for Run 3.

Chapter 4

4.1 Discussion

4.1.4 The study findings

This study presents the development sensitive selective real-time polymerase chain reaction (SPCR) assays for the detection and quantification K103N minor resistance variants in 39 previously genotyped patients infected with HIV-1 subtype C. The prevalence of K103N minor variants ranges from 25.64% (with an assay cut-off of ΔCt 8.23) to 33.33% (with a cut-off of ΔCt 10.33) with a detection limit of 0.01%. The prevalence is lower than the 40-43% observed previously in the subtype C or non-subtype B patients with the lowest detection limit of 0.2% (Johnson, Li et al. 2005; Palmer, Boltz et al. 2006; Balduin, Oette et al. 2009). Balduin and Johnson used the TaqMan fluorescence probes, whereas Palmer used the SYBR Green fluorescence. In this study, two K103N-specific primers were employed with only one derived from Johnson's study (in contrary to three specific primers). Owing to the discriminatory ability and reliability of K103N-specific primers, both SPCR assays detected these subpopulations in 25-33% of the patients. Additionally, the prevalence the major detected by genotyping and the minor K103N variants is equal. The sensitivity (0.01%) was directly proportional to the discriminatory ability of the K103N-specific primers because both assay cut-offs were able to rule out a false positive which was previously detected by genotyping. This sample (STV 289783) had considerable high ΔCt 's relative to the minimum and maximum cut-offs. They ranged from 12.8 to 13.10 after three runs. Sample STV 291337 could not be amplified by either the total copy assay or the K103N-specific SPCR assay.

The plasmid constructs chosen as the standards resulted in highly reproducible total viral copy and K103N-SPCR assays with better amplification efficiencies. The annealing of the total copy primers to the highly conserved sites of the consensus C yielded accurate results, even though a forward primer had a single mismatch near the 5' end. Additional mismatch at this position does not have a significant effect on the primer binding, unlike near the 3' end (Bergroth, Sonnerborg et al. 2005). The same principle as in previous studies was applied regarding primer design and the use of TaqMan technology instead of SYBR green technology (Hance, Lemiale et al. 2001;

Bergroth, Sonnerborg et al. 2005; Johnson, Li et al. 2005). It is about incorporation of a mismatch at the 3' end of specific primers, and the use of TaqMan probes which are labelled with a fluorescent dye because they are more specific. In contrast, the SYBR Green technology is less specific since it detects all double-stranded DNA in the reaction. The presence of a single mismatch in the common mutant standard (MS15-3) encoding AAC (K103N) in comparison to absence of mismatches in the other mutant standards encoding AAT (K103N) did not affect amplification efficiency or the binding of specific primers. A single intentional mismatch introduced at the 3' end position of specific primers reduced the inaccuracy of the K103N-SPCR assay since polymorphisms are prevalent at the binding site for K103N specific primers as shown by data from large population scale in **Appendix B** (multiple alignment of all 2008 subtype C HIV-1 *RT* sequences and primers and probes used in this study).

4.1.2 Detection of HIV-1 K103N minor variants in South Africa

There is a growing health concern that intrapartum single-dose nevirapine which decreases mother-to-child transmission of human immunodeficiency virus type 1 (HIV-1) causes the development of nevirapine resistance mutations (e.g, K103N, Y181C, and G190A) in 20%-44% of women, especially in developing countries (Eshleman, Mracna et al. 2001; Eshleman and Jackson 2002; Abrams 2004). Viral populations harbouring these variants can be found in undetectable levels over time during therapy or in treatment-naive patients. These findings elevate the need to comprehend the exact clinical importance of K103N minor populations. Additionally, global reports suggesting that these minor populations contribute to virologic failure, and that they may cause earlier therapy failure, also led to the development of real-time PCR assays for the detection of quantification these minor populations (Johnson, Li et al. 2005). SPCR assays are not commercially available, but they are only being used in research. The cost of implementing this type of assay for routine drug resistance genotyping is equivalent to a third of the cost of the conventional sequence based genotyping. This is because SPCR is faster and requires less manipulation of data.

In South Africa, sensitive real-time PCR or allele-specific real-time PCR assays were developed to detect and quantify K103N minor resistant variants in SD-NVP-exposed and unexposed women and their babies infected with HIV-1 subtype C (Johnson, Li et al. 2005; Loubser, Balfe et al. 2006; Palmer, Boltz et al. 2006; Coovadia, Hunt et al. 2009; Martinson, Morris et al. 2009; Wind-Rotolo, Durand et al. 2009). Johnson and colleagues, using their developed K103N real-time fluorescence PCR assay, detected 40% K103N out of 40 South African women infected with HIV-1 subtype C at 6-36 weeks postpartum administration of SD-NVP. These samples had no detectable NVP resistant mutations by the conventional sequence analysis, and their limit of the mutation detection was 0.2% (Johnson, Li et al. 2005).

Using the ASPCR assay, Loubser and colleagues detected 87.1% (27/31 of RNA samples) and 52.3% (23/44 of DNA samples) K103N resistance mutation in 67 HIV-1-infected women after six weeks of using SD-NVP. It decayed over time with only 65.4%, 38.9%, and 11.3% detected in the RNA samples at 3, 7, and 12 months respectively. A major decline was noticed in the DNA samples with only 4.2% detected at 12 months. A relative quantitation instead of a standard curve was used (Loubser, Balfe et al. 2006). To assess the persistence and rates of decay of the K103N resistance variants in South African women infected with HIV-1 subtype C after SD-NVP, Palmer and colleagues used a sensitive allele-specific RT-PCR assay. They detected K103N variants in 53% (8/15) of the samples that had no detectable NVP-resistance mutations by standard genotype analysis after 12 months following SD-NVP therapy. The detected mutant virus populations ranged from 0.7-21.6%. In a group that had no detectable NVP-resistance mutations by genotyping at two months, ASPCR detected K103N in 43% (3/7) of the samples, with the mutant virus populations ranging from 0.2-15.3% (Palmer, Boltz et al. 2006).

Unlike 15.1% of women without minor K103N mutations, 60.9% of women with these mutations detected by ASPCR before treatment did not experience viral suppression or viral rebound with subsequent nevirapine treatment (Coovadia, Hunt et al. 2009). Almost all NVP-exposed and unexposed women with K103N at baseline experienced no viral suppression or viral rebound with subsequent antiretroviral therapy containing NVP or other NNRTIs (Coovadia, Hunt et al. 2009; Martinson, Morris et al. 2009). Moreover, 25% (3/15) of NVP-exposed women with K103N

minor variants transmitted HIV-1 to their infants, compared to only 12.5% (1/8) of NVP-unexposed women without K103N (Martinson, Morris et al. 2009). Overall, K103N minor resistant variants or the persisting drug-resistant mutants may affect antiretroviral regimens containing NNRTIs in subsequent pregnancies.

4.1.3 Detection of HIV-1 minor K103N drug-resistant variants globally

Globally, studies developing real-time PCR assays using either the probe-based 5' nuclease or the non-probe based SYBR[®] Green I dye chemistry to detect and/or quantify HIV-1 minor K103N drug-resistant variants are significantly increasing. These assays are referred to as selective/specific real-time PCR (SPCR) or allele-specific real-time PCR (ASPCR) (Hance, Lemiale et al. 2001; Lecossier, Shulman et al. 2005; Metzner, Rauch et al. 2005; Johnson, Li et al. 2007; Church, Towler et al. 2008; Johnson, Li et al. 2008; Rowley, Boutwell et al. 2008; Balduin, Oette et al. 2009; Metzner, Giulieri et al. 2009). A widespread interest in understanding the clinical importance of K103N minor variants, and earlier findings that these variants are associated with reduced treatment efficacy have been the driving force behind the study (Balotta 2000; Aleman 2002). Additionally, K103N mutation develops more rapidly than most other resistance mutations under conditions of incomplete viral suppression. Non-nucleoside reverse transcriptase inhibitors (NNRTIs) have low genetic barrier. Therefore, they induce the highest level of resistance, since a single mutation such as K103N causes subsequent treatment failure with drugs belonging to this class (Schuurman, Demeter et al. 1999; Schuurman, Brambilla et al. 2002; Balduin, Oette et al. 2009). K103N is highly clinically relevant because a majority of HIV-1 patients are treated with nevirapine and efavirenz. K103N minorities were detected in 20.1% of 17 patients, with 40.6% in non-B subtypes and 15.0% in subtype B. Balduin and co-workers discovered that 24% of these patients failed NNRTI therapy after 12 weeks, in contrast with 15% of 67 patients without minorities (Balduin, Oette et al. 2009). Metzner and colleagues detected 10.2% (10/49) and 7.4% (8/109) prevalence for the K103N minorities in treatment-naïve subtype B patients (sero-converters), with mutant populations ranging from 0.01-25% (Metzner, Rauch et al. 2005; Metzner 2010). Johnson and colleagues detected K103N minor populations (ranging from 0.001-11%) in 27% (81/202) and 4% (8/205) of drug-naïve

subtype B patients. A standard curve was used, and the cut-off was defined similar to this study (Johnson, Li et al. 2007; Johnson, Li et al. 2008).

The findings in most of these studies proved that a higher risk of NNRTI treatment failure as a result of K103N minor variants in patients or women receiving intrapartum single-dose nevirapine (Balduin, Oette et al. 2009). These subpopulations can rapidly replace the wild-type virus and become the major virus population and subsequently cause treatment failure in treatment-naïve patients who receive antiretroviral therapy regimens with a low genetic resistance barrier (Metzner, Rauch et al. 2005; Metzner, Giulieri et al. 2009).

The disadvantages of real-time PCR assays include the polymorphism in HIV-1 sequences, and that they are unable to link mutations other than what the assay is targeting. Other more sensitive assays, such as the parallel allele-specific sequencing (PASS), are able to sequece all the virus sequences per sample and report on the resistance mutations present, but they are very expensive and require special expertise (Palmer, Kearney et al. 2005; Cai, Chen et al. 2007). Several studies using this technology revealed that drug-resistant minor variants, especially those encoding resistance to NNRTIs, detected in treatment-naïve and treatment-experienced patients are likely to cause subsequent treatment failure (Hirsch, Gunthard et al. 2008).

4.1.4 Quality control issues

A thorough detection and assessing of the associated mutations is increasingly imperative since all antiretroviral drugs select for resistance (Daar 2007; Johnson, Li et al. 2008). However quality control trial or technical quality for HIV-1 drug resistance testing needs to be improved, especially for the detection of minor species. This testing is challenging as a result of great sequence variability in the HIV-1 genome. The high degree of genetic variability of HIV-1 makes it difficult to design a universal quantification real-time PCR assay for the detection of all the group-M HIV-1 subtypes with a higher specificity, sensitivity and reproducibility (Mackay 2007; Boltz, Maldarelli et al. 2010). These nucleotide polymorphisms in the sequence-specific primer binding site cause primer-template mismatch which in turn results in underestimation or overestimation of drug resistant variants (Bergroth,

Sonnerborg et al. 2005; Palmer, Boltz et al. 2006; Palmer, Boltz et al. 2006; Mackay 2007; Paredes, Marconi et al. 2007; Rowley, Boutwell et al. 2008). This non-specific binding compensates the accuracy of SPCR assays especially in detecting minor variants. To eliminate this problem, nested PCR products are used as templates in the SPCR assays to reduce non-specificity and contamination. Additionally, polymorphism-specific primers are now designed by including intentional nucleotide mismatches (e.g., wobble bases) at positions -1 to -3 of the 3' end to eliminate non-specificity (Rowley, Boutwell et al. 2008). Another modification is the incorporation of degenerate nucleotide bases at the positions where there is great variation or polymorphism, for instance, among sequences of subtypes B or C, consensus B or C, and HIV-1 HXB2 as the background sequence (Mackay 2007). Recently Boltz and colleagues advise that the use of a library of primers and standards based on the patients' HIV-1 consensus sequences can help eliminate the inaccuracies in allele-specific PCR assays as a result of HIV-1 genetic variations (Boltz, Maldarelli et al. 2010).

Despite the high-throughput and faster turn-around time of real-time PCR-based assays, issues of sensitivity and specificity are problematic in detecting and characterizing viral pathogens accurately. The diversity of HIV is making it difficult for scientists to design more sensitive and more specific SPCR assays that can reliably detect a broad spectrum of viral quasispecies. This also limits the use on commercial assays (Mackay, Arden et al. 2002; Mackay 2004; Radonic, Thulke et al. 2004). Quantification of specimens of poor quality due to handling and storage is another problem real-time PCR assays are faced with (Mackay, Arden et al. 2002; Mackay 2004; Radonic, Thulke et al. 2004; Bergroth, Ekici et al. 2009).

A possible limitation to this study is that these newly developed SPCR assays were never tested directly on patient RNA samples or extracted proviral DNA to detect K103N. In future this can be evaluated as an ongoing study. But in the case of RNA, the RT step has to be carried out in order to make cDNA, and a pre-amplification of this in the pre-nested and nested PCR is essential in order to generate the RT fragment which can then be used as a template for SPCR assays. The advantages of using the nested PCR product is that they increase the specificity and sensitivity of the SPCR assays. The disadvantage is many steps prior to SPCR assay which involve a lot of

opening the tube which introduces contamination, and increases *Taq* polymerase error. In the case of extracted proviral DNA being used a template will result in low amplification rate because typically, HIV DNA copy number is low in the CD4 cells. Therefore, a pre-amplification is necessary to increase the DNA copy number.

4.2 Conclusion

In conclusion, the study successfully developed highly sensitive and reproducible SPCR assays for the detection and quantification of K103N resistance variants in the HIV-1 RT gene when using nested PCR products as templates. The assays achieved sensitivities of less than 1 DNA copy per reaction for the K103N resistance mutation. The detection of an additional 40-53.85% of the patients with these resistant subpopulations by both SPCR assays, which was missed by genotyping, proves this. When taken into account that genotyping is still considered the standard-of-care to monitor HIV drug resistance, the study findings that these newly developed SPCR assays were able to detect K103N resistant variants in 7 out of 8 K103N-positive patient samples previously identified by genotyping supports their specificity, reliability and sensitivity. Therefore, these assays could be used on a large spectrum of clinical samples in a laboratory when validated and optimized for routine diagnostic use.

References

- Abrams, E. J. (2004). "Prevention of mother-to-child transmission of HIV-successes, controversies and critical questions." *AIDS Rev* **6**: 131-43.
- Aleman, S., Soderbarg, K., Visco-Comandini, U., Sitbon, G., Sonnerborg, A. (2002). "Drug resistance at low viraemia in HIV-1-infected patients with antiretroviral combination therapy." *AIDS* **16**(7): 1039-44.
- Bachelor, L., S. Jeffrey, et al. (2001). "Genotypic correlates of phenotypic resistance to efavirenz in virus isolates from patients failing nonnucleoside reverse transcriptase inhibitor therapy." *J Virol* **75**(11): 4999-5008.
- Bailey, J. R., A. R. Sedaghat, et al. (2006). "Residual human immunodeficiency virus type 1 viremia in some patients on antiretroviral therapy is dominated by a small number of invariant clones rarely found in circulating CD4+ T cells." *J Virol* **80**(13): 6441-57.
- Balduin, M., M. Oette, et al. (2009). "Prevalence of minor variants of HIV strains at reverse transcriptase position 103 in therapy-naive patients and their impact on the virological failure." *J Clin Virol* **45**(1): 34-8.
- Balotta, C., Berlusconi, A., Pan, A., Violin, M., Riva, C., Colombo, M. C., et al. (2000). "Prevalence of transmitted nucleoside analogue-resistant HIV-1 strains and pre-existing mutations in pol reverse transcriptase and protease region: outcome after treatment in recently infected individuals." *Antivir Ther* **5**(1): 7-14.
- Beerenwinkel, N., M. Daumer, et al. (2003). "Geno2pheno: Estimating phenotypic drug resistance from HIV-1 genotypes." *Nucleic Acids Res* **31**(13): 3850-5.
- Bergroth, T., H. Ekici, et al. (2009). "Difference in drug resistance patterns between minor HIV-1 populations in cerebrospinal fluid and plasma." *HIV Med* **10**(2): 111-5.

Bergroth, T., H. Ekici, et al. (2009). "Selection of drug-resistant HIV-1 during the early phase of viral decay is uncommon in treatment-naive patients initiated on a three- or four-drug antiretroviral regimen including lamivudine." *J Med Virol* **81**(1): 1-8.

Bergroth, T., A. Sonnerborg, et al. (2005). "Discrimination of lamivudine resistant minor HIV-1 variants by selective real-time PCR." *J Virol Methods* **127**(1): 100-7.

Birk, M. and A. Sonnerborg (1998). "Variations in HIV-1 pol gene associated with reduced sensitivity to antiretroviral drugs in treatment-naive patients." *AIDS* **12**(18): 2369-2375.

Blackard, J. T. (2005). "Detection of hepatitis C virus (HCV) in the serum and peripheral-blood mononuclear cells from HCV-monoinfected and HIV/HCV-coinfected persons." *J Infect Dis* **192**: 258-265.

Boltz, V. F., F. Maldarelli, et al. (2010). "Optimization of allele-specific PCR using patient-specific HIV consensus sequences for primer design." *J Virol Methods* **164**(1-2): 122-6.

Brenner, B., D. Turner, et al. (2003). "A V106M mutation in HIV-1 clade C viruses exposed to efavirenz confers cross-resistance to non-nucleoside reverse transcriptase inhibitors." *AIDS* **17**(1): F1-5.

Briones, C., A. de Vicente, et al. (2006). "Minority memory genomes can influence the evolution of HIV-1 quasispecies in vivo." *Gene* **384**: 129-38.

Burd, E. M. (2010). "Validation of developed-laboratory molecular assays for infectious diseases." *Clin. Microbiol. Rev.* **23**(3): 550-76.

Bustin, S. A. (2000). "Absolute quantification of mRNA using real-time reverse transcription polymerase chain reaction assays." *J Mol Endocrinol* **25**: 169-193.

Bustin, S. A. (2002). "Quantification of mRNA using real-time reverse transcription PCR (RT-PCR): trends and problems." *J Mol Endocrinol* **29**: 23-39.

Bustin, S. A. (2010). "Why the need for qPCR publication guidelines? - The case for MIQE." *Methods* **50**: 217-26.

Bustin, S. A., V. Benes, et al. (2009). "The MIQE guidelines: minimum information for publication of quantitative real-time PCR experiments." *Clin Chem* **55**(4): 611-22.

Bustin, S. A. and R. Mueller (2005). "Real-time reverse transcription PCR (qRT-PCR) and its potential use in clinical diagnosis." *Clinical Science* **109**: 365-379.

Bustin, S. A. and T. Nolan (2008) Analysis of mRNA expression by real-time PCR

Cai, F., H. Chen, et al. (2007). "Detection of minor drug-resistant populations by parallel allele-specific sequencing." *Nat Methods* **4**(2): 123-5.

Canales, R. D., Y. Luo, et al. (2006). "Evaluation of DNA microarrays results with quantitative gene expression platforms." *Nat Biotechnol* **24**: 1115-1122.

Church, J. D., W. I. Towler, et al. (2008). "Comparison of LigAmp and an ASPCR assay for detection and quantification of K103N-containing HIV variants." *AIDS Res Hum Retroviruses* **24**(4): 595-605.

Coovadia, A., G. Hunt, et al. (2009). "Persistent minority K103N mutations among women exposed to single-dose nevirapine and virologic response to nonnucleoside reverse-transcriptase inhibitor-based therapy." *Clin Infect Dis* **48**(4): 462-72.

Couto-Fernandez, J. C., C. Silva-de-Jesus, et al. (2005). "Human immunodeficiency virus type 1 (HIV-1) genotyping in Rio de Janeiro, Brazil: assessing subtype and drug-resistance associated mutations in HIV-1 infected individuals failing highly active antiretroviral therapy." *Mem Inst Oswaldo Cruz* **100**(1): 73-8.

- Daar, E. S. (2007). "Incorporating novel virologic tests into clinical practice." *Top HIV Med* **15**(4): 126-9.
- Das, K., S. G. Sarafianos, et al. (2007). "Crystal structures of clinically relevant Lys103Asn/Tyr181Cys double mutant HIV-1 reverse transcriptase in complexes with ATP and non-nucleoside inhibitor HBY 097." *J Mol Biol* **365**(1): 77-89.
- De Clercq, E. (2009). "Anti-HIV drugs: 25 compounds approved within 25 years after the discovery of HIV." *Int J Antimicrob Agents* **33**: 307-20.
- de Mendoza, C., O. Gallego, L. Valer, and Gonzalez-Lahoz (2001). "Update on genotype-guided antiretroviral therapy." *AIDS Res Hum Retroviruses* **3**: 208-215.
- Ding, J., K. Das, et al. (1998). "Structure and functional implications of the polymerase active site region in a complex of HIV-1 RT with a double-stranded DNA template-primer and an antibody Fab fragment at 2.8 Å resolution." *J Mol Biol* **284**(4): 1095-111.
- Eshleman, S. H. and J. B. Jackson (2002). "Nevirapine resistance after single dose prophylaxis." *AIDS Rev* **4**(2): 59-63.
- Eshleman, S. H., M. Mracna, et al. (2001). "Selection and fading of resistance mutations in women and infants receiving nevirapine to prevent HIV-1 vertical transmission (HIVNET 012)." *AIDS* **15**(15): 1951-7.
- Feinberg, M. (1997). "Hidden dangers of incompletely suppressive antiretroviral therapy." *Lancet* **349**(9063): 1408-9.
- Flys, T. S., D. Donnell, et al. (2007). "Persistence of K103N-containing HIV-1 variants after single-dose nevirapine for prevention of HIV-1 mother-to-child transmission." *J Infect Dis* **195**(5): 711-5.
- Freed, E. O. (1998). "HIV-1 gag proteins: diverse functions in the virus life cycle." *Virology* **251**(1): 1-15.

Freed, E. O. (2001). "HIV-1 replication." *Somat Cell Mol Genet* **26**(1-6): 13-33.

Gao, H. Q., P. L. Boyer, et al. (2000). "The role of steric hindrance in 3TC resistance of human immunodeficiency virus type-1 reverse transcriptase." *J Mol Biol* **300**(2): 403-18.

Grant, R. M., F. M. Hecht, et al. (2002). "Time trends in primary HIV-1 drug resistance among recently infected persons." *JAMA* **288**(2): 181-8.

Grant, R. M., Hecht, F. M., Warmerdam, M., Liu, L., Liegler, T., Petropoulos, C.J., (2002). "Time trends in primary HIV-1 drug resistance among recently infected persons." *JAMA* **288**(2): 181-8.

Grant, R. M., D. R. Kuritzkes, et al. (2003). "Accuracy of the TRUGENE HIV-1 genotyping kit." *J Clin Microbiol* **41**(4): 1586-93.

Halfon, P. (2006). "Real-time PCR assays for Hepatitis C virus (HCV) RNA quantitation are adequate for clinical management of patients with chronic HCV infection." *J Clin Microbiol* **44**: 2507-2511.

Hall, T. A. (1999). "BioEdit: user-friendly biological sequence alignment editor and analysis program for Windows 95/98/NT." *Nucl. Acids. Symp, Ser.* **41**: 95-98.

Halvas, E. K., G. M. Aldrovandi, et al. (2006). "Blinded, multicenter comparison of methods to detect a drug-resistant mutant of human immunodeficiency virus type 1 at low frequency." *J Clin Microbiol* **44**(7): 2612-4.

Hance, A. J., V. Lemiale, et al. (2001). "Changes in human immunodeficiency virus type 1 populations after treatment interruption in patients failing antiretroviral therapy." *J Virol* **75**(14): 6410-7.

Hansen, J., T. Schulze, et al. (1988). "Identification and characterization of HIV-specific RNase H by monoclonal antibody." *EMBO J* **7**(1): 239-43.

Harrich, D., C. Ulich, et al. (1996). "A critical role for the TAR element in promoting efficient human immunodeficiency virus type 1 reverse transcription." *J Virol* **70**(6): 4017-27.

Hatzakis, A. E. (2004). "Cellular HIV-1 DNA load predicts HIV-RNA rebound and the outcome of highly active antiretroviral therapy." *AIDS* **18**: 2261-2267.

Higuchi, R., C. Fockler, et al. (1993). "Kinetic PCR analysis: real-time monitoring of DNA amplification reactions." *Biotechnology (N Y)* **11**(9): 1026-30.

Hirsch, M. S., F. Brun-Vezinet, et al. (2003). "Antiretroviral drug resistance testing in adults infected with human immunodeficiency virus type 1: 2003 recommendations of an International AIDS Society-USA Panel." *Clin Infect Dis* **37**(1): 113-28.

Hirsch, M. S., F. Brun-Vezinet, et al. (2000). "Antiretroviral drug resistance testing in adult HIV-1 infection: recommendations of an International AIDS Society-USA Panel." *JAMA* **283**(18): 2417-26.

Hirsch, M. S., H. F. Gunthard, et al. (2008). "Antiretroviral drug resistance testing in adult HIV-1 infection: 2008 recommendations of an International AIDS Society-USA panel." *Clin Infect Dis* **47**(2): 266-85.

Hirsch, M. S., H. F. Gunthard, et al. (2008). "Antiretroviral drug resistance testing in adult HIV-1 infection: 2008 recommendations of an International AIDS Society-USA panel." *Top HIV Med* **16**(3): 266-85.

Holland, P. M., R. D. Abramson, et al. (1991). "Detection of specific polymerase chain reaction product by utilizing the 5'-3' exonuclease activity of *Thermus aquaticus* DNA polymerase." *Proc Natl Acad Sci U S A* **88**: 7276-7280.

Houghton, S. G. and F. R. Cockerill III (2006). "Real-time PCR: overview and applications." *Surg* **139**: 1-5.

Hsiou, Y., J. Ding, et al. (2001). "The Lys103Asn mutation of HIV-1 RT: a novel mechanism of drug resistance." *J Mol Biol* **309**(2): 437-45.

Huang, Y., L. Zhang, et al. (1998). "Characterization of gag and pol sequences from long-term survivors of human immunodeficiency virus type 1 infection." *Virology* **240**(1): 36-49.

Jacobo-Molina, A., J. Ding, et al. (1993). "Crystal structure of human immunodeficiency virus type 1 reverse transcriptase complexed with double-stranded DNA at 3.0 Å resolution shows bent DNA." *Proc Natl Acad Sci U S A* **90**(13): 6320-4.

Johnson, J. A., J. F. Li, et al. (2005). "Emergence of drug-resistant HIV-1 after intrapartum administration of single-dose nevirapine is substantially underestimated." *J Infect Dis* **192**(1): 16-23.

Johnson, J. A., J. F. Li, et al. (2007). "Simple PCR assays improve the sensitivity of HIV-1 subtype B drug resistance testing and allow linking of resistance mutations." *PLoS One* **2**(7): e638.

Johnson, J. A., J. F. Li, et al. (2008). "Minority HIV-1 drug resistance mutations are present in antiretroviral treatment-naïve populations and associate with reduced treatment efficacy." *PLoS Med* **5**(7): e158.

Johnson, V. A., F. Brun-Vezinet, et al. (2008). "Update of the Drug Resistance Mutations in HIV-1." *Top HIV Med* **16**(5): 138-45.

Julias, J. G., M. J. McWilliams, et al. (2003). "Mutation of amino acids in the connection domain of human immunodeficiency virus type 1 reverse transcriptase that contact the template-primer affects RNase H activity." *J Virol* **77**(15): 8548-54.

Julias, J. G., M. J. McWilliams, et al. (2002). "Mutations in the RNase H domain of HIV-1 reverse transcriptase affect the initiation of DNA synthesis and the specificity of RNase H cleavage in vivo." *Proc Natl Acad Sci U S A* **99**(14): 9515-20.

Jung, M., H. Agut, et al. (1992). "Susceptibility of HIV-1 isolates to zidovudine: correlation between widely applicable culture test and PCR analysis." *J Acquir Immune Defic Syndr* **5**(4): 359-64.

Karlsson, A. C., S. Lindback, et al. (1998). "Characterization of the viral population during primary HIV-1 infection." *AIDS* **12**(8): 839-47.

Koralnik, I. J. (1999). "JC virus DNA load in patients with and without progressive multifocal leukoencephalopathy." *Neurology* **52**: 253-260.

Kutyavin, I. V., I. A. Afonina, et al. (2000). "3'-minor groove binder-DNA probes increase sequence specificity at PCR extension temperatures." *Nucleic Acids Res* **28**(2): 655-61.

Larder, B., D. Purifoy, et al. (1987). "AIDS virus reverse transcriptase defined by high level expression in *Escherichia coli*." *EMBO J* **6**(10): 3133-7.

Larder, B. A., P. Kellam, et al. (1991). "Zidovudine resistance predicted by direct detection of mutations in DNA from HIV-infected lymphocytes." *AIDS* **5**(2): 137-44.

Lecossier, D., N. S. Shulman, et al. (2005). "Detection of minority populations of HIV-1 expressing the K103N resistance mutation in patients failing nevirapine." *J Acquir Immune Defic Syndr* **38**(1): 37-42.

Levy, J. A. (1993). "HIV pathogenesis and long-term survival." *AIDS* **7**(11): 1401-10.

Little, S. J., S. Holte, et al. (2002). "Antiretroviral-drug resistance among patients recently infected with HIV." *N Engl J Med* **347**(6): 385-94.

Little, S. J., Holte, S. , Routy, J. P., Daar, E. S., Markowitz, M., Collier, A. C. (2002). "Antiretroviral drug resistance among patients recently infected with HIV." *N Engl J Med* **347**(5): 385-94.

Lori, F., A. I. Scovassi, et al. (1988). "Enzymatically active forms of reverse transcriptase of the human immunodeficiency virus." *AIDS Res Hum Retroviruses* **4**(5): 393-8.

Loubser, S., P. Balfe, et al. (2006). "Decay of K103N mutants in cellular DNA and plasma RNA after single-dose nevirapine to reduce mother-to-child HIV transmission." *AIDS* **20**(7): 995-1002.

Lowe, D. M., A. Aitken, et al. (1988). "HIV-1 reverse transcriptase: crystallization and analysis of domain structure by limited proteolysis." *Biochemistry* **27**(25): 8884-9.

Mackay, I. M. (2004). "Real-time PCR in the microbiology laboratory." *Clin Microbiol Infect* **10**(3): 190-212.

Mackay, I. M. (2007). *Real-time PCR in Microbiology*. Norfolk, Caister academic Press.

Mackay, I. M. (2007). *Real-time PCR in microbiology: from diagnosis to characterization*. Norfolk, UK, Caister Academic Press.

Mackay, I. M., K. E. Arden, et al. (2002). "Real-time PCR in virology." *Nucleic Acids Res* **30**(6): 1292-305.

Malnati, M. S., G. Scarlatti, et al. (2008). "A universal real-time PCR assay for the quantification of group-M HIV-1 proviral load." *Nature protocols* **3**(7): 1-9.

Martinson, N. A., L. Morris, et al. (2009). "Women exposed to single-dose nevirapine in successive pregnancies: effectiveness and nonnucleoside reverse transcriptase inhibitor resistance." *AIDS* **27**(7): 809-16.

Mazzotta, F., S. Lo Caputo, et al. (2003). "Real versus virtual phenotype to guide treatment in heavily pretreated patients: 48-week follow-up of the Genotipo-Fenotipo di Resistenza (GenPheRex) trial." *J Acquir Immune Defic Syndr* **32**(3): 268-80.

McGovern, S. L., E. Caselli, et al. (2002). "A common mechanism underlying promiscuous inhibitors from virtual and high-throughput screening." *J Med Chem* **45**(8): 1712-22.

Menendez-Arias, L. (2009). "Molecular basis of human immunodeficiency virus drug resistance: An update." *Antiviral Res.*

Menendez-Arias, L., M. A. Martinez, et al. (2003). "Fitness variations and their impact on the evolution of antiretroviral drug resistance." *Curr Drug Targets Infect Disord* **3**(4): 355-71.

Metzner, K. J., S. Bonhoeffer, et al. (2003). "Emergence of minor populations of human immunodeficiency virus type 1 carrying the M184V and L90M mutations in subjects undergoing structured treatment interruptions." *J Infect Dis* **188**(10): 1433-43.

Metzner, K. J., S. G. Giulieri, et al. (2009). "Minority quasispecies of drug-resistant HIV-1 that lead to early therapy failure in treatment-naive and -adherent patients." *Clin Infect Dis* **48**(2): 239-47.

Metzner, K. J., P. Rauch, et al. (2005). "Detection of minor populations of drug-resistant HIV-1 in acute seroconverters." *AIDS* **19**(16): 1819-25.

Metzner, K. J., Rauch, P., von Wyl, V., Leemann, C., et al. (2010). "Efficient suppression of minority drug-resistant HIV type 1 (HIV-1) variants present at primary HIV-1 infection by ritonavir-boosted protease inhibitor-containing Antiretroviral therapy." *J Infect Des* **201**: 1063-71.

Mudrow, S. and D. Falke (2003). *Molekulare Virologie*. Berlin, Heidelberg.

Muller, Z., E. Stelzl, et al. (2004). "Evaluation of automated sample preparation and quantitative PCR LCx assay for determination of human immunodeficiency virus type 1 RNA." *J Clin Microbiol* **42**(4): 1439-43.

Nissley, D. V., E. K. Halvas, et al. (2005). "Sensitive phenotypic detection of minor drug-resistant human immunodeficiency virus type 1 reverse transcriptase variants." *J Clin Microbiol* **43**(11): 5696-704.

Palmer, S., V. Boltz, et al. (2006). "Selection and persistence of non-nucleoside reverse transcriptase inhibitor-resistant HIV-1 in patients starting and stopping non-nucleoside therapy." *AIDS* **20**(5): 701-10.

Palmer, S., V. Boltz, et al. (2006). "Persistence of nevirapine-resistant HIV-1 in women after single-dose nevirapine therapy for prevention of maternal-to-fetal HIV-1 transmission." *Proc Natl Acad Sci U S A* **103**(18): 7094-9.

Palmer, S., M. Kearney, et al. (2005). "Multiple, linked human immunodeficiency virus type 1 drug resistance mutations in treatment-experienced patients are missed by standard genotype analysis." *J Clin Microbiol* **43**(1): 406-13.

Palmer, S., A. P. Wiegand, et al. (2003). "New real-time reverse transcriptase-initiated PCR assays with single-copy sensitivity for human immunodeficiency virus type 1 RNA in plasma." *J Clin Microbiol* **41**(10): 4531-4536.

Paredes, R., V. C. Marconi, et al. (2007). "Systematic evaluation of allele-specific real-time PCR for the detection of minor HIV-1 variants with pol and env resistance mutations." *J Virol Methods* **146**(1-2): 136-46.

Parkin, N. T., M. Chamorro, et al. (1992). "Human immunodeficiency virus type 1 gag-pol frameshifting is dependent on downstream mRNA secondary structure: demonstration by expression in vivo." *J Virol* **66**(8): 5147-51.

- Peng, C., N. T. Chang, et al. (1991). "Identification and characterization of human immunodeficiency virus type 1 gag-pol fusion protein in transfected mammalian cells." *J Virol* **65**(5): 2751-6.
- Perez-Elias, M. J., I. Garcia-Arota, et al. (2003). "Phenotype or virtual phenotype for choosing antiretroviral therapy after failure: a prospective, randomized study." *Antivir Ther* **8**(6): 577-84.
- Perrin, L. (2006). "Multicenter performance evaluation of a new TaqMan PCR assay for monitoring human immunodeficiency virus RNA load." *J Clin Microbiol* **44**: 4371-4375.
- Plantier, J. C., R. Dachraoui, et al. (2005). "HIV-1 resistance genotyping on dried serum spots." *AIDS* **19**(4): 391-7.
- Plantier, J. C., M. Leoz, et al. (2009). "A new human immunodeficiency virus derived from gorillas." *Nat Med* **15**(8): 871-2.
- Radonic, A., S. Thulke, et al. (2004). "Guideline to reference gene selection for quantitative real-time PCR." *Biochem Biophys Res Commun* **313**(4): 856-62.
- Ren, J., J. Milton, et al. (2000). "Structural basis for the resilience of efavirenz (DMP-266) to drug resistance mutations in HIV-1 reverse transcriptase." *Structure* **8**(10): 1089-94.
- Ren, J. and D. K. Stammers (2008). "Structural basis for drug resistance mechanisms for non-nucleoside inhibitors of HIV reverse transcriptase." *Virus Res* **134**(1-2): 157-70.
- Resistance, E. G. f. H. (2001). "Clinical and laboratory guidelines for the use of HIV-1 drug resistance testing as part of treatment management: recommendations for the European setting." *AIDS* **15**: 309-320.

Reynisson, E., M. H. Josefsen, et al. (2006). "Evaluation of probe chemistries and platforms to improve the detection limit of real-time PCR." *J Microbiol* **2006**: 206-216.

Rodriguez-Barrios, F. and F. Gago (2004). "Understanding the basis of resistance in the irksome Lys103Asn HIV-1 reverse transcriptase mutant through targeted molecular dynamics simulations." *J Am Chem Soc* **126**(47): 15386-7.

Rodriguez-Barrios, F., C. Perez, et al. (2001). "Identification of a putative binding site for [2',5'-bis-O-(tert-butyldimethylsilyl)-beta-D-ribofuranosyl]-3'-spiro-5"- (4"-amino-1",2"-oxathiole-2",2"-dioxide)thymine (TSAO) derivatives at the p51-p66 interface of HIV-1 reverse transcriptase." *J Med Chem* **44**(12): 1853-65.

Ross, L., R. Boulme, et al. (2005). "A direct comparison of drug susceptibility to HIV type 1 from antiretroviral experienced subjects as assessed by the antivirogram and PhenoSense assays and by seven resistance algorithms." *AIDS Res Hum Retroviruses* **21**(11): 933-9.

Ross, L., R. Boulme, et al. (2005). "Comparison of HIV type 1 protease inhibitor susceptibility results in viral samples analyzed by phenotypic drug resistance assays and by six resistance algorithms: an analysis of a subpopulation of the CHORUS cohort." *AIDS Res Hum Retroviruses* **21**(8): 696-701.

Rowley, C. F., C. L. Boutwell, et al. (2008). "Improvement in allele-specific PCR assay with the use of polymorphism-specific primers for the analysis of minor variant drug resistance in HIV-1 subtype C." *J Virol Methods* **149**(1): 69-75.

Saiki, R. K., S. Scharf, et al. (1985). "Enzymatic amplification of beta-globin genomic sequences and restriction site analysis for diagnosis of sickle cell anemia." *Science* **230**: 1350-1354.

Saladini, F., I. Vicenti, et al. (2009). "Detection of residual HIV-1 reverse transcriptase K103N minority species in plasma RNA and peripheral blood

mononuclear cell DNA following discontinuation of nonnucleoside therapy." *Clin Microbiol Infect*.

Sarafianos, S. G., K. Das, et al. (1999). "Lamivudine (3TC) resistance in HIV-1 reverse transcriptase involves steric hindrance with beta-branched amino acids." *Proc Natl Acad Sci U S A* **96**(18): 10027-32.

Sarafianos, S. G., K. Das, et al. (1999). "Touching the heart of HIV-1 drug resistance: the fingers close down on the dNTP at the polymerase active site." *Chem Biol* **6**(5): R137-46.

Sarafianos, S. G., K. Das, et al. (2004). "Taking aim at a moving target: designing drugs to inhibit drug-resistant HIV-1 reverse transcriptases." *Curr Opin Struct Biol* **14**(6): 716-30.

Sarafianos, S. G., K. Das, et al. (2001). "Crystal structure of HIV-1 reverse transcriptase in complex with a polypurine tract RNA:DNA." *EMBO J* **20**(6): 1449-61.

Sarrazin, C. (2006). "Comparison of conventional PCR with real-time PCR and branched DNA-based assays for hepatitis C virus RNA quantification and clinical significance for genotypes 1 to 5." *J Clin Microbiol* **44**: 729-737.

Schuurman, R., D. Brambilla, et al. (2002). "Underestimation of HIV type 1 drug resistance mutations: results from the ENVA-2 genotyping proficiency program." *AIDS Res Hum Retroviruses* **18**(4): 243-8.

Schuurman, R., L. Demeter, et al. (1999). "Worldwide evaluation of DNA sequencing approaches for identification of drug resistance mutations in the human immunodeficiency virus type 1 reverse transcriptase." *J Clin Microbiol* **37**(7): 2291-6.

Schuurman, R., Demeter, L., Reichelderfer, P., Tijnagel, J., de Groot, T., Boucher, C. (1999). "Worldwide evaluation of DNA sequencing approaches for identification of

drug resistance mutations in the human immunodeficiency virus type 1 reverse transcriptase." *J Clin Microbiol* **37**(7): 2291-6.

Shafer, R. W., S. Y. Rhee, et al. (2008). "Consensus drug resistance mutations for epidemiological surveillance: basic principles and potential controversies." *Antivir Ther* **13 Suppl 2**: 59-68.

Shiramizu, B. (2005). "Circulating proviral HIV DNA and HIV-associated dementia." *AIDS* **19**: 45-52.

Shiramizu, B., S. Gartner, et al. (2004). "Assessment of HIV-1 DNA copies per cell by real-time polymerase chain reaction." *Front Biosci* **9**: 255-61.

Siliciano, J. D., J. Kajdas, et al. (2003). "Long-term follow-up studies confirm the stability of the latent reservoir for HIV-1 in resting CD4+ T cells." *Nat Med* **9**(6): 727-8.

Sluis-Cremer, N. and G. Tachedjian (2008). "Mechanisms of inhibition of HIV replication by non-nucleoside reverse transcriptase inhibitors." *Virus Res* **134**(1-2): 147-56.

Starnes, M. C., W. Y. Gao, et al. (1988). "Enzyme activity gel analysis of human immunodeficiency virus reverse transcriptase." *J Biol Chem* **263**(11): 5132-4.

Stryer, L. and R. P. Haugland (1967). "Energy transfer: a spectroscopic ruler." *Proc Natl Acad Sci U S A* **58**: 719-726.

Tanese, N., V. R. Prasad, et al. (1988). "Structural requirements for bacterial expression of stable, enzymatically active fusion proteins containing the human immunodeficiency virus reverse transcriptase." *DNA* **7**(6): 407-16.

Toni, T. A., E. L. Asahchop, et al. (2009). "Detection of human immunodeficiency virus (HIV) type 1 M184V and K103N minority variants in patients with primary HIV infection." *Antimicrob Agents Chemother* **53**(4): 1670-2.

van Harmelen, J. H., E. Shepard, et al. (2003). "Construction and characterisation of a candidate HIV-1 subtype C DNA vaccine for South Africa." *Vaccine* **21**: 4380-9.

VanGuilder, H. A., K. E. Vrana, et al. (2008). "Twenty-five years of quantitative PCR for gene expression analysis." *Biotechniques* **44**: 619-626.

Various (2008). "HIV Sequence Compendium 2008 Introduction."

Vercauteren, J. and A. M. Vandamme (2006). "Algorithms for the interpretation of HIV-1 genotypic drug resistance information." *Antiviral Res* **71**(2-3): 335-42.

Violin, M., A. Cozzi-Lepri, et al. (2004). "Risk of failure in patients with 215 HIV-1 revertants starting their first thymidine analog-containing highly active antiretroviral therapy." *AIDS* **18**(2): 227-35.

Violin, M., Cozzi-Lepri, A., Velleca, R., Vincenti, A., D'Elia, S., Chiodo, F., et al. (2004). "Risk of failure in patients with 215 HIV-1 revertants starting their first thymidine analog-containing highly active antiretroviral therapy." *AIDS* **18**(2): 227-35.

Walker, N. J. (2002). "A technique whose time has come." *Science* **296**: 557-559.

Watts, J. M., K. K. Dang, et al. (2009). "Architecture and secondary structure of an entire HIV-1 RNA genome." *Nature* **460**(7256): 711-6.

Watzinger, F., K. Ebner, et al. (2006). "Detection and monitoring of virus infections by real-time PCR." *Mol. Aspects Med.* **27**: 254-298.

Weinstein, M. C., S. J. Goldie, et al. (2001). "Use of genotypic resistance testing to guide hiv therapy: clinical impact and cost-effectiveness." *Ann Intern Med* **134**(6): 440-50.

Wensing, A. M., Boucher, C. A. (2003). "Worldwide transmission of drug-resistant HIV." *AIDS Rev* **5**(3): 140-55.

Whiley, D. M. and T. P. Sloots (2006). "Sequence variation can affect the performance of minor groove binder TaqMan probes in viral diagnostic assays." *J Clin Virol* **35**: 81-83.

Wind-Rotolo, M., C. Durand, et al. (2009). "Identification of nevirapine-resistant HIV-1 in the latent reservoir after single-dose nevirapine to prevent mother-to-child transmission of HIV-1." *J Infect Dis* **199**(9): 1301-9.

Wittwer, C. T., M. G. Herrmann, et al. (1997). "Continuous fluorescence monitoring of rapid cycle DNA amplification." *Biotechniques* **22**: 130-138.

Yeni, P. G., S. M. Hammer, et al. (2002). "Antiretroviral treatment for adult HIV infection in 2002: updated recommendations of the International AIDS Society-USA Panel." *JAMA* **288**(2): 222-35.

List of Addendums

Appendix A

Equipments, reagents and software packages used in this study are in Table 1-3.

Table 1: Equipment used in this study.

Equipment	Supplier and location
7900HT Fast Real-Time PCR system	Applied Biosystems, Foster City, California, USA
ABI prism [®] 310 Genetic Analyzer	Applied Biosystems, Foster City, California, USA
Centrifuge 5417C	Eppendorf, New York, USA
GeneAMP [®] 9700 PCR system	Applied Biosystems, Foster City, California, USA
Haake L (water bath)	LabX, California, USA
Labcon [®] shaking incubator	Labcon Ltd., Krugersdorp, South Africa
Nanodrop [™] ND-1000	NanoDrop Technologies Inc., Delaware, USA

Table 2: Commercial reagents and chemicals used this study.

Product	Company	Location	Catalogue Number
1 kb DNA ladder	Promega Corporation	Madison, Wisconsin, USA	G5711
Access RT-PCR system	Promega Corporation	Madison, Wisconsin, USA	A1250
Ampicillin	Invitrogen Corporation	Paisley, UK	11593-027
Bacteriological Agar	Whitehead Scientific	Cape Town, South Africa	1800

BigDye™ Terminator v3.1 Cycle Sequencing Mix	Applied Biosystems	Foster City, California, USA	4337455
Blue/Orange 6X Loading Dye	Promega Corporation	Madison, Wisconsin, USA	G190A
<i>EcoRI</i>	Promega Corporation	Madison, Wisconsin, USA	R6011
Ethidium bromide	Promega Corporation	Madison, Wisconsin, USA	H5041
Ethylenediamine Tetra Acetic Acid (EDTA)	Sigma-Aldrich	Saint-Louis, USA	L4509
GoTaq® Flexi DNA Polymerase	Promega Corporation	Madison, Wisconsin, USA	M8305
Glycerol	Merck	Darmstadt, Germany	28456
Half-dye Buffer	Bioline USA Inc	Randolph, Miami, USA	BIO-36025
Isopropyl-β-D-thiogalactopyranosid (IPTG)	Promega Corporation	Madison, Wisconsin, USA	V3951
Luria-Bertani (LB)	Fluka Biochemika,	Buchs, Switzerland	61748
Molecular grade agarose	Whitehead Scientific (Pty) Ltd.	Burgos, Spain	D1-LE
Nuclease-free water	Promega Corporation	Madison, Wisconsin, USA	P1193
pGEM®-T Easy Vector system II	Promega Corporation	Madison, Wisconsin, USA	A1380
PureYield™ Plasmid Midiprep system,	Promega Corporation	Madison, Wisconsin, USA	A2495
QIAamp® UltraSens™ Virus Kit	Qiagen GmbH	Hilden, Germany	53706
QIAprep® Spin Miniprep Kit	Qiagen GmbH	Hilden, Germany	27106

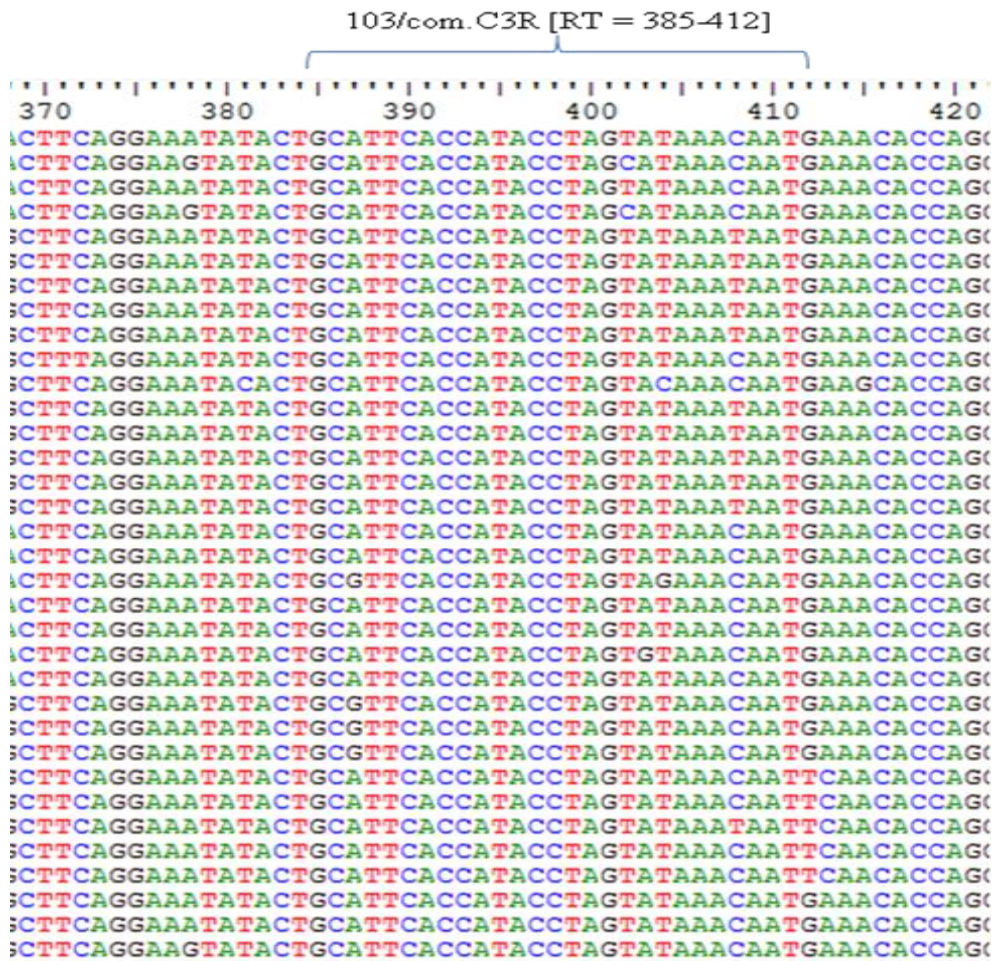
QIAquick® PCR Purification Kit	Qiagen GmbH	Hilden, Germany	28106
QuikChange® Lightning Site-Directed Mutagenesis Kit	Stratagene	La Jolla, Canada	210519
RE 10X Buffer H	Promega Corporation	Madison, Wisconsin, USA	R6011
SOC medium	Sigma-Aldrich	Saint-Louis, USA	S1797-100ML
TaqMan® Gene Expression Master Mix	Applied Biosystems	Foster City, California, USA	4369514
Tris hydrochloride	Roche	Berlin, Germany	708976
X-Galactosidase (X-Gal)	Promega Corporation	Madison, Wisconsin, USA	V3941

Table 3: A list of software packages used in this study.

Program	Version	Company/reference
BioEdit Sequence Alignment Editor	7.0.9.0	(Hall 1999)
Clustal X	1.81.22	(Thompson© et al., 1997)
Geneious Pro	4.5.5	Biomatters Ltd., Auckland, New Zealand. (http://www.geneious.com/)
SDS©	2.3	Applied Biosystems, Foster city, California, USA
Sequencher	4.8	Gene Codes, Ann Arbor, Miami, USA
GeneSnap image acquisition	4.0.0	Synoptics Ltd., Cambridge, UK
QuikChange® Primer Design Program		Stratagene, La Jolla, USA

Appendix B

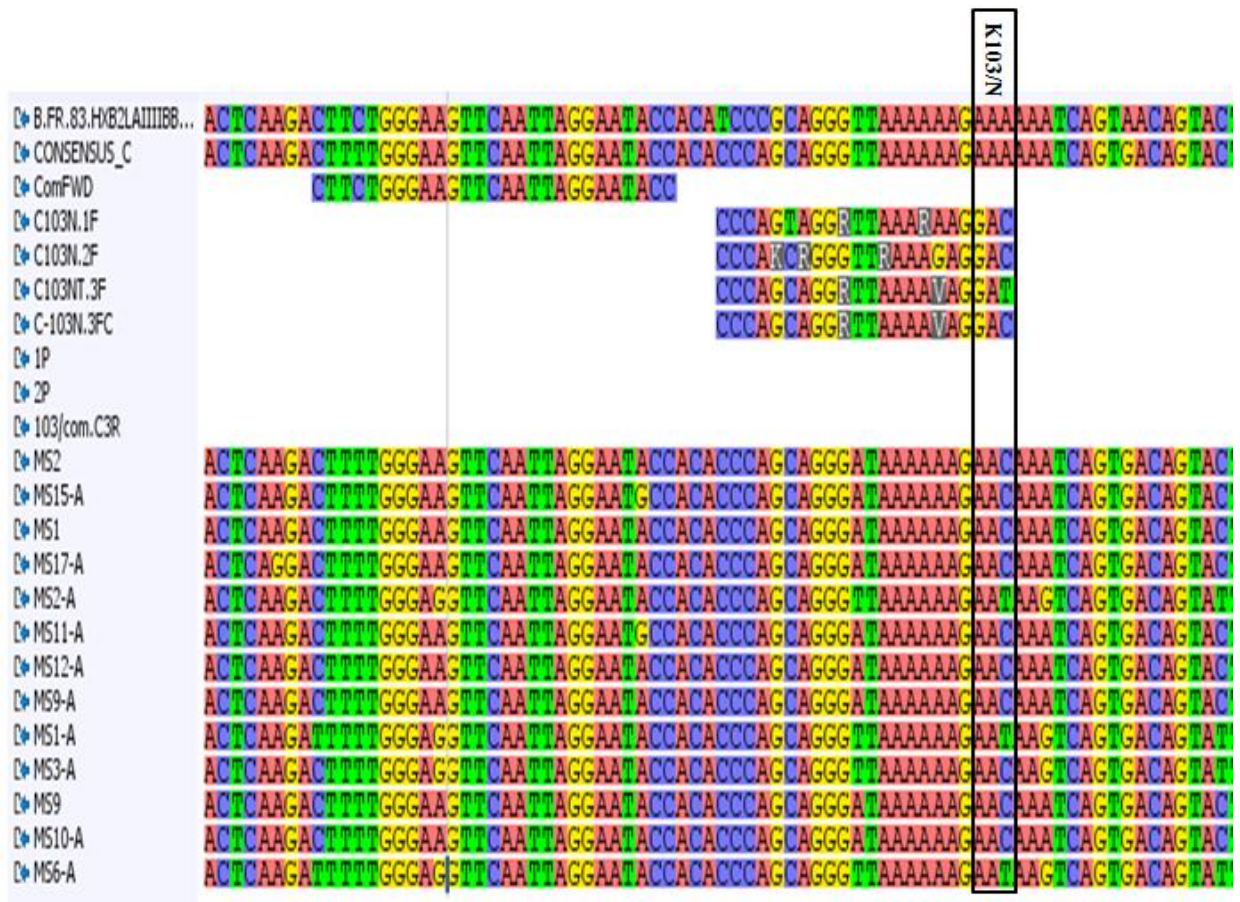
Multiple alignments of all 2008 HIV-1 RT sequences and consensus C: This is a part of the generated multiple sequence alignments of the all 2008 subtype C HIV-1 *RT* sequences from the Los Alamos HIV database. They were generated with ClustalX and viewed with the BioEdit software. The sequences were 494 in total. The coloured bars (green, black, blue and red) represent the sequence similarities and identities. The regions without the bars are diverse.



The alignments end here.

Appendix C

Multiple alignments of plasmid standards, SPCR primers and probes: This is part of the multiple alignment of all primers and probes, pGEM® T-Easy plasmids, with Consensus C and HIV-1 HXB2 as background sequences, showing the mismatches and degenerate bases incorporated in the nucleotide sequences while designing the specific primers when compared to the HIV-1 HXB2.



The alignments continue in the next page...


```

D> B.FR.83.HXB2LAIIIIBB... TGGATGTGGGGATGCATATTTTTCAGTTCCTTAGATGAAGACTTCAGGAAGTATACTGCATTACCATACCTAGTATAAAACAATGAGA
D> CONSENSUS_C TGGATGTGGGGATGCATATTTTTCAGTTCCTTAGATGAAGGCTTCAGGAAATATACTGCATTACCATACCTAGTATAAAACAATGAA
D> ComFWD
D> C103N.1F
D> C103N.2F
D> C103NT.3F
D> C-103N.3FC
D> 1P TGGGGATGCATATTTTTCAGTTCCTTAGATGA
D> 2P TGGGAGATGCATATTTTTCAGTTCCTTAGATGA
D> 103/com.C3R GCATTACCATACCTAGTATAAAACAATG
D> MS2 TAGATGTGGGGATGCATATTTTTCAGTTCCTTAGATGAAGGCTTCAGGAAGTATACTGCATTACCATACCTAGTATAAAACAATGAA
D> MS15-A TAGATGTGGGGATGCATATTTTTCAGTTCCTTAGATGAAGGCTTCAGGAAGTATACTGCATTACCATACCTAGTATAAAACAATGAA
D> MS1 TAGATGTGGGGATGCATATTTTTCAGTTCCTTAGATGAAGGCTTCAGGAAGTATACTGCATTACCATACCTAGTATAAAACAATGAA
D> MS17-A TAGATGTGGGGATGCATATTTTTCAGTTCCTTAGATGAAGGCTTCAGGAAGTATACTGCATTACCATACCTAGTATAAAACAATGAA
D> MS2-A TGGATGTGGGGATGCATATTTTTCAGTTCCTTAGATGAAAGTTTCAGAAAAATACTGCATTACCATACCCAGTATAAAACAATGAA
D> MS11-A TAGATGTGGGGATGCATATTTTTCAGTTCCTTAGATGAAGGCTTCAGGAAGTATACTGCATTACCATACCTAGTATAAAACAATGAA
D> MS12-A TAGATGTGGGGATGCATATTTTTCAGTTCCTTAGATGAAGGCTTCAGGAAGTATACTGCATTACCATACCTAGTATAAAACAATGAA
D> MS9-A TAGATGTGGGGATGCATATTTTTCAGTTCCTTAGATGAAGGCTTCAGGAGGTATACTGCATTACCATACCTAGTATAAAACAATGAA
D> MS1-A TGGATGTGGGGATGCATATTTTTCAGTTCCTTAGATGAAAGTTTCAGAAAAATACTGCATTACCATACCCAGTATAAAACAATGAA
D> MS3-A TGGATGTGGGGATGCATATTTTTCAGTTCCTTAGATGAAAGTTTCAGAAAAATACTGCATTACCATACCCAGCATAGCAATGAA
D> MS9 TAGATGTGGGGATGCATATTTTTCAGTTCCTTAGATGAAGGCTTCAGGAAGTATACTGCATTACCATACCTAGTATAAAACAATGAA
D> MS10-A TAGATGTGGGGATGCATATTTTTCAGTTCCTTAGATGAAGGCTTCAGGAAGTATACTGCATTACCATACCTAGTATAAAACAATGAA
D> MS6-A TGGATGTGGGGATGCATATTTTCAGTTCCTTAGACGAAAGTTTCAGAAAAATACTGCATTACCATACC

```

The alignments end here.